FOLIA BIOLOGICA (KRAKÓW)

e-ISSN 1734-9168 (since 2018)

Volume 66, number 1, June 2018

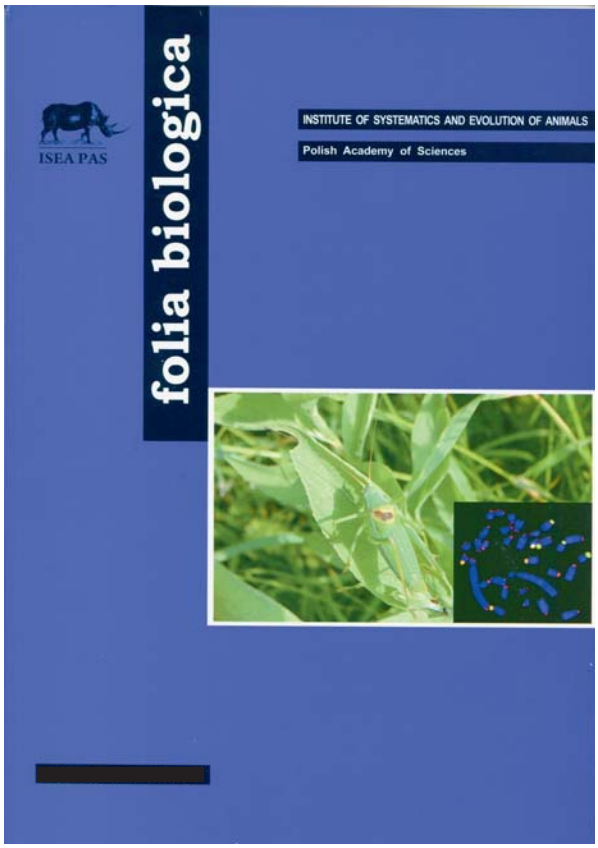

International Open Access journal
publishing original scientific articles
on various aspects of zoology:
experimental zoology,
molecular, chromosomal
and ultrastructural studies

CONTENTS:

ISEA PAS

Institute of Systematics and Evolution of Animals, Polish Academy of Sciences, Kraków, Poland

http://www.isez.pan.krakow.pl

FOLIA BIOLOGICA (KRAKÓW)

INTERNATIONAL QUARTERLY JOURNAL OF BIOLOGICAL RESEARCH

ISEA PAS

is published by the Institute of Systematics and Evolution of Animals, Polish Academy of Sciences

Manuscripts

The language of publication is English. Manuscripts are submitted to external referees for review: a single-anonymous (single-blind) procedure of review is applied. Submission of a manuscript implies that the work has not been published before and that it is not under consideration or accepted elsewhere. Manuscript should strictly conform with the editorial guidelines. Authors of accepted papers are required to participate in publication costs.

Detailed information about journal, Instructions for Authors and submission system are available at:
http://www.isez.pan.krakow.pl/en/folia-biologica.html

All materials should be submitted via the **Editorial System** directly available at: https://www.editorialsystem.com/fbiolkr

Since 2018 the journal is published in electronic form only.

Backfile and current issues are available free of charge at the Publisher's webpage as well as from IngentaConnect (since 2005): http://www.ingentaconnect.com/content/isez/fb

For printed edition of back issues up to 2017 (p-ISSN: 0015-5497) please contact our library: library@isez.pan.krakow.pl

Cover Design

Jerzy ŚWIECIMSKI

The rhinoceros on the cover presents a nearly complete specimen of the Pleistocene *Coelodonta antiquitatis*, excaved in the layers of ozocerite in Starunia (Eastern Carpathians), 1929. This unique exhibit is shown in the Natural History Museum (Institute of Systematics and Evolution of Animals), Kraków.

Cover Photograph

Isophya rhodopensis rhodopensis Ramme, 1951 (Orthoptera, Tettigoniidae).
Chromosomes after fluorescence *in situ* hybridization with 18S rDNA probe (green) and telomeric DNA probe (red).
By courtesy of Elżbieta Warchałowska-Śliwa

Editorial Office

Institute of Systematics and Evolution of Animals,
Polish Academy of Sciences
Sławkowska 17, 31-016 Kraków, Poland
Tel. +48 12 4227006
Telex 0322414 pan pl
Fax +48 12 4224294
E-mail folia@isez.pan.krakow.pl
www.isez.pan.krakow.pl

Journal indexed by

POLISH SCIENTIFIC JOURNALS CONTENTS – AGRIC. & BIOL. SCI.

http://psjc/icm.edu.pl

Index 35811

Indexed in *Current Contents*

e-ISSN 1734-9168
http://www.isez.pan.krakow.pl/en/folia-biologica.html

Folia Biologica (Kraków), vol. 66 (2018), No 1
https://doi.org/10.3409/fb_66-1.01

Effects of MCPA Herbicide on Hematological Parameters and Ultrastructure of Hematopoietic Tissues of Common Carp (*Cyprinus carpio* L.)

Hanna LUTNICKA, Bartosz BOJARSKI✉, Małgorzata WITESKA, Maria CHMURSKA-GĄSOWSKA, Wojciech TRYBUS, Ewa TRYBUS, Anna KOPACZ-BEDNARSKA, and Marcin LIS

Accepted February 20, 2018 *Published online March 21, 2018* *Issue online June 22, 2018*

Original article

LUTNICKA H., BOJARSKI B., WITESKA M., CHMURSKA-GĄSOWSKA M., TRYBUS W., TRYBUS E., KOPACZ-BEDNARSKA A., LIS M.. 2018. Effects of MCPA herbicide on hematological parameters and ultrastructure of hematopoietic tissues of common carp (*Cyprinus carpio* L.). Folia Biologica (Kraków) **66**: 01-11.

Common carp juveniles were subjected to 14 day exposure to 100 µg/l of MCPA (phenoxy acid herbicide) and 30 day depuration. Peripheral blood parameters were analyzed after 1, 3, 7 and 14 days of exposure at 7, 14 and 30 days of depuration. Ultrastructure of hematopoietic tissues of head and trunk kidney and spleen were analyzed after the end of exposure and purification. Results showed that MCPA exposure induced only minor and transient alterations in red blood parameters but more pronounced changes in leukocyte differential count: a significant and persistent depletion of mature neutrophils during both exposure and depuration, and monocytosis during exposure. These changes indicate a possible inflammatory process and immunosuppression caused by this herbicide. Analysis of hematopoietic tissue revealed no major pathologic lesions but some minor ultrastructural anomalies. Hematopoietic precursor cells with blurred ultrastructure, some vacuoles in cytoplasm with different electron density and size, melanomacrophage and myelin-like structures were observed during exposure and particularly during depuration. These changes indicate a weak cytotoxic effect of MCPA on carp hematopoietic system.

Key words: MCPA, herbicide, toxicity, hematology, hematopoietic tissues, common carp.

Hanna LUTNICKA, Maria CHMURSKA-GĄSOWSKA, Institute of Veterinary Science, University Centre of Veterinary Medicine, University of Agriculture in Kraków, Mickiewicza 24/28, 30-059 Kraków, Poland.
Bartosz BOJARSKI✉, Małgorzata WITESKA, Department of Animal Physiology, Institute of Biology, Siedlce University of Natural Sciences and Humanities, Prusa 12, 08-110 Siedlce, Poland.
E-mail: bbojarski@o2.pl
Wojciech TRYBUS, Ewa TRYBUS, Anna KOPACZ-BEDNARSKA, Department of Cell Biology and Electron Microscopy, Institute of Biology, The Jan Kochanowski University, Świętokrzyska 15, 25-406 Kielce, Poland.
Marcin LIS, Department of Veterinary Science, Animal Reproduction and Welfare, University of Agriculture in Kraków, Mickiewicza 24/28, 30-059 Kraków, Poland.

Phenoxy acids, as 2,4-D, MCPA and MCPP, are herbicides widely used in agriculture, forestry and horticulture (KUDSK & STREIBIG 2003). The presence of these substances in the aquatic environment has been reported in monitoring studies. Many scientific studies confirmed that shellfish and fish are good models to evaluate the toxicity in aquatic system due to their ability to metabolize xenobiotics, their sensitivity to pollutants (BARTOSKOVA *et al*. 2013; ALIKO *et al*. 2015; CHROMCOVA *et al*. 2015; BURGOS-ACEVES *et al*. 2016; FAGGIO *et al*. 2016; MATOZZO *et al*. 2016; SAVORELLI *et al*. 2017; SEHONOVA *et al*. 2017a, b; BURGOS-ACEVES *et al*. 2018) and the position into the aquatic food chain (TORRE *et al*. 2013; FAGGIO *et al*. 2016; PAGANO *et al*. 2017; BURGOS-ACEVES & FAGGIO 2017). SADOWSKI *et al*. (2014) detected MCPA (2.20 µg/l) and 2,4-D (1.36 µg/l) in surface water in agricultural areas of Lower Silesia, Poland. MCPA (up to 60 µg/l) was observed in stream water in southern Sweden (KREUGER 1998). The same herbicide, at concentration of 0.27 µg/l, was found in urban water in Melbourne, Australia (ALLINSON *et al*. 2017). GAILLARD *et al*. (2016) revealed that MCPA (26 µg/l) was present in water of fishponds located

in Lorraine Region, France. The presence of herbicides in surface waters may adversely affect fish (GLUSCZAK *et al*. 2007; CATTANEO *et al*. 2008; MORAES *et al*. 2009; BOTELHO *et al*. 2012; GOSIEWSKI *et al*. 2012). Hematological studies are important for environmental monitoring of fish and their health condition during culture because fish are generally so intimately associated with the aquatic environment (FAGGIO *et al*. 2014a; FAZIO *et al*. 2015; NATH *et al*. 2018). These parameters are closely related to the response of the animal to the environment, an indication that the environment where fish lives could exert some influence on the blood characteristics (FAGGIO *et al*. 2014 b, c). Various laboratory techniques are used to evaluate herbicide toxicity (VAN DER OOST *et al*. 2003; CHROMCOVA *et al*. 2015; PLHALOVA *et al*. 2017), including hematological tests, that appear to be a reliable and sensitive indicator of herbicide toxicity to fish (BOJARSKI *et al*. 2015). Anemic response including decrease in the values of red blood parameters such as hematocrit (Ht), hemoglobin concentration (Hb) and erythrocyte count (RBCc) often accompanied by the alterations in the mean cell volume (MCV) and mean corpuscular hemoglobin indices (MCH and MCHC) was observed after exposure to various herbicides: molinate (SANCHO *et al*. 2000), metribuzin (VELISEK *et al*. 2009b), glyphosate (GHOLAMI-SEYEDKOLAEI *et al.* 2013; FIORINO *et al.* 2018), and clomazone (PEREIRAB *et al*. 2013). Very scarce available data indicate that herbicides may also cause leukopenia in fish. Leukocyte count (WBCc) reduction after molinate exposure was reported by SANCHO *et al.* (2000) and after glyphosate exposure by GHOLAMI-SEYEDKOLAEI *et al.* (2013), while decreased leukocrit value after metribuzin treatment was observed by VELISEK *et al*. (2009b). However, the data concerning histopathological lesions caused by herbicides in hematopoietic tissue that may accompany changes in peripheral blood are very scarce (TEH *et al*. 1997; GÓMEZ *et al.* 1998; SANCHO *et al*. 2000; CAPKIN *et al.* 2010).

The presence of the phenoxy acid herbicides may pose a threat to fish living in contaminated environment. The effects of these herbicides on fish organism have not been extensively explored so far. The aim of the study was to determine the influence of phenoxy acid herbicide MCPA on blood parameters and ultrastructure of hematopoietic tissue of common carp (*Cyprinus carpio* Linnaeus, 1758).

Materials and Methods

Animals and experimental conditions

The study was approved by the Ist Local Ethical Committee on Animal Testing in Kraków (permission No. 124/2010). The study was done on common carp juveniles of body mass 60±10 g obtained from the Department of Ichthyobiology and Fishery Management of Polish Academy of Science in Gołysz. The fish were harvested from the rearing pond in spring. Before the experiment they were subjected to clinical and parasitological examination and acclimated for 2 weeks to the laboratory conditions. During the experiment the fish were kept in 14 aquaria (300 l each), 10 fish in each aquarium. Water was constantly aerated using LP-60 aerator (Resun, China) and filtered using external filters Unimax (Aquael, Poland). Water quality parameters were measured every 3 days (temperature, pH, dissolved oxygen level, total hardness, concentrations of ammonia, nitrite and nitrate) using reagent kits and multiparameter photometer HI83200 (Hanna Instruments, Olsztyn, Poland). The average values of these parameters during the experiment were: temperature 17-18°C, pH 7.2-8.0, O_2 8.26-9.15 mg/l, hardness 16-18 n, NH_3 0.02-0.07 mg/l, NO_2^- 1-2 mg/l and NO_3^- 18-24 mg/l. Water was renewed every 3-4 days during exposure to maintain the nominal concentration of the tested herbicide and prevent the accumulation of fish nitrogen metabolites. Similarly, water was exchanged every 3-4 days during the purification period. Fish were fed daily *ad libitum* with barley flakes and frozen chironomid larvae.

Experimental design

The fish (140 individuals) were equally divided into 2 groups: control and MCPA-exposed. The fish were exposed to tested herbicide at sublethal concentration of 100 µg/l for 14 days and then subjected to depuration in clean water for another 30 days. Blood was sampled from 10 fish of each group after 1, 3, 7 and 14 days of exposure and after 7, 14 and 30 days of depuration. Blood was sampled by heart puncture using glass heparinized Pasteur pipettes (sodium heparin 5000 IU/ml, Polfa, Poland) to heparinized plastic Eppendorf tubes. Blood from each fish was taken only once (after anesthesia with MS-222) and subjected to standard hematological analysis. RBCs and WBCs were counted in blood diluted 1:200 with Natt-Herrick solution using Bürker hemocytometer. Hematocrit value (Ht) was measured using microhematocrit method. Hemoglobin concentration (Hb) was measured spectrophotometrically at 540 nm wave length after conversion of hemoglobin to cyanmethemoglobin with Drabkin solution. Next, mean cell volume (MCV), mean corpuscular hemoglobin (MCH), and mean corpuscular hemoglobin concentration (MCHC) were calculated. Blood smears were also made and stained using Hemacolor® staining kit (Merck, Germany) to evaluate differential leukocyte count. Various types of leukocytes were identified per 100 cells at ×600 magnification. The

following types of cells were identified: lymphocytes, monocytes, juvenile neutrophils, mature neutrophils and eosinophils. Ultrastructural analysis of hematopoietic organs was also performed. Head and trunk kidney and spleen tissues were sampled from 5 fish of the control and MCPA-exposed groups twice: immediately after the end of exposure (14 days) and after the end of purification (44 days of the experiment). The sections were treated using standard method (KARNOVSKY 1965) and embedded in epoxy resin (Epoxy Embedding Medium, Sigma Aldrich). The preparations were subjected to transmission electron microscope analysis (TEM) using JOEL JEM-100 SX and Tecna G2 Spirit (FEI Company).

Chemical tested

MCPA (2-methyl-4-chlorophenoxyacetic acid $C_9H_9ClO_3$) is a systemic postemergence herbicide used to control annual and perennial dicotyledon weeds in cereal, linen, rice, peas and potato crops. It is also used in grasslands and forestry. MCPA is a component of 33 commercial formulas available in Poland, in 11 being a unique active substance, and in remaining 22 – one of at least 2 different active substances (THE REGISTER OF PLANT PROTECTION PRODUCTS, Polish Ministry of Agriculture and Rural Development, https://bip.minrol.gov.pl/Informacje-Branzowe/Produkcja-Roslinna/Ochrona-Roslin/Rejestr-Srodkow-Ochrony-Roslin, February 2017). MCPA is quite persistent in aquatic environment with half-life of 13.5 days (PESTICIDE PROPERTIES DATABASE – PPDB, University of Hertfordshire, https://sitem.herts.ac.uk/aeru/ppdb, February 2017). Analytical standard of purity 99.7 ± 0.1% obtained from the Institute of Organic Industry in Warsaw (Branch in Pszczyna) was used.

Statistical analysis of data

Normality of distribution was tested by the Shapiro-Wilk's test, and homogeneity of variance using Levene's test. The data were analyzed by ANOVA, followed by Tukey's post-hoc test. For the data that did not meet the assumptions of ANOVA (differential leukocyte count), a non-parametric U Mann–Whitney test was performed. The level of significance was set at $\alpha = 0.05$. Data were presented as means ± SD. Results were analyzed using STATISTICA 10 program.

Results

Hematological parameters

During the experiment neither mortality nor distress symptoms were observed in the exposed fish. The values of red blood parameters are shown in Table 1. RBCc in the control group ranged from 0.70 ± 0.11 to 1.12 ± 0.18 $\times 10^6$/µl. After 7 days of MCPA exposure RBCc value significantly increased and after 14 days of purification decreased compared to the control. Ht in the control fish ranged from 27.0 ± 4.5 to 34.7 ± 5.1% and no sta-

Table 1

Values of red blood cell parameters in common carp during exposure to MCPA (100 µg/l) and purification (asterisks indicate the values significantly different from the control at the same sampling time, Tukey's test, $P<0.05$)

Time of blood collecting/parameter tested		Exposure to MCPA herbicide (100 µg/l)				Purification		
		1 day	3 days	7 days	14 days	7 days	14 days	30 days
RBCc ($\times 10^6$/µl)	Control	0.81 ± 0.16	1.06 ± 0.10	0.88 ± 0.20	1.00 ± 0.08	0.70 ± 0.11	1.12 ± 0.18	1.08 ± 0.07
	MCPA	0.85 ± 0.30	1.06 ± 0.38	1.20* ± 0.25	0.80 ± 0.19	0.73 ± 0.15	0.82* ± 0.23	0.93 ± 0.15
Ht (%)	Control	27.00 ± 4.52	31.00 ± 2.78	32.90 ± 5.90	28.70 ± 3.62	27.40 ± 2.72	34.70 ± 5.10	34.00 ± 2.58
	MCPA	30.20 ± 4.02	32.90 ± 4.86	35.40 ± 4.25	29.30 ± 3.89	28.50 ± 2.68	31.00 ± 4.67	30.60 ± 4.90
Hb (g/dl)	Control	6.08 ± 1.42	8.33 ± 1.37	5.88 ± 0.86	7.93 ± 1.37	6.85 ± 1.77	7.79 ± 0.94	4.80 ± 0.57
	MCPA	9.98* ± 1.13	8.62 ± 1.14	4.53 ± 0.80	6.19* ± 0.76	6.89 ± 0.78	6.27 ± 0.86	5.65 ± 0.76
MCV (fl)	Control	342.07 ± 75.93	302.57 ± 48.30	394.50 ± 117.69	290.29 ± 49.31	399.44 ± 75.65	319.65 ± 82.80	319.23 ± 38.67
	MCPA	393.58 ± 134.22	350.13 ± 137.56	311.13 ± 63.48	389.45 ± 141.11	411.92 ± 111.34	399.04 ± 99.00	334.14 ± 55.61
MCH (pg)	Control	78.10 ± 26.06	78.93 ± 14.58	69.14 ± 13.79	79.70 ± 13.00	97.48 ± 21.65	71.02 ± 12.51	44.51 ± 5.05
	MCPA	129.05* ± 40.22	91.18 ± 34.23	40.12 ± 10.55	80.55 ± 20.73	100.70 ± 35.76	80.32 ± 18.49	61.98 ± 10.90
MCHC (g/dl)	Control	22.53 ± 4.62	26.20 ± 3.77	18.21 ± 3.38	28.00 ± 5.80	25.08 ± 6.70	22.66 ± 2.63	14.04 ± 1.63
	MCPA	33.37* ± 4.27	26.71 ± 5.38	13.06 ± 3.36	21.37* ± 3.25	24.44 ± 4.15	20.37 ± 2.11	19.16 ± 5.71

tistically significant differences between the control and herbicide-exposed fish were observed. Hb in blood of the control fish ranged from 4.80 ± 0.57 to 7.93 ± 1.37 g/dl. Hb significantly increased in MCPA-exposed group already after 1 day of exposure, while after 14 days significantly decreased compared to the control. MCV in the control fish was between 290.29 ± 49.31 fl and 399.44 ± 75.65 fl. In MCPA-exposed fish MCV values were usually slightly higher but no significant differences were observed compared to the control. MCH of the control fish was from 44.51 ± 5.05 to 97.48 ± 21.65 pg, while in the MCPA-exposed group it was more variable and after 1 day of exposure to the herbicide MCH value was significantly higher compared to the control. MCHC in the control showed the values between 14.04 ± 1.63 and 28.0 ± 5.80 g/dl. In MCPA-exposed group MCHC significantly increased after 1 day of exposure and decreased at the end of exposure compared to the control.

The results of leukocyte analysis are presented in Table 2. WBCc in the control ranged from 23.4 ± 4.7 to 45.8 ± 9.4 $\times 10^3/\mu l$. A significant increase in WBCc was observed in MCPA group after 7 days of exposure compared to the control. In the control group lymphocytes comprised from 85.0 ± 6.4 to 96.8 ± 1.6%. After 3 days of exposure to the herbicide a significant decrease in lymphocyte percentage was observed, followed by an increase after 30 days of purification. Percentage of immature neutrophils in the control fish was between 1.9 ± 1.1 and 8.0 ± 4.3% and no significant differences were observed between the groups. Percentage of mature neutrophils in the control ranged from 1.5 ± 0.9 to 7.7 ± 3.0%. After 1 day of exposure to MCPA a significant decrease occurred followed by an increase in 7 days compared to the control. Percentage of mature neutrophils decreased again in fish subjected to the herbicide treatment after 7, 14 and 30 days of purification compared to the control. Percentage of monocytes in the control was low and ranged from 0.3 ± 0.4 to 1.4 ± 1.2%. After 3 and 7 days of MCPA exposure contribution of monocytes significantly increased compared to the control.

Histology of hematopoietic organs

Head kidney

In fish from the control group head kidney hematopoietic tissue ultrastructure showed no pathological lesions and the results obtained after 14 and 44 days of experiment were similar (Fig. 1A and B). Head kidney of the control fish showed firm structure. Juvenile blood cells: promyelocytes, metamyelocytes, eosinophils, lymphocytes and scarce erythrocytes were present in the stroma, usually tightly packed. In the cells following organelles were observed: mitochondria, short RER sections, free ribosomes, single Golgi apparatuses, single vacuoles containing various materials, and granulocytes showed also numerous granules (Fig. 1A and B). After 14 days of MCPA exposure the head kidney structure was still firm and blood precursor cells were tightly packed (Fig. 2A and B). However, focally the cells were slightly deformed (Fig. 2B). Numerous neutrophil precursors, eosinophils and lymphocytes were observed (Fig. 2A). Single cells with electron-light nuclei or cytoplasm were observed among the normal cells (Fig. 2A and B). These cells showed also melanomacrophage struc-

Table 2

Values of white blood cell parameters in common carp during exposure to MCPA (100 μg/l) and purification (asterisks indicate the values significantly different from the control at the same time, Tukey's test for WBCc and U-Mann Whitney test for differential leukocyte count, $P<0.05$)

Time of blood collecting / parameter tested		Exposure to MCPA herbicide (100 μg/l)				Purification		
		1 day	3 days	7 days	14 days	7 days	14 days	30 days
WBCc ($\times 10^3/\mu l$)	Control	35.00 ± 5.90	42.60 ± 5.41	34.20 ± 5.29	33.80 ± 9.82	23.40 ± 4.72	24.20 ± 3.33	45.80 ± 9.36
	MCPA	36.80 ± 16.06	65.20 ± 25.98	77.10* ± 20.29	47.90 ± 11.70	30.20 ± 9.31	66.20* ± 15.16	52.00 ± 17.00
Lymphocytes (%)	Control	90.50 ± 2.58	93.60 ± 1.74	96.80 ± 1.60	95.60 ± 1.91	92.10 ± 4.06	88.70 ± 2.03	85.00 ± 6.36
	MCPA	94.08 ± 2.34	86.78* ± 3.42	89.10 ± 3.75	94.35 ± 4.06	96.15 ± 2.25	93.00 ± 3.55	92.85* ± 2.68
Juvenile neutrophils (%)	Control	3.85 ± 2.04	1.65 ± 0.85	1.90 ± 1.17	1.90 ± 1.11	2.90 ± 1.98	4.65 ± 2.71	8.00 ± 4.33
	MCPA	2.23 ± 1.51	5.47 ± 2.73	1.80 ± 1.49	1.75 ± 1.80	1.55 ± 0.42	4.00 ± 2.98	3.90 ± 1.78
Mature neutrophils (%)	Control	4.65 ± 2.20	3.80 ± 1.92	1.50 ± 0.85	1.50 ± 0.85	3.90 ± 1.82	5.70 ± 2.54	7.72 ± 3.00
	MCPA	2.03* ± 1.47	2.99 ± 1.50	2.85* ± 1.20	2.20 ± 1.32	1.65* ± 0.97	2.20* ± 1.99	3.20* ± 1.77
Monocytes (%)	Control	1.60 ± 1.07	1.40 ± 1.18	0.95 ± 0.55	0.75 ± 0.68	1.40 ± 1.22	0.50 ± 0.53	0.60 ± 0.22
	MCPA	1.53 ± 0.78	4.71* ± 1.83	3.75* ± 1.67	1.40 ± 1.02	0.95 ± 0.93	0.40 ± 0.61	0.05 ± 0.16

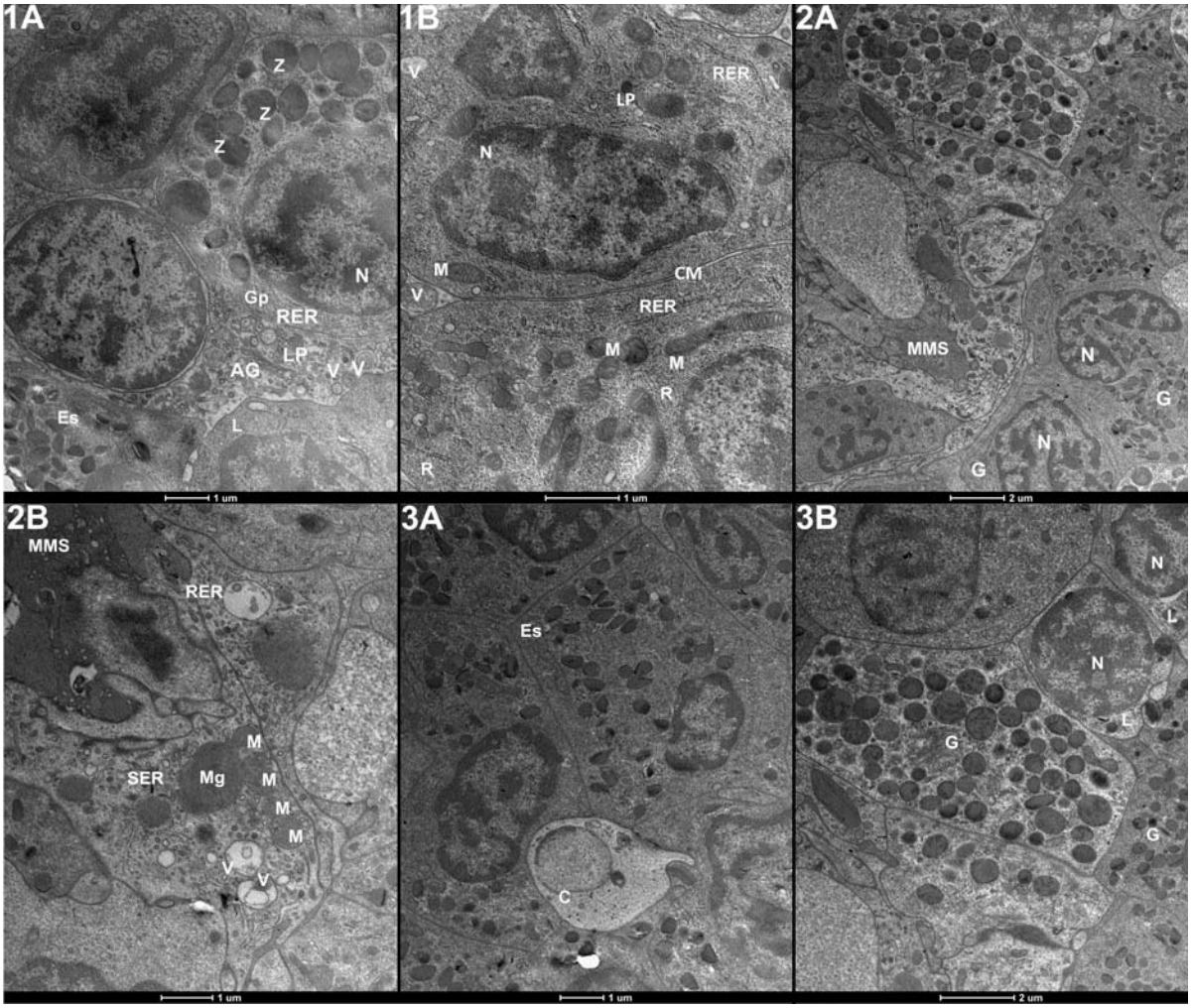

Figs 1-3.
Fig. 1A. Electron micrograph of common carp head kidney, control. Hematopoietic precursors: promyelocyte (Gp), eosinophil (Es) and lymphocyte (L). Numerous granules (Z), vacuoles (V), Golgi apparatus (AG) and primary lysosome (LP) in granulocytes. 9900 x. Fig. 1B. Electron micrograph of common carp head kidney, control. Organelles in hematopoietic precursor cells: rough endoplasmic reticulum (RER), free ribosomes (R), mitochondria (M), single vacuoles (V), primary lysosome (LP), cell nuclei (N) and cellular membrane (CM) 16500 x.
Fig. 2A. Electron micrograph of common carp head kidney after 14 days of exposure to 100 µg/l of MCPA. Numerous usually correct granulocytes (G) with nucleus (N) and damaged cell with melanomacrophage structure (MMS). 6000 x. Fig. 2B. Electron micrograph of common carp head kidney after 14 days of exposure to 100 µg/l of MCPA. Large melanomacrophage structure (MMS), numerous vacuoles (V) of different size and electron density, rough endoplasmic reticulum (RER), smooth endoplasmic reticulum (SER), mitochondria (M) and megamitochondria (Mg). 11500 x.
Fig. 3A. Electron micrograph of common carp head kidney after 30 days of depuration post MCPA exposure. In firm tissue structure eosinophils (Es) and electron-light cells (C). 9900 x. Fig. 3B. Electron micrograph of common carp head kidney after 30 days of depuration post MCPA exposure. Normal structure of granulocytes (G) and lymphocytes (L) with correct nucleus (N). 6000 x.

tures of various size. In granulocytes numerous granules were visible (Fig. 2A). After 30 days of depuration of MCPA-exposed fish their head kidneys usually had firm structure (Fig. 3A and B). Among the hematopoietic precursors granulocytes predominated. Cell nuclei showed chromatin diversification: both euchromatin and heterochromatin were observed. Nuclei of some cells were slightly deformed. Electron-light cells or cells with electron-light cytoplasm also occurred. Nuclei of lymphocytes were often cleft.

Trunk kidney – hematopoietic tissue

Analyses of trunk kidney hematopoietic tissue ultrastructure revealed no pathological alterations in fish from the control group and no differences between the samples taken after 14 and 44 days of experiment (Fig. 4A and B). The organ had firm structure and tightly packed cells. Mitochondria showed distinct cristae. RER and single Golgi apparatuses were also observed. Granulocytes showed numerous granules. In nuclei heterochromatin and euchromatin zones were visible. Hematopoietic tissue of trunk kidney consisted mainly of granulocyte and lymphocyte precursors. After 14 days of MCPA exposure hematopoietic and excretory parts of trunk kidney were connected and the cells were usually tightly packed (Fig. 5A) but some of them were slightly separated (Fig. 5B). Various types of granulocytes accompanied by

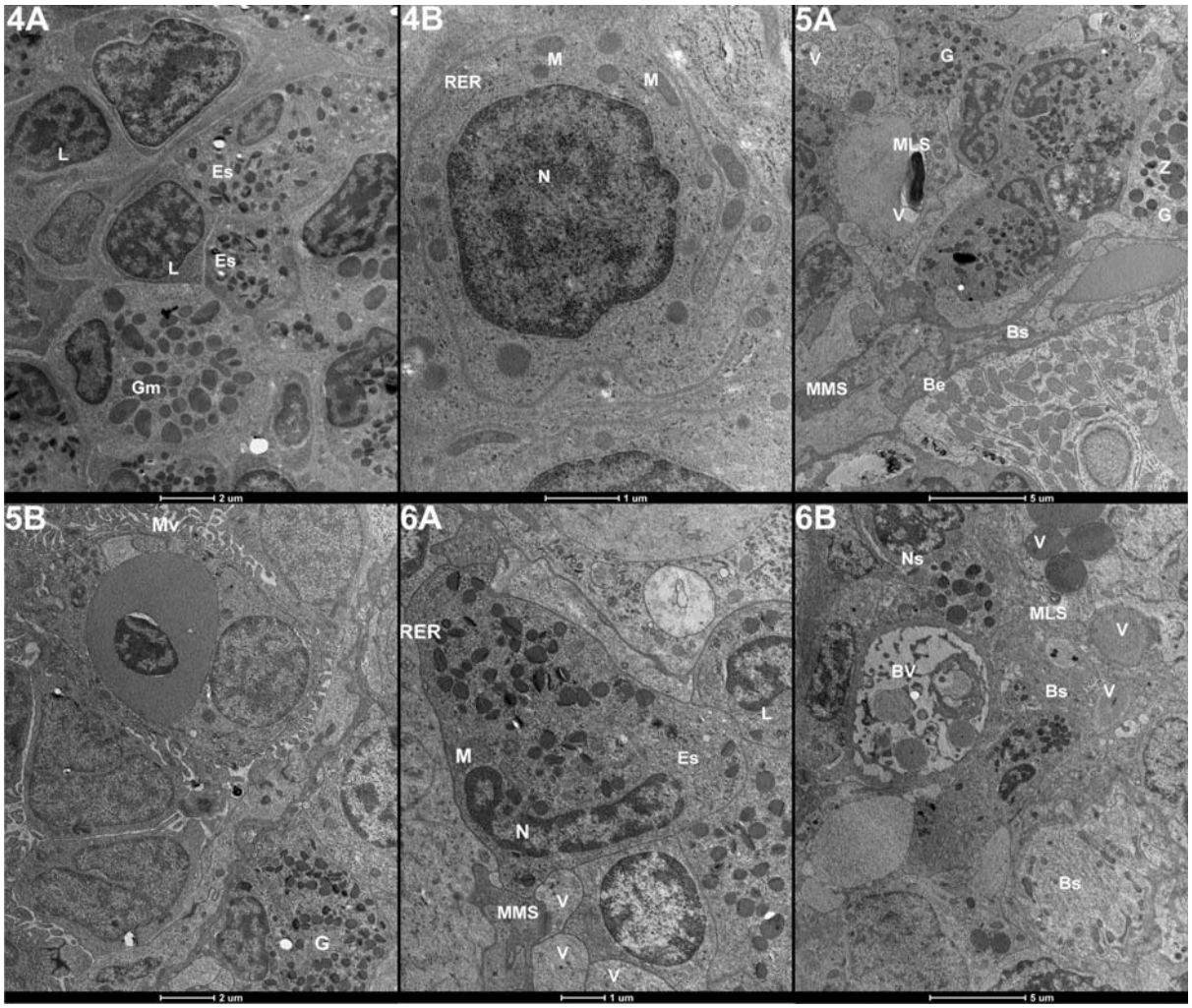

Figs 4-6.
Fig. 4A. Electron micrograph of common carp trunk kidney hematopoietic tissue, control. Firm tissue structure, numerous neutrophil precursors (Gm), eosinophils (Es) and lymphocytes (L). 6000 x. Fig. 4B. Electron micrograph of common carp trunk kidney hematopoietic tissue, control. Lymphocyte precursor with visible mitochondria (M), rough endoplasmic reticulum (RER) and nucleus (N). 16500 x.
Fig. 5A. Electron micrograph of common carp trunk kidney hematopoietic tissue near the boundary (Be) of excretory part after 14 days of exposure to 100 µg/l of MCPA. Firm tissue structure with some hematopoietic precursor cells of blurred ultrastructure (Bs). Granulocytes (G) containing numerous granules (Z) and damaged cells with single vacuoles (V) of various size and content. Single melanomacrophage (MMS) and myelin-like (MLS) structures. 4200 x. Fig. 5B. Electron micrograph of common carp trunk kidney hematopoietic tissue after 14 days of exposure to 100 µg/l of MCPA. Slight tissue structure loosening. Single granulocyte (G) and numerous microvilli (Mv) 6000 x.
Fig. 6A. Electron micrograph of common carp trunk kidney hematopoietic tissue after 30 days of depuration post MCPA exposure. Lymphocyte (L) and correct eosinophil (Es) with mitochondria (M), rough endoplasmic reticulum (RER) and nucleus (N). Hematopoietic precursor cells showing blurred ultrastructure, some vacuoles (V), and melanomacrophage structure (MMS). 9900 x. Fig. 6B. Electron micrograph of common carp trunk kidney hematopoietic tissue after 30 days of depuration post MCPA exposure. Hematopoietic precursor cells of normal (Ns) and blurred (Bs) ultrastructure near blood vessel (BV). Vacuoles (V) and myelin-like structures (MLS) in the cells. 4200 x.

lymphocytes were observed (Fig. 5A and B). They usually showed correct ultrastructure but in some cells it was slightly blurred (Fig 5A). Granulocytes (particularly eosinophils) showed numerous granules (Fig. 5A and B). In some cells single vacuoles, melanomacrophage structures and myelin-like bodies occurred (Fig. 5A). After 30 days of depuration hematopoietic and excretory parts of trunk kidney were connected or partly separated. Hematopoietic tissue showed firm structure (Fig. 6A and B) but cell ultrastructure was often blurred, particularly near excretory zone and blood vessels (Fig. 6B). Hematopoietic cells contained melanomacrophage and myelin-like structures accompanied by vacuoles (Fig 6A and B).

Spleen

Ultrastructure of splenic hematopoietic cells of the control fish revealed no pathological lesions and histological picture after 14 and 44 days of experiment did not differ (Fig. 7A and B). The spleen tissue showed numerous hematopoietic precursors and erythrocytes. Erythrocytes at various stages of

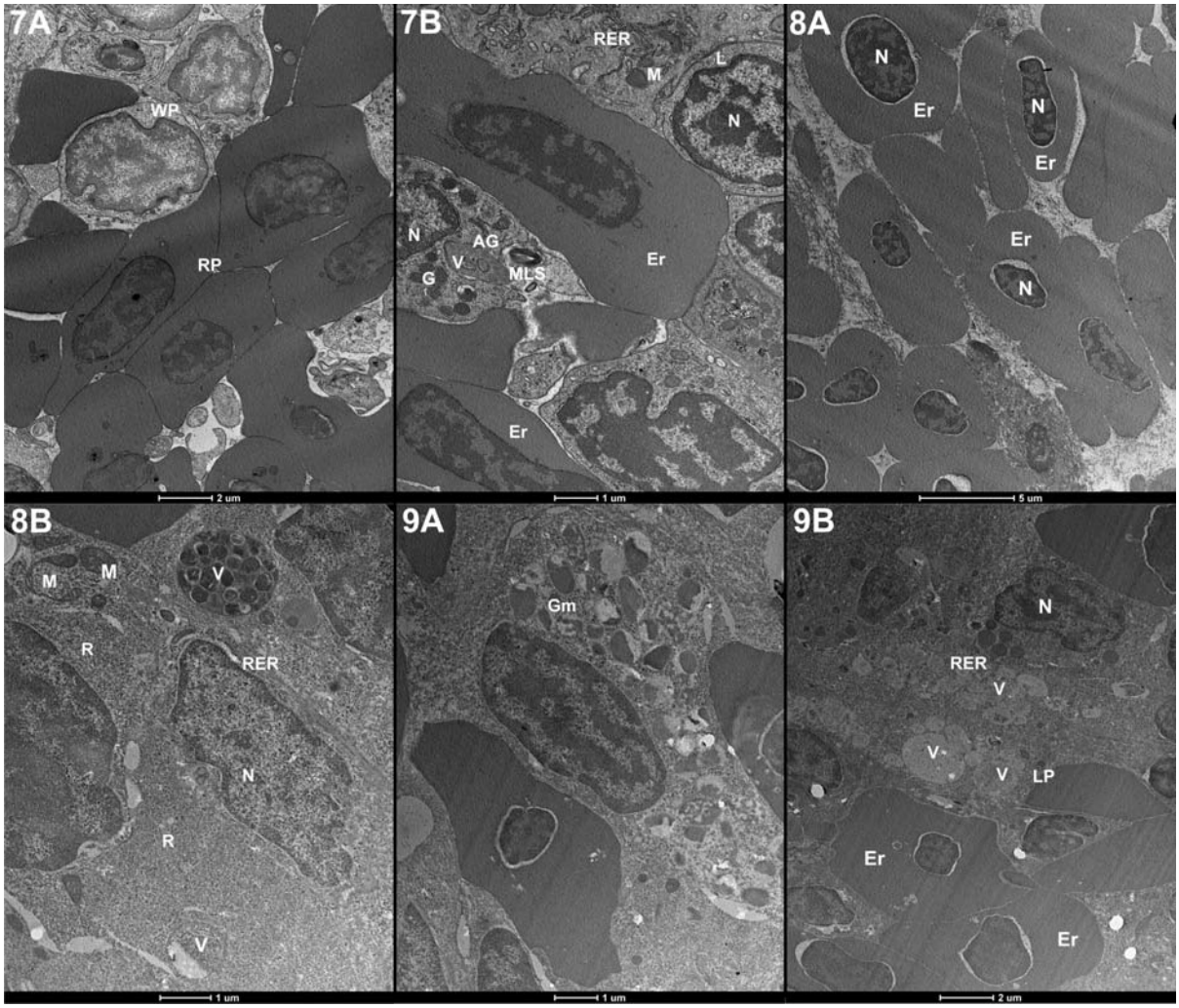

Figs 7-9.
Fig. 7A. Electron micrograph of common carp spleen, control. Firm tissue structure, numerous red pulp (RP) and white pulp (WP) cells. 6000 x.Fig. 7B. Electron micrograph of common carp spleen, control. Lymphocytes (L) and granulocytes (G) with ultrastructure: mitochondria (M), rough endoplasmic reticulum (RER), single mielin-like structure (MLS), Golgi apparatus (AG), vacuoles (V) and nuclei (N); single erythrocytes (Er) also visible. 9900 x.
Fig. 8A. Electron micrograph of common carp spleen after 14 days of exposure to 100 µg/l of MCPA. Group of erythrocytes (Er) with nuclei (N) at various stages of physiological degradation and electron-light stroma. 4200 x. Fig. 8B. Electron micrograph of common carp spleen after 14 days of exposure to 100 µg/l of MCPA. White pulp cell ultrastructure showing mitochondra (M) of different size and single in dividing process, short rough endoplasmic reticulum sections (RER), free ribosomes (R), vacuoles (V) and nuclei with euchromatin and heterochromatin. 11500 x.
Fig. 9A. Electron micrograph of common carp spleen after 30 days of depuration post MCPA exposure. Damaged metamyelocyte (Gm). 9900 x. Fig. 9B. Electron micrograph of common carp spleen after 30 days of depuration post MCPA exposure. Numerous vacuoles (V), primary lysosome (LP), rough endoplasmic reticulum (RER) in blurred ultrastructure of white pulp cells. Cell with nucleus (N) and some erythrocytes (Er) also visible. 6000 x.

physiological degradation were organized in lines or groups with lymphoid tissue among them or they surrounded lymphoid tissue forming sinus-like figures. The cells were usually tightly packed but sometimes empty intercellular spaces were observed. White pulp contained granulocytes: eosinophils and neutrophils at various development stages, and lymphocytes (Fig. 7B). After 14 days of exposure to MCPA spleen structure was generally compact (Fig. 8B). Red pulp consisted of lesser or larger groups of erythrocytes at various stages of more pronounced destruction compared to the control. (Fig. 8A). White pulp consisted of correct and abnormal cells – showing blurred ultrastructure (Fig. 8B). The cells showed mitochondria, RER, free ribosomes and vacuoles of different electron density, and the nuclei with euchromatin and heterochromatin zones (Fig. 8B). After 30 days of depuration white pulp had firm structure with tightly packed hematopoietic cells (Fig. 9A and B). Most of the cells showed correct ultrastructure but some cells with blurred ultrastructure and distinct anomalies were observed. These anomalies included numerous vacuoles of uniform or diverse electron density (Fig. 9B). The red pulp contained numerous erythrocytes undergoing physiological destruction.

Discussion

Exposure of fish to MCPA resulted in a significant but transient alterations in red blood parameters: increase in Hb, MCH and MCHC on the 1 day of exposure that might have resulted from stress followed by a decrease in Hb and MCHC after 14 days. After 14 days of depuration erythropenia was also observed. These results indicate that MCPA may induce in fish a transient anemic response. According to VOSYLIENE (1999), the quantitative red blood parameters in fish are rather stable and little sensitive to environmental factors, due to considerable compensatory abilities of organism.

It is known that different pesticides present in the aquatic environment can cause chemical stress in fish, which is expressed by changes in hematological parameters (SVOBODOVÁ *et al*. 2003; LI *et al*. 2011; LUTNICKA *et al*. 2016). However, little works concerning the effects of herbicides on the hematological profile of fish has been published. Alterations in the values red blood cell parameters of fish exposed to herbicides were observed by various authors but most data concern acute exposures. Anemia was reported by VELISEK *et al.* (2009b) who revealed that short-term (96 h) metribuzin exposure of *Cyprinus carpio* (175.1 mg/l) caused a significant decrease in Ht, Hb, MCV, and RBCc values. Similarly, short-time (96 h) Roundup exposure (3-20 mg/l) of *Leporinus obtusidens* reduced RBCc, Ht and Hb levels. RAMESH *et al*. (2009) showed that acute atrazine treatment (24 h, 18.5 mg/l) caused significant reduction of RBCc and Hb content in *C. carpio*. HUSSEIN *et al*. (1996) revealed that the exposure of *Oreochromis niloticus* and *Chrysichthyes auratus* to 3 and 6 mg/l of atrazine resulted in significant decrease in RBCc, Hb and Ht compared the control group in both species. DOBŠÍKOVÁ *et al*. (2011) observed a decrease of Ht in *C. carpio* exposed for 96 h to 13 mg/l of Gardoprim Plus Gold 500 SC (corresponding to 2.25 mg/l and 3.75 mg/l of terbuthylazine and S-metolachlor, respectively). KREUTZ *et al*. (2011) revealed a significant decrease in RBCc of *Rhamdia quelen* exposed to glyphosate (96 h, 0.73 mg/l). CRESTANI *et al*. (2006) observed that clomazone caused a significant decrease of Ht values in *Rhamdia quelen* after 96 h of exposure at a concentration of 0.05 mg/l and after 192 h at concentrations of 0.05 mg/l and 1.0 mg/l. After purification (192 h), the Ht levels in treated fish (0.5 and 1.0 mg/l) were similar to control values indicating a recovery. Butachlor administration for 48-72 h at concentrations 0.5-1.0 mg/l led to hematological alterations in *Labeo rohita* including time- and concentration-related decrease in RBCc and Ht values (GHAFFAR *et al*. 2015). Sublethal exposure of *Anguilla anguilla* to molinate (96 h, 11.15 mg/l) induced a significant decrease in Ht, Hb and RBCc (SANCHO *et al*. 2000). Some authors, however, reported that herbicide exposures of fish caused increase in the values of their red blood parameters. The results obtained by MODESTO and MARTINEZ (2010) demonstrated a significant increase of Ht and RBCc in *Prochilodus lineatus* exposed to Roundup Transorb® (24 and 96 h at 5 mg/l). Sub-chronic exposure of *C. carpio* to terbutryn (2-40 mg/l) led to a significant increase in RBCc (VELISEK *et al.* 2010). The results obtained by BOJARSKI *et al*. (2015) revealed that exposure of *C. carpio* to pendimethalin was time- and concentration-related in a non-linear way: at 2.5 μg/l a significant increase of Hb and MCHC were observed after 7 days of treatment. At 25 μg/l Hb decreased after 1 day and Ht after 3 days, while RBCc, Ht and Hb increased after 7 days of herbicide exposure. Ethofumesate (7 days, 0.11 μg/l) caused increase of RBCc, Ht and Hb, while at 1.1 μg/l Hb and MCHC values increased after 3 days of exposure. In fish exposed to mixture of both herbicides (2.5 μg/l of pendimethalin + 0.11 μg/l of ethofumesate or 25 μg/l and 1.1 μg/l, respectively) RBCc and Ht increased after 1 and 3 days of exposure, while longer exposures (7 days) resulted in reduction of RBCc and Ht values and increase of MCV and MCHC.

More pronounced alterations occurred in white blood cell system: despite transient leukocytosis after 7 days of exposure and 14 days post exposure, a persistent depletion of mature neutrophils, both during and after the end of exposure was observed, accompanied by significant monocytosis in 7 and 14 days of exposure. These changes indicate a possible inflammatory and immunosuppressive response in fish exposed to MCPA and increased migration of granulocytes to the affected tissues.

Little literature concerning the effects of herbicides on white blood parameters in fish is available and reported results are divergent. According to VELISEK *et al. (*2009b), 96 h exposure of *C. carpio* to 175.1 mg/l of metribuzin caused a significant WBCc decrease. Similar reaction was reported in *C. carpio* by RAMESH *et al*. (2009) after acute atrazine treatment (18.5 mg/l, 24 h). DOBŠÍKOVÁ *et al*. (2011) observed a decrease of WBCc and lymphopenia in *C. carpio* exposed for 96 h to 13 mg/l of Gardoprim Plus Gold 500 SC. According to KREUTZ *et al*. (2011), WBCc significantly decreased in the blood of glyphosate-exposed *Rhamdia quelen* (96 h, 0.73 mg/l). Also in molinate-exposed (96 h, 11.15 mg/l) *Anguilla anguilla* WBCc significantly decreased (SANCHO *et al*. 2000). On the other hand, increase in WBCc accompanied by lymphocytosis and neutropenia were reported by MODESTO and MARTINEZ (2010) in *Prochilodus lineatus* exposed to Roundup Transorb® (24 and 96 h, 5 mg/l). Butachlor exposure (48-72 h, 0.5-1.0 mg/l) re-

sulted in WBCc increase in *Labeo rohita* (GHAFFAR *et al*. 2015). BOJARSKI *et al*. (2015) found that exposure of *C. carpio* to 0.11 µg/l of ethofumesate caused increase of WBCc after 3 days of exposure. Hematological alterations induced in fish by various contaminants may be different and probably depend on various factors: type of toxic compound and its concentration, time of exposure, fish species, water quality parameters and other factors.

The observed hematological disturbances might have been related to herbicide-induced pathological lesions in hematopoietic organs: head and trunk kidneys and spleen. Our electron microscope observations of the hematopoietic organs suggest that MCPA caused minor ultrastructural alterations: deformed and blurred blood precursor cells, numerous vacuoles with auto- and heterophagic content, myelin-like and melanomacrophage structures were observed. In the spleen, ultrastructure of white and red pulp cells was usually correct but some cells were destroyed. The presence of abundant vacuoles, myelin-like and melanomacrophage structures in the cells indicates cell recovery and elimination of degenerated debris after herbicide-induced damage. The decrease in frequency of mature neutrophils during depuration period after fish exposure to MCPA might have been related to their destruction or migration to damaged tissues and involvement in the inflammatory process. Very few literature data are available concerning histopathological lesions in hematopoietic organs of fish exposed to aquatic contaminants, and their correlation with coexisting hematological changes. GÓMEZ *et al*. (1998) studied the lesions in hematopoietic part of posterior (trunk) kidney tissue in tench (*Tinca tinca*) caused by a continuous exposure to 400 mg/l of 2,4-dichlorophenoxyacetic acid (2,4-D). Using light microscope they found marked alterations characterized by progressive swelling and cell necrosis, and degeneration in the intertubular space in 48 h after intoxication. Intracytoplasmic vacuoles of different size were also visible. The lesions increased with time. Ultrastructural analysis revealed that at the beginning of exposure necrosis and phagocyte activation occurred. After 5 days the cells showed increased necrotic degeneration, numerous myelin figures and auto- and heterophagic vacuoles. Maximum necrosis level was observed after 12 days when mass disruption of cell-specific granules was observed, particularly in heterophils. Occasionally, electron-dense hyaline droplets were observed in venous sinus myoepithelial cells in the hematopoietic portion, arranged along the major axis of the cell. Hematopoietic tissue lesions were accompanied by changes in peripheral blood: Ht and Hb values decreased progressively. According to the authors, these hematological alternations indicated changes in cell membrane permeability, complementing the findings in hematopoietic tissue. CAPKIN *et al*. (2010) studied the effects of sublethal concentrations of carbofuran (25, 50 and 200 µg/l), propineb (3, 6 and 24 mg/l) and benomyl (2, 5 and 20 mg/l) on trunk kidney and spleen of juvenile rainbow trout (*Oncorhynchus mykiss*). The fish were exposed to the pesticides for 14 days. The most important lesions were observed at the highest concentrations of pesticides. Trunk kidney and spleen showed necrosis and abundant melanomacrophage centers. In the spleen lipid infiltration and increase of sinusoidal space were observed. TEH *et al.* (1997) observed histopathologic alterations of spleen of feral fish (sunfish, *Lepomis auritus* and bass, *Micropterus salmoides*) from three freshwater ecosystems polluted with discharges from a nuclear weapons facility, bleached craft mill or showing high levels of PCBs. Lymphopenia vascular congestion and reticuloendothelial cell necrosis were found in fish from first and third ecosystem. Melanomacrophage aggregations were also abundant in the spleen of sunfish from first ecosystem. VELISEK *et al*. (2009a) found no histological effects in the spleen of common carp (*C. carpio*) exposed for 96 h at 57.5 µg/l of bifenthrin (Talstar EC 10) HAAPARANTA *et al.* (1996) observed melanomacrophage centers in spleen, liver and hematopoietic part of the trunk kidney of two species of fish: perch (*Perca fluviatilis*) and roach (*Rutilus rutilus*). Similarly as in the present study, the results obtained by other authors (TEH *et al*. 1997; CAPKIN *et al*. 2010) showed that abundance and the surface of melanomacrophage centers and structures in the internal organs usually increased as a result of water contamination by different toxic substances. These results indicate high intensity of elimination of cellular debris after damage caused by herbicide intoxication in hematopoietic cells, particularly during depuration period.

Changes in the values of hematological parameters accompanied by the ultrastructural lesions in the hematopoietic organs caused by sublethal exposure to 100 µg/l of MCPA may be interpreted as a result of chemical stress. Most of hematological alterations were transient but ultrastructural lesions in hematopoietic organs seemed more persistent which was probably related to cellular regeneration processes.

Acknowledgments

The studies were carried out in the University of Agriculture in Kraków, Faculty of Animal Science, Institute of Veterinary Sciences, Department of Veterinary Science, Animal Reproduction and Welfare; Mickiewicza 24/28, 30-059 Krakow, Poland.

Funding

This work has been supported by grant NN304279440 (National Science Center, Poland) and UCMW-UR (University Center of Veterinary Medicine – University of Agriculture in Krakow, Poland).

Author Contributions

Research concept and design: H.L., B.B.; Collection and/or assembly of data: H.L., B.B., M.Ch.-G., W.T., E.T., A.K.-B.; Data analysis and interpretation: H.L., B.B., M.W., W.T., E.T., A.K.-B., M.L.; Writing the article: H.L., B.B., M.W., W.T., E.T., A.K.-B.; Critical revision of the article: H.L., B.B., M.W., M.Ch.-G., M.L.; Final approval of article: H.L., B.B., M.W., M.L.

Conflict of Interest

The authors declare no conflict of interest.

References

ALIKO V., HAJDARAJ G., CACI A., FAGGIO C. 2015. Copper induced lysosomal membrane destabilisation in haemolymph cells of mediterranean green crab (*Carcinus aestuarii*, Nardo, 1847) from the Narta Lagoon (Albania). Braz. Arch. Biol. Technol. **58**: 750-756.

ALLINSON M., ZHANG P., BUI A., MYERS J.H., PETTIGROVE V., ROSE G., SALZMAN S.A., WALTERS R., ALLINSON G. 2017. Herbicides and trace metals in urban waters in Melbourne, Australia (2011-12): concentrations and potential impact. Environ. Sci. Poll. Res. **24**: 7274-7284.

BARTOSKOVA M., DOBSIKOVA R., STANCOVA V., ZIVNA D., BLAHOVA J., MARSALEK P., ZELNÍCKOVA L., BARTOS M., DI TOCCO F.C., FAGGIO C. 2013. Evaluation of ibuprofen toxicity for zebrafish (*Danio rerio*) targeting on selected biomarkers of oxidative stress. Neuro. Endocrinol. Lett. **34**: 102-108.

BOJARSKI B., LUDWIKOWSKA A., KUREK A., PAWLAK K., TOMBARKIEWICZ B., LUTNICKA H. 2015. Hematological alterations in common carp (*Cyprinus carpio* L.) exposed to herbicides: pendimethalin and ethofumesate tested separately and in mixture. Folia Biol. (Kraków) **63**: 167-174.

BOTELHO R.G., BARBOSA DOS SANTOS J., FERNANDES K.M., NEVES C.A. 2012. Effects of atrazine and picloram on grass carp: acute toxocity and histological assessment. Toxicol. Environ. Chem. **94**: 121-127.

BURGOS-ACEVES M.A., COHEN A., SMITH Y., FAGGIO C. 2016. Estrogen regulation of gene expression in the teleost fish immune system. Fish Shellfish Immunol. **58**: 42-49.

BURGOS-ACEVES M.A., COHEN A., SMITH Y., FAGGIO C. 2018. A potential microRNA regulation of immune-related genes in invertebrate haemocytes. Sci. Total Environ. **621**: 302-307.

BURGOS-ACEVES M.A., FAGGIO C. 2017. An approach to the study of the immunity functions of bivalve haemocytes: Physiology and molecular aspects. Fish Shellfish Immunol. **67**: 513-517.

CAPKIN E., TERZI E., BORAN H., YANDI I., ALTINOOK I. 2010. Effects of some pesticides on the vital organs of juvenile rainbow trout (*Oncorhynchus mykiss*). Tissue Cell **42**: 376-382.

CATTANEO R., LORO V.L., SPANEVELLO R., SILVEIRA F.A., LUZ L., MIRON D.S., FONSECA M.B., MORAES B.S., CLASEN B. 2008. Metabolic and histological parameters of silver catfish (*Rhamdia quelen*) exposed to commercial formulation of 2,4-dichlorophenoxiacetic acid (2,4-D) herbicide. Pest. Biochem. Physiol. **92**: 133-137.

CHROMCOVA L., BLAHOVA J., ZIVNA D., PLHALOVA L., CASUSCELLI DI TOCCO F., DIVISOVA L., PROKES M., FAGGIO C., TICHY F., SVOBODOVA Z. 2015. NeemAzal T/S – toxicity to early-life stages of common carp (*Cyprinus carpio* L.). Vet. Medic. **60**: 23-30.

CRESTANI M., MENEZES C., GLUSCZAK L., MIRON D., DOS SANTOS MIRON D., LAZZARI L., DUARTE M.F., MORSCH V.M., PIPPI A.L., VIEIRA V.P. 2006. Effects of clomazone herbicide on hematological and some parameters of protein and carbohydrate metabolism of silver catfish *Rhamdia quelen*. Ecotoxicol. Environ. Safety **65**: 48-55.

DOBŠÍKOVÁ R., BLAHOVÁ J., MODRÁ H., ŠKORIČ M., SVOBODOVÁ Z. 2011. The effect of acute exposure to herbicide Gardoprim Plus Gold 500 SC on haematological and biochemical indicators and histopathological changes in common carp (*Cyprinus carpio* L.). Acta Vet. Brno **80**: 359-363.

FAGGIO C., FEDELE G., ARFUSO F., PANZERA M., FAZIO F. 2014a. Haematological and biochemical response of *Mugil cephalus* after acclimation to captivity. Cah. Biol. Mar. **55**: 31-36.

FAGGIO C., PAGANO M., ALAMPI R., VAZZANA I., FELICE M.R. 2016. Cytotoxicity, haemolymphatic parameters, and oxidative stress following exposure to sub-lethal concentrations of quaternium-15 in *Mytilus galloprovincialis*. Aquat. Toxicol. **180**: 258-265.

FAGGIO C., PICCIONE G., MARAFIOTI S., ARFUSO F., FORTINO G., FAZIO F. 2014b. Metabolic response to monthly variations of *Sparus aurata* reared in Mediterranean off-shore tanks. Turk. J. Fish. Aquat. Sci. **14**: 567-574.

FAGGIO C., PICCIONE G., MARAFIOTI S., ARFUSO F., TRISCHITTA F., FORTINO G., FAZIO F. 2014c. Monthly variations of haematological parameters of *Sparus aurata* and *Dicentrarchus labrax* reared in Mediterranean land offshore tanks. Cah. Biol. Mar. **55**: 437-443.

FAZIO F., PICCIONE G., ARFUSO F., FAGGIO C. 2015. Peripheral blood and head kidney haematopoietic tissue response to experimental blood loss in Mullet (*Mugil cephalus*). Mar. Biol. Res. **11**: 197-202.

FIORINO E., SEHONOVA P., PLHALOVA L., BLAHOVA J., SVOBODOVA Z., FAGGIO C. 2018. Effect of glyphosate on early life stages: comparison between *Cyprinus carpio* and *Danio rerio*. Environ. Sci. Poll. Res. DOI 10.1007/s11356-017-1141-5 (in press).

GAILLARD J., THOMAS M., IURETIG A., PALLEZ Ch., FEIDT C., DAUCHY X., BANAS D. 2016. Barrage fishponds: Reduction of pesticide concentration peaks and associated risk of adverse ecological effects in headwater streams. J. Environ. Manag. **169**: 261-271.

GHAFFAR A., HUSSAIN R., KHAN A., ABBAS R.Z., ASAD M. 2015. Butachlor Induced Clinico-Hematological and Cellular Changes in Fresh Water Fish *Labeo rohita* (Rohu). Pak. Vet. J. **35**: 201-206.

GHOLAMI-SEYEDKOLAEI S.J., MIRVAGHEFI A., FARAHMAND H., KOSARI A.A. 2013. Effect of a glyphosate-based herbicide in *Cyprinus carpio*: Assessment of acetylcholinesterase activity, hematological responses and serum biochemical parameters. Ecotoxicol. Environ. Safety **98**: 135-141.

GLUSCZAK L., DOS SANTOS MIRON D., MORAES B.S., SIMÕES R.R., SCHETINGER M.R.Ch., MORSCH V.M., LORO V.L. 2007. Acute effects of glyphosate herbicide on metabolic

and enzymatic parameters of silver catfish (*Rhamdia quelen*). Comp. Biochem. Physiol. **146**: 519-524.

GÓMEZ L., MASOT J., MARTINEZ S., DURÁN E., SOLER F., RONCERO V. 1998. Acute 2,4-D poisoning in tench (*Tinca tinca* L.): Lesions in the hematopoietic portion of the kidnay. Arch. Environ. Contam. Toxicol. **35**: 479-483.

GOSIEWSKI G., SOCHA M., NOWAK E., KUCHINKA J., SOKOŁOWSKA-MIKOŁAJCZYK M. 2012. Influence of short- and long-term exposition to Roundup on the spontaneous and hormonally stimulated LH secretion and gills condition in Prussian carp (*Carassius gibelio*). Adv. Environ. Sci. – Int. J. Bioflux Soc. **4**: 146-152.

HAAPARANTA A., VALTONEN E.T., HOFFMANN R., HOLMES J. 1996. Do macrophage centres in freshwater fishes reflect the differences in water quality? Aquat. Toxicol. **34**: 253-272.

HUSSEIN S.Y., EL-NASSER M.A., AHMED S.M. 1996. Comparative studies on the effects of herbicide atrazine on freshwater fish *Oreochromis niloticus* and *Chrysichthyes auratus* at Assiut, Egypt. Bull. Environ. Contam. Toxicol. **57**: 503-510.

KARNOVSKY M. J. 1965. A formaldehyde-glutaraldehyde fixative of high osmolality for use in electron microscopy. J. Cell Biol. **27**: 137-138.

KREUGER J. 1998. Pesticides in stream water within an agricultural catchment in southern Sweden, 1990-1996. Sci. Total Environ. **216**: 227-251.

KREUTZ L.C., BARCELLOS L.J.G., DE FARIA VALLE S., DE OLIVEIRA SILVA T., ANZILIERO D., DOS SANTOS E.D., PIVATO M., ZANATTA R. 2011. Altered hematological and immunological parameters in silver catfish (*Rhamdia quelen*) following short term exposure to sublethal concentration of glyphosate. Fish Shellfish Immunol. **30**: 51-57.

KUDSK P., STREIBIG J.C. 2003. Herbicides – a two-edged sword. Weed Res. **43**: 90-102.

LI Z.H., VELISEK J., GRABIC R., LI P., KOLAROVA J., RANDAK T. 2011. Use of hematological and plasma biochemicalparameters to assess the chronic effects of a fungicide propiconazole on a freshwater teleost. Chemosphere **83**: 572-578.

LUTNICKA H., BOJARSKI B., LUDWIKOWSKA A., WROŃSKA D., KAMIŃSKA T., SZCZYGIEŁ J., TROSZOK A., SZAMBELAN K., FORMICKI G. 2016. Hematological alterations as a response to exposure to selected fungicides in common carp (*Cyprinus carpio* L.). Folia Biol. (Kraków) **64**: 235-244.

MATOZZO V., PAGANO M., SPINELLI A., CAICCI F., FAGGIO C. 2016. *Pinna nobilis*: A big bivalve with big haemocytes? Fish Shellfish Immunol. **55**: 529-34.

MODESTO K.A., MARTINEZ C.B.R. 2010. Effects of Roundup Transorb in fish: hematology, antioxidant defenses and acetylocholinesterase activity. Chemosphere **81**: 781-787.

MORAES B.S., LORO V.L., PRETTO A., DA FONSECA M.B., MENEZES Ch., MARCHESAN E., REIMCHE G.B., DE AVILA L.A. 2009. Toxicological and metabolic parameters of the teleost fish (*Leporinus obtusidens*) in response to commercial herbicides containing clomazone and propanil. Pest. Biochem. Physiol. **95**: 57-62.

NATH S., MATOZZO V., BHANDARI D., FAGGIO C. 2018. Growth and liver histology of *Channa punctatus* exposed to a common biofertilizer. Nat. Prod. Res. DOI 10.1080/14786419.2018.1428586 (in press).

PAGANO M., PORCINO C., BRIGLIA M., FIORINO E., VAZZANA M., SILVESTRO S., FAGGIO C. 2017. The influence of exposure of cadmium chloride and zinc chloride on haemolymph and digestive gland cells from *Mytilus galloprovincialis*. Int. J. Environ. Res. **11**: 207-216.

PEREIRAB L., FERNANDES M.N., MARTINEZC C.B.R. 2013. Hematological and biochemical alterations in the fish Prochilodus lineatus caused by the herbicide clomazone. Environ. Toxicol. Pharm. **36**: 1-8.

PESTICIDE PROPERTIES DATABASE – PPDB, University of Hertfordshire, https://sitem.herts.ac.uk/aeru/ppdb, February 2017.

PLHALOVA L., BLAHOVA J., DIVISOVA L., ENEVOVA V., CASUSCELLI DI TOCCO F., FAGGIO C., TICHY F., VECEREK V., SVOBODOVA Z. 2017. The effects of subchronic exposure to NeemAzal T/S on zebrafish (*Danio rerio*). Chem. Ecol. DOI 10.1080/02757540.2017.1420176 (in press).

RAMESH M., SRINIVASAN R., SARAVANAN M. 2009. Effect of atrazine (herbicide) on blood parameters of common carp *Cyprinus carpio* (Actinopterygii: Cypriniformes). African J. Environ. Sci. Technol. **3**: 453-458.

SADOWSKI J., KUCHARSKI M., DZIĄGWA M. 2014. Influence of changes in the scope of registered plant protection products on the level of herbicide contamination of waters in agricultural areas. Prog. Pant. Prot. **54**: 191-197.

SANCHO E., CERÓN J.J., FERRANDO M.D. 2000. Cholinesterase activity and hematological parameters as biomarkers of sublethal molinate exposure in *Anguilla anguilla*. Ecotoxicol. Environ. Safety **46**: 81-86.

SAVORELLI F., MANFRA L., CROPPO M., TORNAMBÈ A., PALAZZI D., CANEPA S., TRENTINI P.L., CICERO A.M., FAGGIO C. 2017. Fitness evaluation of *Ruditapes philippinarum* exposed to nickel. Biol. Trace El. Res. **177**: 384-393.

SEHONOVA P., PLHALOVA L., BLAHOVA J., DOUBKOVA V., MARSALEK P., PROKES M., TICHY F., SKLADANA M., FIORINO E., MIKULA P., VECEREK V., FAGGIO C., SVOBODOVA Z. 2017a. Effects of selected tricyclic antidepressants on early-life stages of common carp (*Cyprinus carpio*). Chemosphere **185**: 1072-1080.

SEHONOVA P., PLHALOVA L., BLAHOVA J., DOUBKOVA V., PROKES M., TICHY F., FIORINO E., FAGGIO C., SVOBODOVA Z. 2017b. Toxicity of naproxen sodium and its mixture with tramadol hydrochloride on fish early life stages. Chemosphere **188**: 414-423.

SVOBODOVÁ Z., LUSKOVÁ V., DRASTICHOVÁ J., SVOBODA M., ŽLÁBEK V. 2003. Effect of deltamethrin on haematological indices of common carp (*Cyprinus carpio* L.). Acta Vet. Brno **72**: 79-85.

TEH S.J., ADAMS S.M., HINTON D.E. 1997. Histopathological biomarkers in feral freshwater fish populations exposed to different types of contaminant stress. Aquat. Toxicol. **37**: 51-70.

THE REGISTER OF PLANT PROTECTION PRODUCTS, Polish Ministry of Agriculture and Rural Development, https://bip.minrol.gov.pl/Informacje-Branzowe/Produkcja-Roslinna/Ochrona-Roslin/Rejestr-Srodkow-Ochrony-Roslin, February 2017.

TORRE A., TRISCHITTA F., FAGGIO C. 2013. Effect of $CdCl_2$ on regulatory volume decrease (RVD) in *Mytilus galloprovincialis* digestive cells. Toxicol. *in Vitro* **27**: 1260-1266.

VAN DER OOST R., BEYER J., VERMEULEN N.P.E. 2003. Fish bioaccumulation and biomarkers in environmental risk assessment: a review. Environ. Toxicol. Pharm. **13**: 57-149.

VELISEK J., SUDOVA E., MACHOVA J., SVOBODOVA Z. 2010. Effects of sub-chronic exposure to terbutryn in common carp (*Cyprinus carpio* L.). Ecotoxicol. Environ. Safety **73**: 384-390.

VELISEK J., SVOBODOVA Z., MACHOVA J. 2009a. Effects of bifenthrin on some haematological, biochemical and histopathological parameters of common carp (*Cyprinus carpio* L.). Fish Physiol. Biochem. **35**: 583-590.

VELISEK J., SVOBODOVA Z., PIACKOVA V., SUDOVA E. 2009b. Effect of acute exposure to metribuzin on some hematological, biochemical and histological parameters of common carp (*Cyprinus carpio* L.). Bull. Environ. Contam. Toxicol. **82**: 492-495.

VOSYLIENE M.Z. 1999. The effect of heavy metals on haematological indices of fish (survey). Acta Zool. Lituanica **9**: 76-82.

e-ISSN 1734-9168
http://www.isez.pan.krakow.pl/en/folia-biologica.html

Folia Biologica (Kraków), vol. 66 (2018), No 1
https://doi.org/10.3409/fb_66-1.02

An Unusual Symbiotic System in *Elymana kozhevnikovi* (Zachvatkin, 1938) and *Elymana sulphurella* (Zetterstedt, 1828) (Insecta, Hemiptera, Cicadellidae: Deltocephalinae)

Michał KOBIAŁKA, Anna MICHALIK and Teresa SZKLARZEWICZ✉

Accepted March 07, 2018 *Published online March 21, 2018* *Issue online June 22, 2018*

Original article

KOBIAŁKA M., MICHALIK A., SZKLARZEWICZ T. 2018. An unusual symbiotic system in *Elymana kozhevnikovi* (Zachvatkin, 1938) and *Elymana sulphurella* (Zetterstedt, 1828) (Insecta, Hemiptera, Cicadellidae: Deltocephalinae). Folia Biologica (Kraków) **66**: 13-24.

Morphological and molecular analyses revealed that the Deltocephalinae leafhoppers *Elymana kozhevnikovi* and *E. sulphurella* are host to four bacteriocyte-associated microorganisms: *Sulcia* (phylum Bacteroidetes), *Nasuia* (phylum Proteobacteria, class Betaproteobacteria), *Arsenophonus* (phylum Proteobacteria, class Gammaproteobacteria) and *Sodalis*-like bacteria (phylum Proteobacteria, class Gammaproteobacteria). Ultrastructural observations showed that in some bacteriocytes, apart from *Sulcia,* small elongated, rod-shaped bacteria are likewise present. The use of fluorescence *in situ* hybridization (FISH) revealed the occurrence of *Sodalis*-like bacteria in these bacteriocytes. *Sodalis*-like bacteria were also distributed in some cells of the bacteriome sheath. *Nasuia* and *Arsenophonus* co-existed in the same bacteriocytes. Moreover, *Arsenophonus* bacteria were dispersed in fat body cells. *Wolbachia* and *Rickettsia* were also detected alongside bacteriocyte-associated symbionts in *E. kozhevnikovi* and *E. sulphurella*. *Sulcia*, *Nasuia*, *Arsenophonus* and *Sodalis*-like bacteria are transovarially transmitted from one generation to the next.

Key words: Symbiotic microorganisms, *Sulcia*, *Nasuia*, *Arsenophonus*, *Sodalis*-like bacteria, *Wolbachia*, *Rickettsia*, transovarial transmission.

Michał KOBIAŁKA, Anna MICHALIK, Teresa SZKLARZEWICZ✉, Department of Developmental Biology and Morphology of Invertebrates, Institute of Zoology and Biomedical Research, Jagiellonian University, Gronostajowa 9, 30-387 Kraków, Poland.
E-mail: teresa.szklarzewicz@uj.edu.pl

Deltocephalinae leafhoppers, as other plant sap-sucking hemipterans, live in mutualistic relations with microorganisms including bacteria and/or yeast-like symbionts. The presence of these associates is connected with the restricted diet of host insects, poor in essential nutrients (mainly amino acids) (reviewed e.g. in BUCHNER 1965; DOUGLAS 1998; BAUMANN 2005). It is generally accepted that the occurrence of obligate symbionts is a result of an ancient acquisition of microorganisms by the ancestor of these insects resulting in the presence of microorganisms in all the descendants. As a consequence of the long-term co-evolution between host insects and their symbionts, neither can survive as separate entities (i.e. host insects devoid of microorganisms cannot properly develop or reproduce, microorganisms cannot be cultivated on laboratory media). On account of this mutualistic relationship, BUCHNER (1965) termed the obligate microorganisms "primary symbionts". BUCHNER (1965) also distinguished "accessory symbionts" (later termed "facultative symbionts" or "secondary symbionts") which may occur in some populations only. The presence of the latter in host insects is a consequence of, as a rule, their more recent acquisition. Secondary symbionts may fulfill different functions, e.g. they may protect host insects against parasites or heat stress (MONTLLOR *et al.* 2002; OLIVER *et al*. 2003; ŁUKASIK *et al*. 2013). Recent genomic analyses have shown that they may also be engaged in the synthesis of amino acids or other factors in metabolic pathways in different groups of hemipterans (TAKIYA *et al.* 2006; LAMELAS *et al.* 2011; SLOAN & MORAN 2012; LUAN *et al*. 2015; HUSNIK & MCCUTCHEON 2016). On ac-

count on the metabolic complementarity of symbionts residing in auchenorrhynchous hemipterans and their mutualistic association with host insects, TAKIYA and co-workers (2006) termed these symbionts "coprimary symbionts".

Previous histological observations by MÜLLER (1962) and BUCHNER (1965) have shown that auchenorrhynchous hemipterans (cicadas, leafhoppers, treehoppers, spittlebugs and planthoppers) generally harbor several different symbionts. More recent molecular work determined their systematic affinity and function, revealing that auchenorrhynchous hemipterans host the ancient symbionts: Candidatus *Sulcia muelleri* (hereafter *Sulcia*) (phylum Bacteroidetes) and betaproteobacterial symbionts (phylum Proteobacteria) (MORAN *et al.* 2005; TAKIYA *et al*. 2006; BRESSAN *et al*. 2009; NODA *et al*. 2012; URBAN & CRYAN 2012; BENNETT & MORAN 2013; ISHII *et al.* 2013; KOGA *et al.* 2013; SZKLARZEWICZ *et al.* 2016; KOBIAŁKA *et al.* 2015, 2016; MAO *et al*. 2017). In some auchenorrhynchous hemipterans, the ancient betaproteobacterial symbiont has been lost and replaced by other bacteria (e.g. Gammaproteobacteria or Alphaproteobacteria) (MORAN *et al.* 2003; TAKIYA *et al.* 2006; MCCUTCHEON *et al.* 2009; KOGA *et al*. 2013; MICHALIK *et al*. 2014). Moreover, in some groups of auchenorrhynchous hemipterans, the ancient symbionts (only the betaproteobacterial symbiont or both *Sulcia* and the betaproteobacterial symbiont) have been eliminated and replaced by yeast-like microorganisms (NODA 1977; NODA *et al.* 1995; SACCHI *et al.* 2008; MICHALIK *et al.* 2009; NISHINO *et al.* 2016; KOBIAŁKA *et al.* 2016, 2017). Since the Deltocephalinae possess diverse symbiotic associates in comparison to other auchenorrhynchous hemipterans (SACCHI *et al.* 2008; ISHII *et al.* 2013; BENNETT & MORAN 2013; KOBIAŁKA *et al.* 2015, 2016, 2017), in this work we described the symbiotic systems of two unexamined representatives of these leafhoppers, *Elymana kozhevnikovi* and *E. sulphurella,* by means of molecular and ultrastructural methods.

Material and Methods

Insects

The adult females of *Elymana kozhevnikovi* (Zachvatkin, 1938) and *Elymana sulphurella* (Zetterstedt, 1828) were collected in the southern part of Poland (Kraków, Częstochowa, Gliwice, Katowice) from June to September 2012-2016 from the grasses of the family Poaceae.

Light and electron microscopy

The dissected abdomens of adult females of all species examined were fixed in 2.5% glutaraldehyde in 0.1 M phosphate buffer (pH 7.4) at 4°C for three months. Next, the material was rinsed in the phosphate buffer with the addition of sucrose (5.8 g/100 ml) and postfixed in 1% osmium tetroxide in the same buffer. Then, the material was dehydrated in a graded series of ethanol and acetone and embedded in epoxy resin Epon 812 (Serva, Heidelberg, Germany). The semithin sections (1 µm thick) obtained from about twenty five females of *E. kozhevnikovi* and about twenty five females of *E. sulphurella* were stained with 1% methylene blue in 1% borax and photographed using a Nikon Eclipse 80i light microscope (LM). The ultrathin sections (90 nm thick) were contrasted with uranyl acetate and lead citrate and examined using a Jeol JEM 2100 electron transmission microscope (TEM) at 80 kV.

DNA analyses

DNA was extracted individually from the dissected abdomens of ten females preserved in 100% ethanol. DNA extraction was conducted using the Sherlock AX extraction kit (A&A Biotechnology) according to the manufacturer's protocol and next DNA was stored at 4°C for further analyses. Molecular identification of bacteria associated with examined species was performed based on their 16S rDNA sequences which were obtained by amplifications with symbiont-specific primers (listed in Table 1). PCR reactions were run in a total volume of 20 µl made up of 10 µl of the PCR Mix Plus HGC mixture (A&A Biotechnology), 8 µl of water, 0.5 µl of each of the primers (10 µM) and 1 µl of the DNA template (1 µg/µl) under the following protocol: an initial denaturation step at 94°C for a duration of 3 min, followed by 33 cycles at 94°C for 30 s, 54-56°C for 40 s (see Table 1), 70°C for 1 min 40 s and a final extension step of 5 min at 72°C. The PCR products were visualized by electrophoresis in 1.5% agarose gel stained with Midori Green (Nippon Genetics Europe). The positive PCR products were sent to an external company (Genomed) for DNA sequencing. The GenBank accession numbers of sequences obtained are listed in Table 2.

Phylogenetic analyses

The phylogenetic analyses were performed based on sequences of 16S rDNA of symbionts of *E. kozhevnikovi* and *E. sulphurella* and selected symbionts of Deltocephalinae leafhoppers deposited in the GenBank database. The sequences were then edited using BioEdit Sequence Alignment

Table 1

Primers and fluorochrome-labeled probes used in this study

Purpose	Primer name	Primer sequence (5'-3')	Target gene	Annealing temperature	Source
Diagnostic PCR	10CFB	AGAGTTTGATCATGGCTCAGGATG	16S rRNA gene of *Sulcia*	54°C	MORAN *et al.* 2005
	CFB1515R	GTACGGCTACCTTGTTACGACTTAG			
	16SA1	AGAGTTGATCMTGGCTCAG	16S rRNA gene of *Sodalis*-like symbionts	54°C	FUKATSU & NIKOH 1998
	Sod1248R	TCCGCTGACTCTCGCGAGAT			
	ArsF	TGGCTCAGATTGAACGCTG	16S rRNA gene of *Arsenophonus*	54°C	This study
	ArsR	CACCGCAGTCATGAATCAC			
	Nasuia2F	TAAAGCGGGGAAAACCTCGT	16S rRNA gene of *Nasuia*	56°C	KOBIAŁKA *et al.* in preparation
	Nasuia2R	GCATGCTGATCCGCGATTAC			
	Nasuia5F	GCTTGATCCAGCAATGTYRC	16S rRNA gene of *Nasuia*	56°C	KOBIAŁKA *et al.* in preparation
	Nasuia5R	ACCTTCCAGTACGGCTACCT			
	Rick158F	CGGAGG AAAGAT TTATCG CTG	16S rRNA gene of *Rickettsia*	54°C	ISHII *et al*. 2013
	Rick1206R	CACGTC ACCGTC TTGCTC			
	WspF	TGGTCCAATAAGTGAGAGAAAC	16S rRNA gene of *Wolbachia*	55°C	ZHOU *et al*. 1998
	WspR	AAAAATTAAACGCTACTCCA			
FISH	Ars2	Cy5-TCATGACCACAACCTCCAAA	16S rRNA gene of *Arsenophonus*	Not applicable	GOTTLIEB *et al*. 2008
	BET940R	Cy5-TTAATCCACATCATCCACCG	16S rRNA gene of Betaproteobacteria	Not applicable	DEMANÈCHE *et al.* 2008
	Sod1248R	Cy3-TCCGCTGACTCTCGGGAGAT	16S rRNA gene of *Sodalis*-like symbionts	Not applicable	KOGA *et al*. 2013
	Sul664R	Cy3-CCMCACATTCCAGYTACTCC	16S rRNA gene of *Sulcia*	Not applicable	KOGA *et al*. 2013

Table 2

List of investigated symbiotic microorganisms with the accession numbers of the sequences

Species	Symbionts	GenBank number
Elymana kozhevnikovi (Zachvatkin, 1938)	*Sulcia*	MG840399
	Nasuia	MG878963
	Arsenophonus	MG894669
	Sodalis	MG835278
	Wolbachia	MG873552
Elymana sulphurella (Zetterstedt, 1828)	*Sulcia*	MG840400
	Nasuia	MG878964
	Arsenophonus	MG894670
	Sodalis	MG835279
	Wolbachia	MG873553

Editor 5.0.9 (HALL 1999), and following this, the sequence alignments were generated using ClustalX 1.8 (THOMPSON *et al*. 1997). The phylogenetic analyses were conducted using MrBayes 3.2.2 software (HUELSENBECK & RONQUIST 2001). In this analysis four incremental Metropolis-coupled MCMC chains (3 heated and 1 cold) were run for ten million generations with sampling every 1000 generations. The convergence of analyses was validated using Tracer software (RAMBAUT & DRUMMOND 2007) and the first 25 % of trees were discarded as 'burn-in'. The results of the Bayesian analysis were visualized using FigTree 1.4.0 software (RAMBAUT 2009).

Fluorescence *in situ* hybridization (FISH)

Fluorescence *in situ* hybridization (FISH) was conducted with symbiont-specific probes (see Table 1). Ten females preserved in 100% ethanol were rehydrated, fixed in 4% formaldehyde and dehydrated through incubations in 80%, 90% and

100% ethanol and acetone. Then, material was embedded in Technovit 8100 resin and cut into sections. Hybridization was performed using a hybridization buffer containing: 1 ml 1M Tris-HCl (pH 8.0), 9 ml 5 M NaCl, 25 µl 20% SDS, 15 ml 30% formamide and about 15 ml of distilled water. The slides were incubated in 200 µl of hybridization solution (hybridization buffer + probes) overnight, at room temperature (ŁUKASIK *et al.* 2017). Next, the slides were washed in PBS three times for 10 minutes, dried and covered with ProLong Gold Antifade Reagent (Life Technologies). The hybridized slides were then examined using a confocal laser scanning microscope Zeiss Axio Observer LSM 710.

Results

Molecular identification of symbiotic microorganisms

Analysis of the 16S rDNA sequences of symbionts associated with *Elymana kozhevnikovi* and *Elymana sulphurella* indicated that the examined species of deltocephalinae leafhoppers are host to six kinds of bacteria: *Sulcia*, *Nasuia*, *Arsenophonus*, *Sodalis*, *Wolbachia* and *Rickettsia*. *Sulcia*, *Nasuia*, *Arsenophonus* and *Sodalis* were detected in all the examined individuals. The 16S rDNA sequences of *Sulcia*, *Nasuia* and *Arsenophonus* symbionts of both *Elymana* species were identical. Sequences of *Sulcia* and *Nasuia* show a high similarity (99%) to 16S rDNA sequences of *Sulcia* and *Nasuia* occurring in other representatives of Deltocephalinae, whereas 16S rDNA sequences of *Arsenophonus* symbionts are similar to those in *Arsenophonus* bacteria detected in the bat fly *Basilia boardmani* [KC597734] and aphid *Aphis melosae* [KF824532]. In turn, the sequences of 16S rDNA of *Sodalis*-like bacteria of *E. kozhevnikovi* and *E. sulphurella* are almost identical (99% identity) and display 99% similarity to the 16S rDNA of bacteria *Sodalis praecaptivus* [CP006569] and the *Sodalis* symbiont of the clown stink bug *Poecilocoris lewisi* [AB915782]. In some of the examined individuals, bacteria belonging to the genera *Wolbachia* (*E. kozhevnikovi* 2/6; *E. sulphurella* 2/8) and *Rickettsia* (*E. kozhevnikovi* 3/7; *E. sulphurella* 3/7) were also detected.

Phylogenetic analyses of the obtained 16S rDNA sequences of *Sulcia* and *Nasuia* symbionts confirmed their systematic affiliation (Figs 1, 2). The topologies resulting from the Bayesian inference of the *Sulcia* and *Nasuia* symbionts are shown in Figs 1 and 2, respectively.

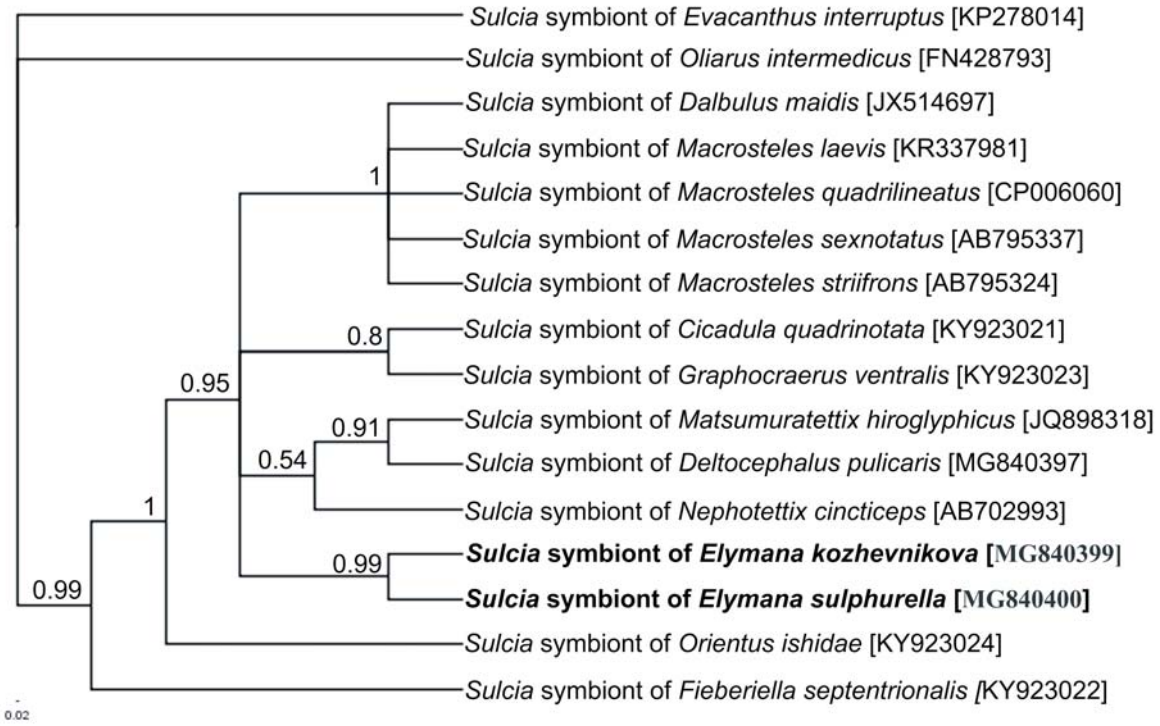

Fig. 1. Phylogenetic tree showing the relationships of *Sulcia* symbionts of the examined *Elymana kozhevnikovi* and *E. sulphurella* leafhoppers and other representatives of the subfamily Deltocephalinae, based on 16S RNA gene sequences. The numbers associated with the branches indicate the Bayesian posterior probability values. The accession numbers of the sequences used in the phylogenetic analysis have been put in brackets. For outgroups, *Sulcia* symbionts of the planthopper *Oliarus intermedicus* (Fulgoromorpha) and leafhopper *Evacanthus interruptus* (Cicadellidae) were used.

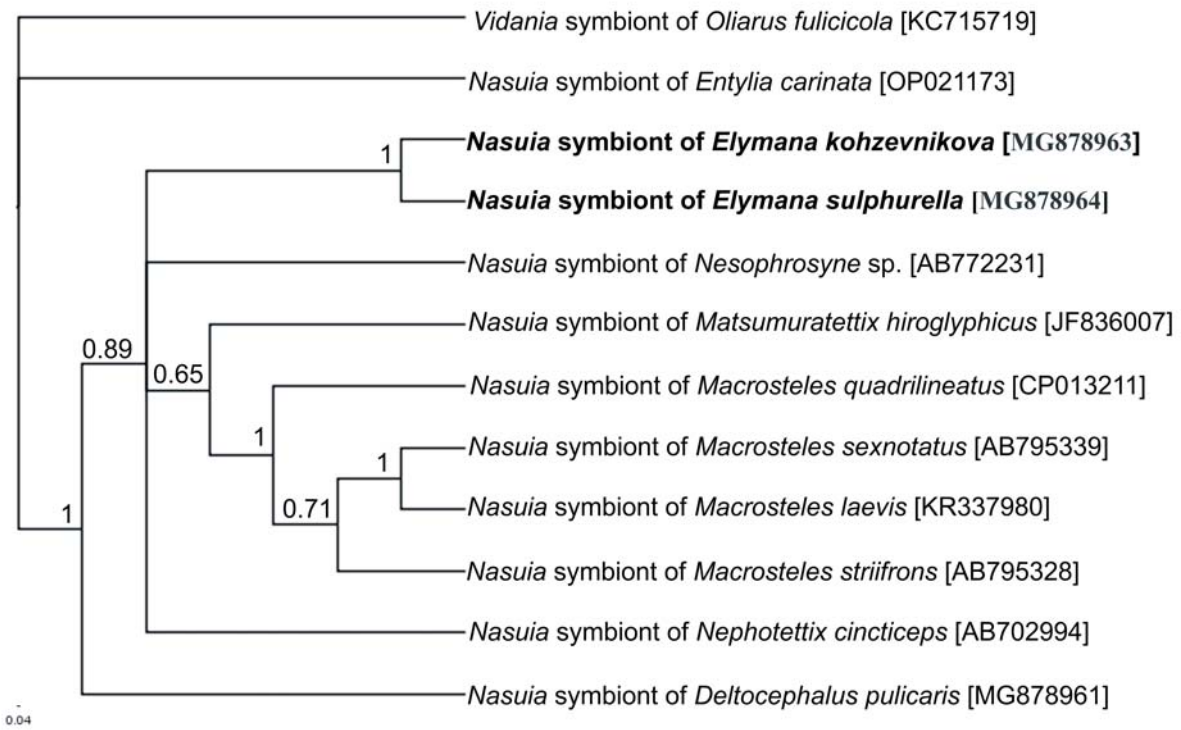

Fig. 2. Phylogenetic tree based on 16S rRNA sequences of *Nasuia* symbiont of the examined *Elymana kozhevnikovi and E. sulphurella* leafhoppers and other representatives of the subfamily Deltocephalinae, based on 16S RNA gene sequences. The numbers associated with the branches indicate Bayesian posterior probability values. The accession numbers of the sequences used in the phylogenetic analysis have been put in brackets. The *Vidania* symbiont of the planthopper *Oliarus fulicicola* was used as an outgroup.

Ultrastructure and distribution of symbiotic microorganisms

Histological observations revealed that paired bacteriomes occur in the females of *Elymana kozhevnikovi* and *E. sulphurella* (Fig. 3). Each bacteriome is composed of large bacteriocytes (Fig. 3). Two easily recognizable zones can be distinguished in the bacteriomes: a peripheral zone (Fig. 3) containing bacteriocytes with large, pleomorphic bacteria (Fig. 4) and a central zone (Fig. 3) with bacteriocytes containing large, lobated bacteria (Figs 7, 9) and large, elongated bacteria (Figs 7, 8, 8 insert, 9). Fluorescence *in situ* hybridization of the bacteriocyte-associated symbionts identified the pleomorphic microorganisms residing in peripheral bacteriocytes as *Sulcia* bacteria (Fig. 13), and the lobated microorganisms as *Nasuia* bacteria (Fig. 13). *Sulcia* stain more intensely with methylene blue (Figs 3, 8) and are more electron-dense under an electron transmission microscope (Figs 4, 5) compared to *Nasuia* (Figs 7, 9). In all the examined individuals of *E. kozhevnikovi* and *E. sulphurella*, in the cytoplasm and in the nuclei of some bacteriocytes with bacteria *Sulcia* (Fig. 5) and in some cells of the bacteriome sheath (Fig. 6) small, elongated, rod-shaped microorganisms occur. These microorganisms measure about 0.4 μm in diameter. FISH experiments using specific probes showed that *Sodalis*-like bacteria are present in bacteriocytes with *Sulcia* bacteria as well as in cells of the bacteriome sheath (Fig. 13 insert). In all the bacteriocytes with *Nasuia* large, elongated microorganisms also occur (Figs 7, 8, 8 insert, 9). The latter measure 1-1.2 μm in diameter. The use of the FISH technique identified these microorganisms as *Arsenophonus* bacteria (Fig. 14). It was observed that both in the younger females and in older (i.e. reproductive) females in some bacteriocytes *Arsenophonus* bacteria undergo degeneration (Figs 8, 10). In consequence, in these bacteriocytes numerous fagosomes and lamellar bodies appear (Fig. 10). Ultrastructural observations (Figs 11, 12) as well as FISH identification (Fig. 14 insert) revealed that both in *E. kozhevnikovi* and *E. sulphurella*, *Arsenophonus* bacteria are also present in fat body cells. Some *Arsenophonus* bacteria residing in fat body cells likewise undergo degeneration (Fig. 12).

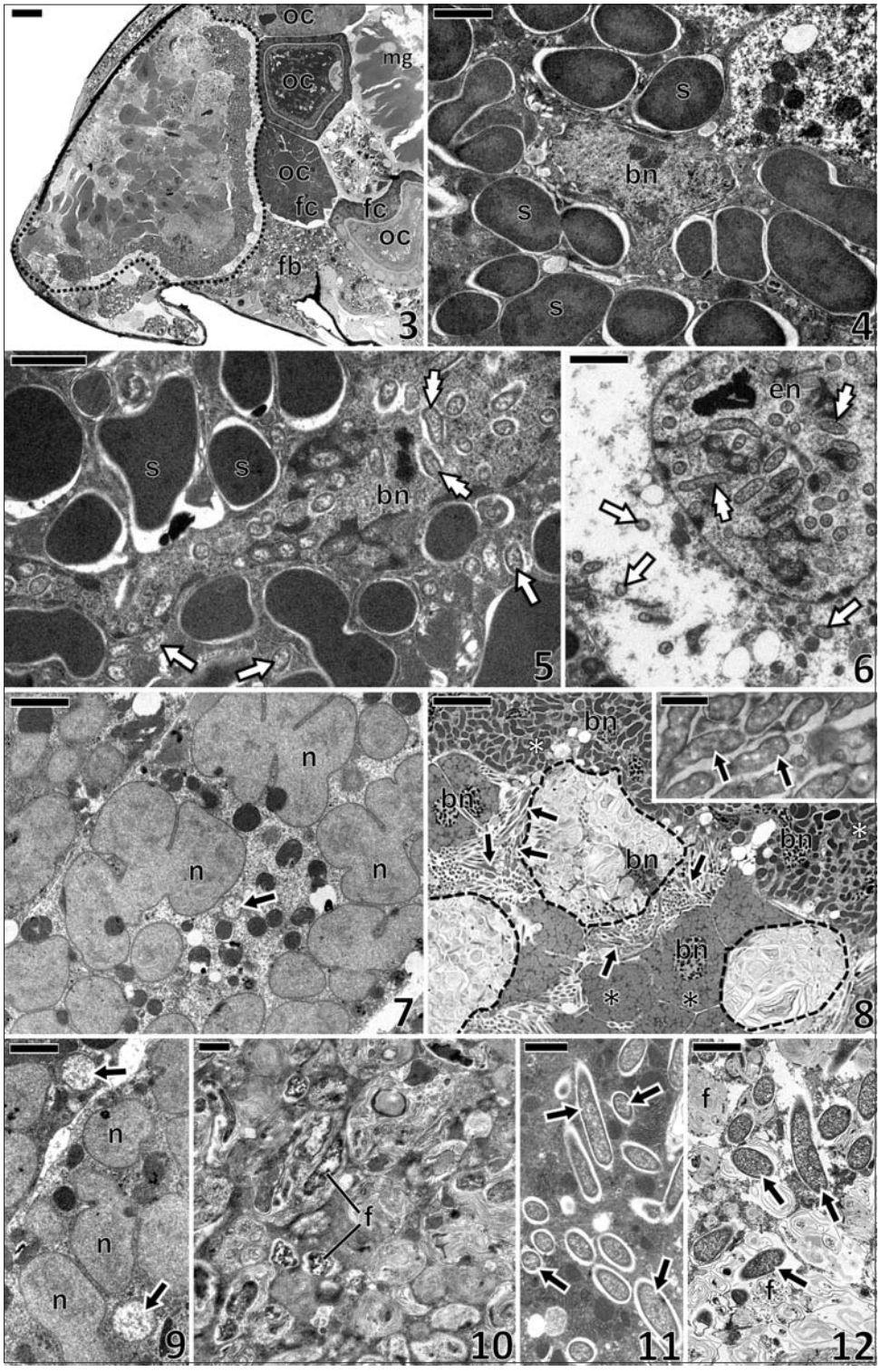

Figs 3-12. Distribution of symbiotic bacteria in the body of *Elymana kozhevnikovi* and *E. sulphurella*. Fig. 3. *E. sulphurella*. Cross section through the abdomen. Note the large bacteriome localized ventrolaterally (marked with a black, dotted line). Fig. 4. *E. sulphurella*. Bacteriocyte with bacteria *Sulcia* (s). Fig. 5. *E. kozhevnikovi*. Bacteriocyte with bacteria *Sulcia* (s). Note small, elongated, rod-shaped bacteria in the bacteriocyte cytoplasm (white arrows) and in the nucleus (white, double arrows). Fig. 6. *E. kozhevnikovi*. Cell of the bacteriome sheath surrounding the bacteriome. Note small, elongated, rod-shaped bacteria in the bacteriocyte cytoplasm (white arrows) and in the nucleus (white, double arrows). Fig. 7. *E. kozhevnikovi*. Bacteriocyte with bacteria *Nasuia* (n). Note single bacterium *Arsenophonus* (black arrow) accompanying bacteria *Nasuia*. Fig. 8. *E. kozhevnikovi*. Fragment of the bacteriome containing bacteriocytes with bacteria *Sulcia* (white asterisks) and bacteriocytes with *Nasuia* (black asterisks) and *Arsenophonus* (black arrows). Note degenerating *Arsenophonus* bacteria (marked with a black, dashed line). Fig. 8 insert. *E. sulphurella*. *Arsenophonus* bacteria (black arrows). Fig. 9. *E. kozhevnikovi*. Fragment of two bacteriocytes with *Nasuia* (n). Note single *Arsenophonus* bacteria (black arrows) among *Nasuia*. Fig. 10. *E. sulphurella*. Fragment of bacteriocyte with *Nasuia* and *Arsenophonus*. Note fagosomes containing degenerating *Arsenophonus* bacteria (f). Figs 11, 12. *E. kozhevnikovi*. Fragment of fat body lobes with *Arsenophonus* bacteria. Note *Arsenophonus* (black arrows) and fagosomes (f). Figs 3, 8. LM, methylene blue, scale bar = 25µm. Figs 4–7, 7 insert, 9–12. TEM, scale bar =2µm. bn – bacteriocyte nucleus; en – nucleus of the cell of the bacteriome sheath; fb – fat body; fc – follicular epithelium; mg – midgut; oc – oocyte.

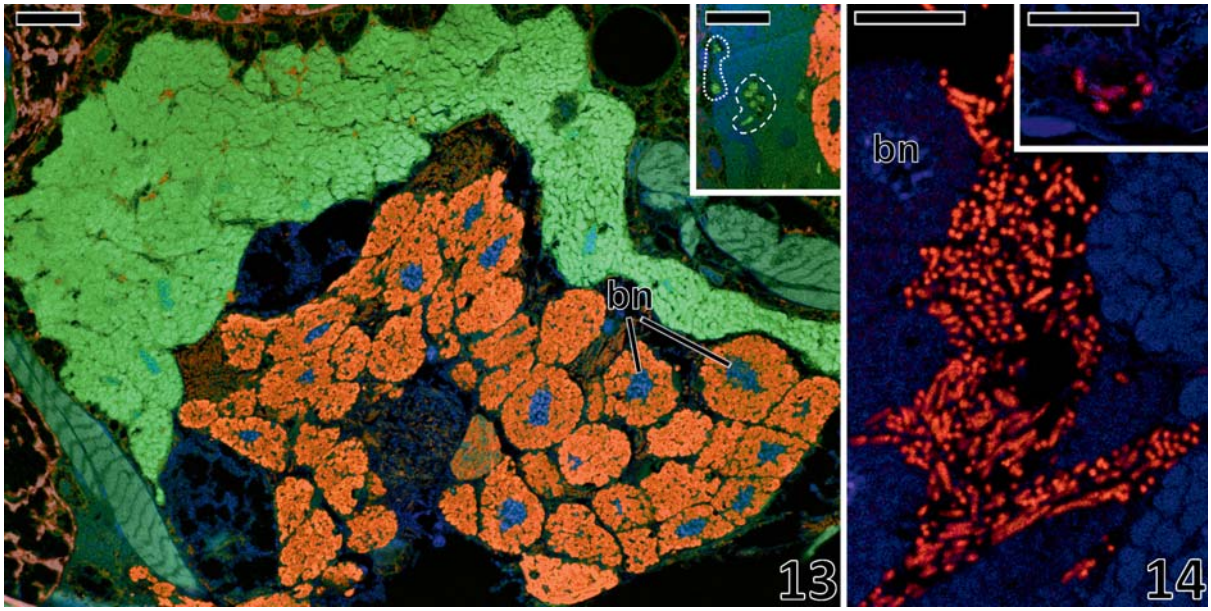

Figs 13-14. Fluorescence *in situ* identification of symbionts of *Elymana sulphurella*. Fig. 13. Bacteriocytes with *Sulcia* (shown in green) and *Nasuia* (shown in red) bacteria. Fig. 13 insert. *Sodalis*-like bacteria (shown in green) residing in bacteriocytes (marked with a white, dashed line) and in cells of the bacteriome sheath (marked with a white, dotted line). *Nasuia* is shown in red. Fig. 14. *Arsenophonus* bacteria residing in bacteriocytes (shown in red). Fig. 14 insert. *Arsenophonus* residing in fat body cells (shown in red). Confocal microscope, scale bar = 25μm. bn – bacteriocyte nucleus stained with DAPI.

Transovarial transmission of symbionts

In reproductive females the bacteria leave the bacteriomes and invade ovaries. Ovaries of leafhoppers consist of seven elongated tubes called ovarioles. In each ovariole several linearly arranged oocytes are present. The oocytes are surrounded with a single layer of follicular cells (for further details concerning the organization of insect ovaries and course of oogenesis, see BÜNING 1994; BILIŃSKI 1998). The bacteria are released from the bacteriocytes and begin to invade follicular cells surrounding the posterior pole of the terminal oocytes which are at the stage of late vitellogenesis (Fig. 15). *Sulcia*, *Nasuia, Arsenophonus* and *Sodalis*-like bacteria enter the cytoplasm of follicular cells (Figs 16, 17). After passing through the follicular epithelium, bacteria accumulate in the space between the former and the oocyte surface (termed the perivitelline space), finally forming a "symbiont ball" (Fig. 18). The bacteria residing inside the "symbiont ball" closely adhere to each other (Figs 19, 20).

Discussion

Our morphological and molecular analyses revealed that in two species of Deltocephalinae leafhoppers, *Elymana kozhevnikovi* and *E. sulphurella*, an unusual combination of four microorganisms, *Sulcia*, *Nasuia*, *Arsenophonus* and *Sodalis*-like bacteria, occurs. To our knowledge, the co-existence of both ancient symbionts (i.e. *Sulcia* and betaproteobacteria) and more recently acquired *Arsenophonus* and *Sodalis*-like bacteria has not been observed in any other auchenorrhynchous hemipteran. Moreover, even the co-residence of three bacterial associates such as *Sulcia*, *Nasuia* and novel *Arsenophonus/Sodalis*-like bacteria is a very rare phenomenon within these insects. Both ancestral symbionts co-residing with *Arsenophonus* bacteria have only been found in the Deltocephalinae leafhopper *Macrosteles laevis* (KOBIAŁKA *et al*. 2016), whereas these symbionts co-residing with *Sodalis*-like bacteria have only been observed in the spittlebug, *Aphrophora quadrinotata* (Cicadomorpha, Cercopoidea: Aphrophoridae) (KOGA *et al*. 2013) and in the planthopper *Ommatidiotus dissimilis* (MICHALIK *et al*. 2018a). According to KOGA and co-workers (2013), the three-symbiont association in *A. quadrinotata* may be a transitional situation in which the novel symbiont *Sodalis* did not yet eliminate the ancestral betaproteobacterial symbiont *Zinderia*. The similarity in the organization of the symbiotic systems in *A. quadrinotata* and Deltocephalinae leafhoppers *E. kozhevnikovi* and *E. sulphurella* indicates a similar evolutionary scenario occurring in these hemipterans.

The situation observed in *E. kozhevnikovi* and *E. sulphurella* is of special interest. To our knowledge, the co-existence of *Nasuia* and *Arsenophonus* bacteria in the same bacteriocytes has never been reported for auchenorrhynchous hemipter-

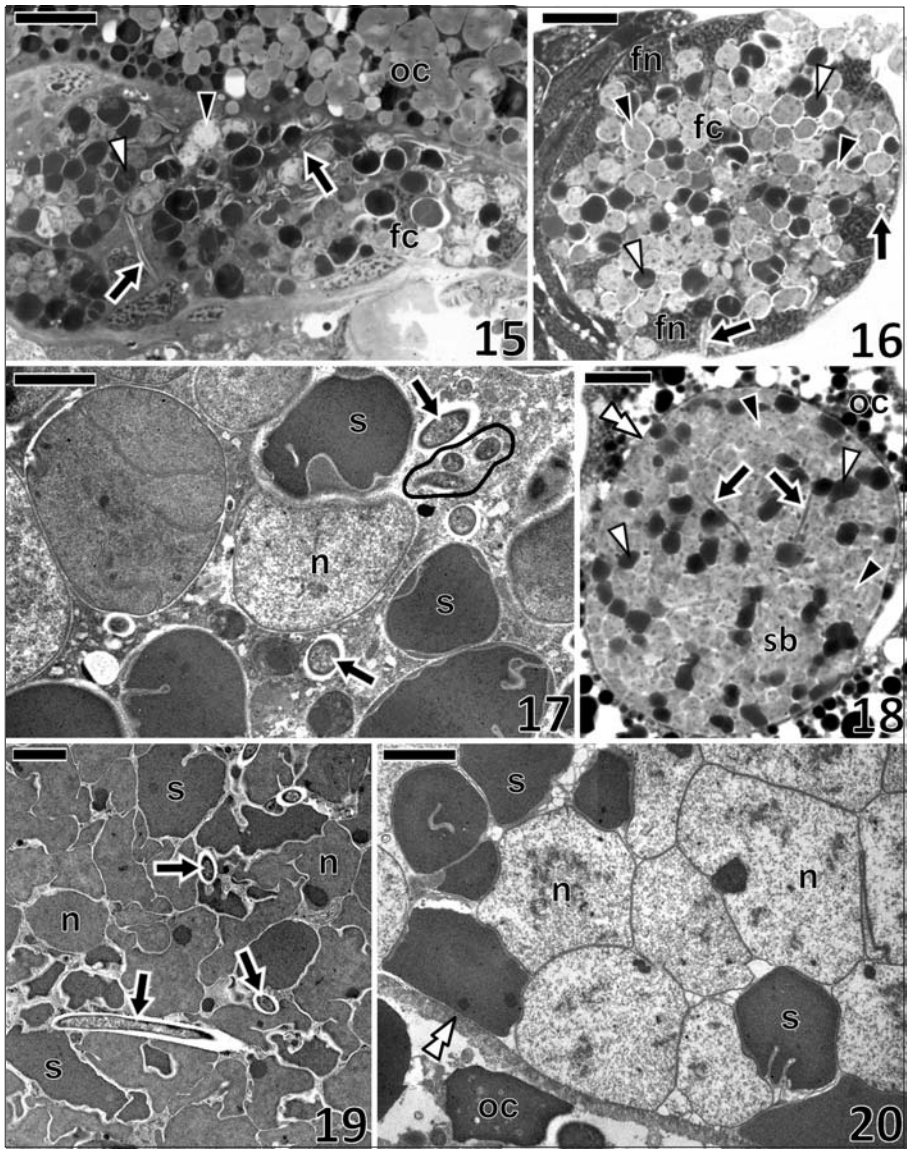

Figs 15-20. Consecutive stages of transovarial transmission of symbiotic bacteria in *Elymana kozhevnikovi* and *E. sulphurella*. Fig. 15. *E. kozhevnikovi. Sulcia* (white arrowheads), *Nasuia* (black arrowheads) and *Arsenophonus* bacteria (black arrows) invade follicular cells surrounding the terminal (longitudinal section). Fig.16. *E. sulphurella.* Posterior pole of the ovariole (cross section). Follicular cells are tightly packed with symbiotic *Sulcia* (white arrowheads), *Nasuia* (black arrowheads) and *Arsenophonus bacteria* (black arrows) bacteria. Fig. 17. *E. kozhevnikovi. Sulcia* (s), *Nasuia* (n), *Arsenophonus* bacteria (black arrows) and small, rod-shaped *Sodalis*-like bacteria (marked with a black, continuous line) migrate through the cytoplasm of the follicular cell. Figs 18-20. "Symbiont ball" containing *Sulcia* (white arrowheads in LM images, s in TEM images), *Nasuia* (black arrowheads in LM images, n in TEM images) and *Arsenophonus* (black arrows) bacteria in a deep invagination of the oolemma (white, double arrowheads) at the posterior pole of the oocyte. Figs 18, 20. *E. sulphurella.* Fig. 19. *E. kozhevnikovi*. Figs 15, 16, 18. LM, methylene blue, scale bar =25μm. Figs 17, 19, 20. TEM, scale bar = 2μm. fc – follicular cell; fn – follicular cell nucleus; oc – oocyte; sb – symbiont ball.

ans. Moreover, ultrastructural observations clearly indicate that in all the examined females of *E. kozhevnikovi* and *E. sulphurella*, both in bacteriocytes and in fat body cells, numerous *Arsenophonus* bacteria undergo degeneration (see Figs 8, 10, 12). Based on morphological observations, it is very difficult to comment on this phenomenon. Additionally, it cannot be excluded that some of the lamellar bodies in the bacteriocytes may represent remnants of *Nasuia* bacteria. It may be speculated that *Arsenophonus*, as a novel symbiont of *E. kozhevnikovi* and *E. sulphurella*, may be neutralized by the host insect. This, in turn, corresponds well with the above-mentioned hypothesis of the intermediate state between the *Sulcia* and *Nasuia* system and the *Sulcia* and *Arsenophonus* system. Thus, in both of these leafhoppers, the ancestral *Nasuia* still exists and functions, but newly acquired *Arsenophonus* bacteria have already begun the long process of elimination of this symbiont. It seems that the occurrence of *Arsenophonus* both in the specialized bacteriocytes and in the fat body cells confirms the intermediate state of symbiosis in *Elymana*. The verification of this hypothesis will be the subject of further work with the use of genomic analyses.

Our PCR analyses revealed that *Sodalis*-like bacteria occur within all of the examined individuals of *E. kozhevnikovi* and *E. sulphurella*. The combination of results of ultrastructural observations and FISH method indicates that the microorganisms present in bacteriocytes with *Sulcia* and in the cells of the bacteriome sheath represent *Sodalis*-like bacteria. However, based on these results, we are unable to determine whether these bacteria are present both in the cytoplasm and in the cell nuclei. Taking into account the fact that *E. kozhevnikovi* and *E. sulphurella* are host to *Rickettsia* and *Wolbachia* which may occur intracellularly (ARNEODO *et al*. 2008; SCHULZ & HORN 2015; KOBIAŁKA in preparation), it cannot be excluded that *Sodalis*-like bacteria are distributed in the cytoplasm, whereas *Rickettsia* or *Wolbachia* may reside inside the nucleus. To resolve this question, further detailed studies are required. The role of *Sodalis*-like bacteria in the biology of *E. kozhevnikovi* and *E. sulphurella* remains unclear. Several facts such as: (1) the occurrence of these bacteria in all the examined individuals detected by means of ultrastructural and molecular methods, (2) their transovarial transmission between generations and (3) lack of any symptoms of negative influence on host insects, suggest that *Sodalis*-like bacteria may be beneficial to their host insects. This, in turn, leads to the conclusion that these bacteria may represent the most recently acquired symbionts.

Both *Arsenophonus* and *Sodalis*-like bacteria are widely distributed within insects (reviewed in DURON *et al.* 2008; NOVÁKOVÁ *et al*. 2009; WILKES *et al*. 2011). The interactions between *Arsenophonus* and insects may be parasitic or symbiotic (reviewed in WILKES *et al*. 2011). The symbiotic *Arsenophonus* (or its close relatives) has been found in hematophagous insects, for which it provides B vitamins (reviewed in WILKES *et al*. 2011). Within plant sap-feeding hemipterans, *Arsenophonus* has been detected in Cixiidae planthoppers, aphids, psyllids, whiteflies, the Deltocephalinae leafhopper *Macrosteles laevis* and the scale insect *Greenisca brachypodii* (WILKES *et al*. 2011; HALL *et al*. 2016; KOBIAŁKA *et al*. 2016; MICHALIK *et al*. 2018b). *Sodalis*-like symbionts have been observed, e.g. in tsetse flies (DALE & MAUDLIN 1999), heteropterans (KAIWA *et al*. 2010), scale insects (GATEHOUSE *et al*. 2011; KOGA *et al*. 2013; GRUWELL *et al*. 2014; HUSNIK & MCCUTCHEON 2016; SZKLARZEWICZ *et al*. 2018), leafhoppers (MICHALIK *et al*. 2014), spittlebugs (KOGA *et al.* 2013; KOGA & MORAN 2014), aphids (BURKE *et al*. 2009; MANZANO-MARIN *et al*. 2017), psyllids (THAO *et al*. 2000; HALL *et al*. 2016), phtirapterans (FUKATSU *et al*. 2007; BOYD *et al*. 2016), and weevils (TOJU & FUKATSU 2011; TOJU *et al*. 2013). Such a wide distribution of *Arsenophonus* and *Sodalis*-like symbionts among different groups of insects indicates the expansive nature of these bacteria and their tendency to replace the ancient symbionts.

Using PCR diagnostics we detected that apart from *Sulcia*, *Nasuia*, *Arsenophonus* and *Sodalis*-like symbionts, *E. kozhevnikovi* and *E. sulphurella* may harbor *Wolbachia* and *Rickettsia* bacteria widely distributed among arthropods. It seems probable that both these bacterial associates are dispersed in different tissues of these insects. However, to determine the detailed distribution of *Wolbachia* and *Rickettsia*, their role in the biology of the host insects and mode of transmission between generations, further comprehensive molecular and ultrastructural analyses are needed.

Our results provide new data on the symbionts of plant sap-sucking hemipterans and corroborate the previous observations that Deltocephalinae leafhoppers, uniquely among other hemipteran groups, are characterized by a large diversity of symbiotic systems. Numerous species of Deltocephalinae leafhoppers (*Deltocephalus pulicaris*, *Athysanus argentarius, Euscelis incisus, Doratura stylata, Arthaldeus pascuellus, Errastunus ocellaris, Jassargus flori, Jassargus pseudocellaris, Psammotettix alienus, Psammotettix confinis, Turrutus socialis and Verdanus abdominalis, Macrosteles quadripunctatus*, *Macrosteles quadrilineatus*, *Macrosteles sexnotatus, Macrosteles striifrons, Matsumuratettix hiroglyphicus*, *Nephotettix cincticeps*) retained the ancient symbionts, i.e. *Sulcia* and *Nasuia* (WANGKEEREE *et al*. 2011; NODA *et al*. 2012; BENNETT & MORAN 2013; ISHII *et al.* 2013; KOBIAŁKA *et al.* 2015; BENNETT *et al.* 2016; KOBIAŁKA *et al*. in preparation). In *E. kozhevnikovi* and *E. sulphurella*, apart from ancient symbionts, novel symbionts – *Arsenophonus* and *Sodalis*-like bacteria are present (this study), whereas in *Macrosteles laevis* – the ancient symbionts are accompanied by *Arsenophonus* (KOBIAŁKA *et al.* 2016). It should be stressed that in *M. laevis*, the bacterium *Arsenophonus* does not occur individually, but is hidden inside cells of *Sulcia* bacteria. In *Cicadula quadrinotata*, *Fieberiella septentrionalis*, *Graphocraerus ventralis* and *Orientus ishidae*, the bacterium *Nasuia* has been lost and replaced by yeast-like symbionts (KOBIAŁKA *et al.* 2017), whereas in *Balclutha calamagrostis* and *Balclutha punctata* – by *Sodalis*-like bacteria (KOBIAŁKA *et al*. in preparation). In *Dalbulus maidis*, in turn, only *Sulcia* has been detected (BRENTASSI *et al.* 2017). These results indicate that ancient symbionts of Deltocephalinae leafhoppers undergo elimination and replacement by novel symbionts, such as *Arsenophonus*, *Sodalis* and yeast-like microorganisms.

Observations of the course of transmission of symbionts from the mother to offspring in different species of Deltocephalinae leafhoppers indicate that this process is uniform in this group of hemipterans (MÜLLER 1962; BUCHNER 1965; KOBIAŁKA *et al.*

2015, 2016, 2017; BRENTASSI *et al.* 2017). In all the hitherto examined Deltocephalinae leafhoppers, the symbiotic microorganisms (both the ancient symbionts and novel associates – bacteria or yeast-like symbionts) invade the posterior pole of the ovariole. The symbionts individually migrate through the cytoplasm of follicular cells surrounding the terminal oocytes and next they gather in the perivitelline space in the deep invagination of oolemma in the form of a "symbiont ball". The single exception is *M. laevis* in which the novel associate *Arsenophonus* does not infect the ovarioles individually, but is transported inside cells of *Sulcia*. Thus, this atypical behavior of *Arsenophonus* is probably connected with the young condition of association between this microorganism and *M. laevis*. Our ultrastructural observations have shown that in *E. kozhevnikovi* and *E. sulphurella, Arsenophonus* and *Sodalis*-like bacteria are individually transmitted to the ovariole. This, in turn, indicates that both species of *Elymana* have already developed a stable system of novel symbiont transmission.

Acknowledgments

We are greatly indebted to M.Sc. Ada JANKOWSKA for her skilled technical assistance and Dr. Dariusz ŚWIERCZEWSKI and Dr. Marcin WALCZAK for providing and identifying the insects. This work was carried out using a Jeol 2100 transmission electron microscope in the Laboratory of Microscopy, Department of Cell Biology and Imaging, Institute of Zoology and Biomedical Research, Jagiellonian University.

Funding

This work was supported by funds from the National Science Centre, Poland, research grant 2015/17/N/NZ8/01573.

Author contributions

Research concept and design: M.K., T.S.; Collection and/or assembly of data: M.K.; Data analysis and interpretation: M.K., A.M., T.S.; Writing the article: M.K., A.M., T.S.; Critical revision of the article: T.S.; Final approval of article: T.S.

Conflict of Interest

The authors declare no conflict of interest.

References

ARNEODO J.D., BRESSAN A., LHERMINIER J., MICHEL J., BOUDON-PADIEU E. 2008. Ultrastructural detection of an unusual intranuclear bacterium in *Pentastiridius leporinus* (Hemiptera: Cixiidae). J. Invertebr. Pathol. **97**: 310-313.

BAUMANN P. 2005 Biology of bacteriocyte-associated endosymbionts of plant sup-sucking insects. Annu. Rev. Microbiol. **59**: 155-189.

BENNETT G.M., MORAN N.A. 2013. Small, smaller, smallest: the origin and evolution of ancient dual symbioses in a phloem-feeding insect. Genome Biol. Evol. **5**: 1675-1688.

BENNETT G.M., ABBÀ S., KUBE M., MARZACHÌ C. 2016. Complete genome sequences of the obligate symbionts "*Candidatus* Sulcia muelleri" and "*Ca.* Nasuia deltocephalinicola" from the pestiferous leafhopper *Macrosteles quadripunctulatus* (Hemiptera: Cicadellidae). Genome Announc. **4**: e01604-1615.

BILIŃSKI S. 1998. Introductory remarks. Folia Histochem. Cytobiol. **3**: 143-145.

BOYD B.M., ALLEN J.M., KOGA R., FUKATSU T., SWEET A.D., JOHNSON K.P., REED D.L. 2016. Two bacterial genera, *Sodalis* and *Rickettsia*, associated with the seal louse *Proechinophthirus fluctus* (Phthiraptera: Anoplura). Appl. Environ. Microbiol. **82**: 3185-3197.

BRENTASSI M.E., FRANCO E., BALATTI P., MEDINA R., BERNABEI F., DE REMES LENICOV A.M.M. 2017. Bacteriomes of the corn leafhopper, *Dalbulus maidis* (DeLong & Wolcott, 1923) (Insecta, Hemiptera, Cicadellidae: Deltocephalinae) harbor *Sulcia* symbiont: molecular characterization, ultrastructure and transovarial transmission. Protoplasma **254**: 1421-1429.

BRESSAN A., ARNEODO J., SIMONATO M., HAINES W.P., BOUDON-PADIEU E. 2009. Characterization and evolution of two bacteriome-inhabiting symbionts in cixiid planthoppers (Hemiptera: Fulgoromorpha: Pentastirini). Environ. Microbiol. **11**: 3265-3279.

BUCHNER P. 1965. Endosymbiosis of Animals with Plant Microorganisms. Interscience, New York.

BÜNING J. 1994. The ovary of Ectognatha, the insects *s. str*. (In: The Insect Ovary: Ultrastructure, Previtellogenic Growth and Evolution. J. BÜNING ed. Chapman and Hall, London): 31-305.

BURKE G.R., NORMARK B.B., FAVRET C., MORAN N.A. 2009. Evolution and diversity of facultative symbionts from the aphid subfamily Lachninae. Appl. Environ. Microbiol. **75**: 5328-5335.

DALE C., MAUDLIN I. 1999. *Sodalis* gen. nov. and *Sodalis glossinidius* sp. nov., a microaerophilic secondary endosymbiont of the tsetse fly *Glossina morsitans morsitans*. Int. J. Syst. Bacteriol. **49**: 267-275.

DEMANÈCHE S., SANGUIN H., POTE J., NAVARRO E., BERNILLON D., MAVINGUI P., WILDI W., VOGEL T.M., SIMONET P. 2008. Antibiotic-resistant soil bacteria in transgenic plant fields. PNAS **105**: 3957-3962.

DOUGLAS A.E. 1998. Nutritional interactions in insect-microbial symbioses: aphids and their symbiotic bacteria *Buchnera*. Annu. Rev. Entomol. **43**: 17-37.

DURON O., BOUCHON D., BOUTIN S., BELLAMY S., ZHOU L., ENGELSTÄDTER J., HURST G.D. 2008. The diversity of reproductive parasites among arthropods: *Wolbachia* do not walk alone. BMC Biol. **6**: 27.

FUKATSU T., NIKOH N. 1998. Two intracellular symbiotic bacteria from the mulberry psyllid *Anomoneura mori* (Insecta, Homoptera). Appl. Environ. Microbiol. **64**: 3599-3606.

FUKATSU T., KOGA R., SMITH W.A., TANAKA K., NIKOH N., SASAKI-FUKATSU K., YOSHIZAWA K., DALE C., CLAYTON D.H. 2007. Bacterial endosymbiont of the slender pigeon louse, *Columbicola columbae*, allied to endosymbionts of grain

weevils and tsetse flies. *Appl. Environ. Microbiol.* **73**: 6660-6668.

GATEHOUSE L.N., SUTHERLAND P., FORGIE S.A., KAJI R., CHRISTELLER J.T. 2011. Molecular and histological characterization of primary (Betaproteobacteria) and secondary (Gammaproteobacteria) endosymbionts of three mealybug species. Appl. Environ. Microbiol. **78**: 1187-1197.

GOTTLIEB Y., GHANIM M., GUEGUEN G., KONTSEDALOV S., VAVRE F., FLEURY F., ZCHORI-FEIN E. 2008. Inherited intracellular ecosystem: symbiotic bacteria share bacteriocytes in whiteflies. FASEB J. **22**: 2591-2599.

GRUWELL M.E., DUDA Z., MACCREADY J. 2014. Investigation of endosymbiotic bacteria associated with scale insects of the family Putoidae (Hemiptera: Coccoidea). Acta Zool. Bulg. **6**: 29-34.

HALL T.A. 1999. BIOEDIT: an user-friendly biological sequence alignment editor and analysis program for Windows 95/98/NT. Nucleic Acids Symp. Ser. **41**: 95-98.

HALL A. A.G., MORROW J.L., FROMONT C., STEINBAUER M.J., TAYLOR G.S., JOHNSON S.N., COOK J.M., RIEGLER R. 2016. Codivergence of the primary bacterial endosymbiont of psyllids versus host switches and replacement of their secondary bacterial endosymbionts. Environ. Microbiol. **18**: 2591-2603.

HUELSENBECK J.P., RONQUIST F. 2001. MRBAYES: Bayesian inference of phylogenetic trees. Bioinformatics **17**: 754-755.

HUSNIK F., MCCUTCHEON J.P. 2016. Repeated replacement of an intrabacterial symbiont in the tripartite nested mealybug symbiosis. PNAS **113**: E5416-E5424.

ISHII Y., MATSUURA Y., KAKIZAWA S., NIKOH N., FUKATSU T. 2013. Diversity of bacterial endosymbionts associated with *Macrosteles* leafhoppers vectoring phytopathogenic phytoplasmas. Appl. Environ. Microbiol. **79**: 5013-5022.

KAIWA N., HOSOKAWA T., KIKUCHI Y., NIKOH N., MENG X.Y., KIMURA N., ITO M., FUKATSU T. 2010. Primary gut symbiont and secondary, *Sodalis*-allied symbiont of the scutellerid stinkbug *Cantao ocellatus*. Appl. Environ. Microbiol. **76**: 3486-3494.

KOBIAŁKA M., MICHALIK A., WALCZAK M., JUNKIERT Ł., SZKLARZEWICZ T. 2015. Symbiotic microorganisms of the leafhopper *Deltocephalus pulicaris* (Fallén, 1806) (Insecta, Hemiptera, Cicadellidae: Deltocephalinae): molecular characterization, ultrastructure and transovarial transmission. Pol. J. Entomol. **84**: 155-162.

KOBIAŁKA M., MICHALIK A., WALCZAK M., JUNKIERT Ł., SZKLARZEWICZ T. 2016. *Sulcia* symbiont of the leafhopper *Macrosteles laevis* (Ribaut, 1927) (Insecta, Hemiptera, Cicadellidae: Deltocephalinae) harbors *Arsenophonus* bacteria. *Protoplasma* **253**: 903-912.

KOBIAŁKA M., MICHALIK A., WALCZAK M., SZKLARZEWICZ T. 2017. Dual 'bacterial-fungal' symbiosis in Deltocephalinae leafhoppers (Insecta, Hemiptera, Cicadomorpha: Cicadellidae). Microb. Ecol. https://doi.org/10.1007/s00248-017-1075-y.

KOGA R., MORAN N.A. 2014. Swapping symbionts in spittlebugs: evolutionary replacement of a reduced genome symbiont. ISME J. **8**: 1237-1246.

KOGA R., BENNETT G.M., CRYAN J.R., MORAN N.A. 2013. Evolutionary replacement of symbionts in an ancient and diverse insect lineage. Environ. Microbiol. **15**: 2073-2081.

LAMELAS A., GOSALBES M. J., MOYA A., LATORRE A. 2011. New clues about the evolutionary history of metabolic losses in bacterial endosymbionts, provided by the genome of *Buchnera aphidicola* from the aphid *Cinara tujafilina.* Appl. Environ. Microbiol. **77**: 4446-4454.

LUAN J-B., CHEN W., HASEGAWA D.K., SIMMONS A.M., WINTERMANTEL W.M., LING K-S., FEI Z., LIU S-S., DOUGLAS A.E. 2015. Metabolic coevolution in the bacterial symbiosis of whiteflies and related plant sap-feeding insects. Genome Biol. Evol. **7**: 2635-2647.

ŁUKASIK P., M. VAN ASCH M., GUO H., FERRARI J. GODFRAY H.C. 2013. Unrelated facultative endosymbionts protect aphids against a fungal pathogen. Ecol. Lett **16**: 214-218.

ŁUKASIK P., NEWTON J.A., SANDERS J.G., HU Y., MOREAU C.S., KRONAUER D.J.C., O'DONNELL S., KOGA R., RUSSELL J.A. 2017. The structured diversity of specialized gut symbionts of the New World army ants. Mol. Ecol. **26**: 3808-3825.

MANZANO-MARIN A., SZABO G., SIMON J-C., HORN M., LATORRE A. 2017. Happens in the best of subfamilies: establishment and repeated replacements of co-obligate secondary endosymbionts within Lachninae aphids. Environ. Microbiol. **19**: 393-408.

MCCUTCHEON J.P., MCDONALD B.R., MORAN N.A. 2009. Convergent evolution of metabolic roles in bacterial co-symbionts of insects. PNAS **106**: 15394-15399.

MAO M., YANG X., POFF K., BENNETT G. 2017. Comparative genomics of the dual-obligate symbionts from the treehopper, *Entylia carinata* (Hemiptera: Membracidae), provide insight into the origins and evolution of an ancient symbiosis. Genome Biol. Evol. **9**: 1803-1815.

MICHALIK A., JANKOWSKA W., SZKLARZEWICZ T. 2009. Ultrastructure and transovarial transmission of endosymbiotic microorganisms in *Conomelus anceps* and *Metcalfa pruinosa* (Insecta, Hemiptera, Fulgoromorpha). Folia Biol. (Kraków) **57**: 131-137.

MICHALIK A., SZWEDO J., STROISKI A., WIERCZEWSKI D., SZKLARZEWICZ T. 2018a. Symbiotic cornucopia of the monophagous planthopper *Ommatidiotus dissimilis* (Fallén, 1806) (Hemiptera, Fulgoromorpha: Caliscelidae). Protoplasma, https://doi.org/10.1007/s00709-018-1234-0.

MICHALIK A., JANKOWSKA W., KOT M., GOŁAS A., SZKLARZEWICZ T. 2014. Symbiosis in the green leafhopper, *Cicadella viridis* (Hemiptera, Cicadellidae). Association *in statu nascendi*? Arthropod Struct. Dev. **43**: 579-587.

MICHALIK A., SZWEDO J., STROIŃSKI A., ŚWIERCZEWSKI D., SZKLARZEWICZ T. 2018a. Symbiotic cornucopia of the monophagous planthopper *Ommatidiotus dissimilis* (Fallén, 1806) (Hemiptera, Fulgoromorpha: Caliscelidae). Protoplasma, https://doi.org/10.1007/s00709-018-1234-0.

MICHALIK A., SCHULZ F., MICHALIK K., WASCHER F., HORN M., SZKLARZEWICZ T. 2018b. Coexistence of novel gammaproteobacterial and *Arsenophonus* symbionts in the scale insect *Greenisca brachypodii* (Hemiptera, Coccomorpha: Eriococcidae). Environ. Microbiol. https://doi.org/10.1111/1462-2920.14057.

MONTLLOR C.B., MAXMEN A., PURCELL A.H. 2002. Facultative bacterial endosymbionts benefit pea aphids *Acyrthosiphon pisum* under heat stress. Ecol. Entomol. **27**: 189-195.

MORAN N.A, DALE C., DUNBAR H., SMITH W.A., OCHMAN H. 2003. Intracellular symbionts of sharpshooters (Insecta, Hemiptera: Cicadellinae) form a distinct clade with a small genome. Environ. Microbiol. **5**: 116-126.

MORAN N.A., TRAN P., GERARDO N.M. 2005. Symbiosis and insect diversification: an ancient symbiont of sap-feeding insects from the phylum Bacteroidetes. Appl. Environ. Microbiol. **71**: 8802-8810.

MÜLLER H.J. 1962. Neuere Vorstellungen über Verbreitung und Phylogenie der Endosymbiosen der Zikaden. Z. Morphol. Ökol. Tiere **51**: 190-210.

NISHINO T., TANAHASHI M., LIN C.P., KOGA R., FUKATSU T. 2016. Fungal and bacterial endosymbionts of eared leafhoppers of the subfamily Ledrinae (Hemiptera: Cicadellidae). Appl. Entomol. Zool. **51**: 465-477.

NODA H. 1977. Histological and histochemical observation of intracellular yeast-like symbiotes in the fat body of the small brown planthopper, *Laodelphax striatellus* (Homoptera: Delphacidae). Appl. Entomol. Zool. **12**: 134-141.

NODA H., NAKASHIMA N., KOIZUMI M. 1995. Phylogenetic position of yeast-like symbiotes of rice planthoppers based

on partial 18S rDNA sequences. Insect Biochem. Mol. Biol. **25**: 639-646.

NODA H., WATANABE K., KAWAI S., YUKUHIRO F., MIYOSHI T., TOMIZAWA M., KOIZUMI Y., NIKOH N., FUKATSU T. 2012. Bacteriome-associated endosymbionts of the green rice leafhopper *Nephotettix cincticeps* (Hemiptera: Cicadellidae). Appl. Entomol. Zool. **47**: 217-225.

NOVÁKOVÁ E., HYPŠA V., MORAN N.A. 2009. *Arsenophonus*, an emerging clade of intracellular symbionts with a broad host distribution. BMC Microbiol. **9**: 143.

OLIVER K.M., RUSSELL J.A., MORAN N.A., HUNTER M.S. 2003. Facultative bacterial symbionts in aphids confer resistance to parasitic wasps. PNAS **100**: 1803-1807.

RAMBAUT A. 2009. FigTree v1. 4.0: Tree Figure Drawing Tool. Available: http://tree.bio.ed.ac.uk/software/figtree/. Accessed 2014 Jul 2

RAMBAUT A., DRUMMOND A.J. 2007. Tracer v1.4: MCMC trace analyses tool. Available: http://beast.bio.ed.ac.uk/Tracer.

SACCHI L., GENCHI M., CLEMENTI E., BIGLIARDI E., AVANZATTI A.M., PAJOROI M., NEGRI I., MARZORATI M., GONELLA E., ALMA A., DAFFONCHIO D., BANDI C. 2008. Multiple symbiosis in the leafhopper *Scaphoideus titanus* (Hemiptera: Cicadellidae): details of transovarial transmission of *Cardinium sp.* and yeast-like endosymbionts. Tissue Cell **40**: 231-242.

SCHULZ F., HORN M. 2015. Intranuclear bacteria: inside the cellular control center of eukaryotes. Trends Cell Biol. **25**: 339-346.

SLOAN D.B., MORAN N.A. 2012. Genome reduction and coevolution between the primary and secondary bacterial symbionts of psyllids. Mol. Biol. Evol. **29**: 3781-3792.

SZKLARZEWICZ T., GRZYWACZ B., SZWEDO J., MICHALIK A. 2016. Bacterial symbionts of the leafhopper *Evacanthus interruptus* (Linnaeus, 1758) (Insecta, Hemiptera, Cicadellidae: Evacanthinae). Protoplasma **253**: 379-391.

SZKLARZEWICZ T., KALANDYK-KOŁODZIEJCZYK M., MICHALIK K., JANKOWSKA W., MICHALIK A. 2018. Symbiotic microorganisms in *Puto superbus* (Leonardi, 1907) (Insecta, Hemiptera, Coccomorpha: Putoidae). Protoplasma **255:** 129-138.

TAKIYA D.M., TRAN P., DIETRICH C.H., MORAN N.A. 2006. Co-cladogenesis spanning three phyla: leafhoppers (Insecta: Hemiptera: Cicadellidae) and their dual bacterial symbionts. Mol. Ecol. **15**: 4175-4191.

THAO M.L., CLARK M.A., BAUMANN L., BRENNAN E.B., MORAN N.A., BAUMANN P. 2000. Secondary endosymbionts of psyllids have been acquired multiple times. Curr. Microbiol. **41**: 300-304.

THOMPSON J.D., GIBSON T.J., PLEWNIAK F., JEANMOUGIN F., HIGGINS D.G. 1997. The ClustalX windows interface: flexible strategies for multiple sequence alignment aided by quality analysis tools. Nucleic Acids Res. **25**: 4876-4882.

TOJU H., FUKATSU T. 2011. Diversity and infection prevalence of endosymbionts in natural populations of the chestnut weevil: relevance of local climate and hostplants. Mol. Ecol. **20**: 853e868.

TOJU H., TANABE A.S., NOTSU Y., SOTA T., FUKATSU T. 2013. Diversification of endosymbiosis: replacements, cospeciation and promiscuity of bacteriocyte symbionts in weevils. ISME J. **7**: 1378-1390.

URBAN J., CRYAN J. 2012. Two ancient bacterial endosymbionts have coevolved with the planthoppers (Insecta: Hemiptera: Fulgoroidea). BMC Evol. Biol. **12**: 87.

WANGKEEREE J., MILLER T.A., HANBOONSONG Y. 2011. Predominant bacteria symbionts in the leafhopper *Matsumuratettix hiroglyphicus* – the vector of sugarcane white leaf phytoplasma. Bull. Insectol. **64**: 215-216.

WILKES T.E., DURON O., DARBY A.C., HYPŠA V., NOVÁKOVÁ E., HURST G.D.D. 2011. The genus *Arsenophonus*. (In: Manipulative Tenants: Bacteria Associated with Arthropods. E. ZCHORI-FEIN, K. BOURTZIS eds. CRC Press, Danvers): 225-244.

ZHOU W., ROUSSET F., O'NEIL S. 1998. Phylogeny and PCR-based classification of *Wolbachia* strains using wsp gene sequences. Proc. Biol. Sci. **265**: 509-515.

e-ISSN 1734-9168
http://www.isez.pan.krakow.pl/en/folia-biologica.html

Folia Biologica (Kraków), vol. 66 (2018), No 1
https://doi.org/10.3409/fb_66-1.03

Molecular Cloning of *AZIN2* and its Expression Profiling in Goose Tissues and Follicles

Bo KANG, Ting DENG, Ziyu CHEN, Xinxing WANG, Zhixin YI, and Dongmei JIANG

Accepted March 14, 2018 *Published online May 18, 2018* *Issue online June 22, 2018*

Original article

KANG B., DENG T., CHEN Z.Y., WANG X.X., YI Z.X., JIANG D.M. 2018. Molecular cloning of *AZIN2* and its expression profiling in goose tissues and follicles. Folia Biologica (Kraków) **66**: 25-31.

Ornithine decarboxylase antizyme inhibitor 2 (AZIN2) plays key roles in regulating the biosynthesis and content of polyamines and other amines such as serotonin and histamine. The *AZIN2* coding sequence in the goose was cloned and analysed in this experiment. *AZIN2* expression levels in goose tissues and follicles were also measured. A full-length *AZIN2* coding sequence (GenBank accession no. MF939648) encoding a 457-amino acid protein was 1374 bp in length. The molecular weight of putative AZIN2 protein was 49.10 kDa. The mRNA expression of *AZIN2* was not observed in heart, adrenal gland, breast muscle, thigh muscle and pineal gland tissues in the goose. The highest and lowest expression levels of *AZIN2* in all examined tissues were observed in cerebrum and kidney tissues, respectively. The mRNA expression levels of *AZIN2* in the cerebrum, cerebellum and hypothalamus were 61.95-, 15.87- and 15.04-fold higher compared to the liver, respectively. The mRNA expression of *AZIN2* was observed in all examined follicles. The mRNA expression level of *AZIN2* was 6.48-fold higher in the F1 follicle compared to the SWF. Taken together, *AZIN2* mRNA has a restricted pattern of expression in the goose. AZIN2 may play important roles in modulating physiological functions of the brain and regulating follicular development and ovulation of goose ovaries.

Key words: Goose, ornithine decarboxylase, ornithine decarboxylase antizyme inhibitor 2, follicle.

Bo KANG, Ting DENG, Ziyu CHEN, Xinxing WANG, Zhixin YI, Dongmei JIANG✉, College of Animal Science and Technology, Sichuan Agricultural University, Chengdu 611130, China. E-mail: jiangdm@sicau.edu.cn

Polyamines regulate cell proliferation, differentiation, apoptosis, reproduction, and cancer (THOMAS & THOMAS 2001; LEFEVRE *et al*. 2011). Polyamine levels are precisely regulated through various processes including polyamine biosynthesis, catabolism and transport (PEGG 2009). An autoregulatory circuit consisting of ornithine decarboxylase (ODC), ornithine decarboxylase antizyme (OAZ) and ornithine decarboxylase antizyme inhibitor (AZIN) control the intracellular level of polyamines (HOSHINO *et al*. 2005; OLSEN & ZETTER 2011; QIU *et al*. 2017). OAZs inhibit the activity of ODC and target its degradation. AZIN binds to OAZ with a higher affinity than ODC and rescues ODC from the ODC-OAZ complex (LIU *et al*. 2011; QIU *et al*. 2017).

Up to date, the AZIN family was made up of AZIN1 and AZIN2 proteins (KAHANA 2009; MA *et al*. 2015). Both AZIN1 and AZIN2 bind to OAZ with the same affinity. AZINs are highly homologous to ODC but lack decarboxylase activity (MURAKAMI *et al*. 1996). Recently, several studies demonstrated that AZIN2 enhanced the stability and activity of ODC and polyamine influx through counteracting the inhibition of OAZ (LOPEZ- CONTRERAS *et al*. 2006; KANERVA *et al*. 2008).

AZIN2 has a significant role in maintaining polyamine homeostasis and regulating cell proliferation, similar to that found for AZIN1 (KEREN-PAZ *et al*. 2006; SILVA *et al*. 2015). High expression of AZIN2 is found in the testis and brain and differentiated resting cells (PITKANEN *et al*. 2001; MAKITIE *et al*. 2010; LOPEZ-GARCIA *et al*. 2013). The expression level of AZIN2 is positively correlated to the polyamine level in the brain of Alzheimer's patients (MAKITIE *et al*. 2010; INOUE *et al*. 2013). Recently, several studies have suggested that AZIN2 plays a role in regulating the biosynthesis of serotonin and histamine and may have a role in the endocrine function of adrenal glands and pancreas (KANERVA *et al*. 2009; LOPEZ-GARCIA *et al*. 2013; ACOSTA-ANDRADE *et al*. 2016). These reports suggest that AZIN2 has multiple biological functions. Our previous study cloned and characterized the *AZIN1* gene of the Sichuan white goose, and implied that AZIN1 played important roles in follicular development (MA *et al*. 2015). Thus far, the goose *AZIN2* gene and its expression profiles remain to be determined. To characterize the goose *AZIN2* gene, we cloned the *AZIN2* cDNA sequence and measured mRNA expression levels of *AZIN2* in different tissues and ovarian follicles.

Materials and Methods

Preparation of experimental animals and tissue collection

All experimental procedures were performed in accordance with the Institutional Review Board (IRB14044) and the Institutional Animal Care and Use Committee of the Sichuan Agricultural University under permit number DKY-B20140302. The heart, liver, spleen, lungs, kidneys, adrenal glands, breast muscles, thigh muscles, cerebrum, cerebellum, pineal gland, hypothalamus, pituitary gland, uterus, follicles and ovarian stroma in laying Sichuan white geese were collected and prepared on ice as described previously (MA *et al*. 2015).

Total RNA extraction and amplification of *AZIN2*

Total RNA from goose tissue samples was extracted with a Trizol reagent (Takara, Dalian) following the manufacturer's instructions. The reverse transcription of each RNA sample isolated from all examined tissues was completed using a PrimeScript® RT reagent Kit (Takara). Primers for amplifying the *AZIN2* coding sequence were as follows:
AZIN2-1: 5'-CACGAGTGCCGTCACACTTT-3', 5'-TATCACAGCAGCGATCTCCTC-3';
AZIN2-2: 5'-GCCAACAACCTCCACAGCCT-3', 5'-ACGACGCGGCGATGGTGTAT-3' and
AZIN2-3: 5'-AGAAGCCTTGCCCAGACCA-3', 5'-AAGAGGCCCGCACCGATCG-3'. The 50 μl reaction was composed of 2 μl of cDNA, 0.5 μl of each primer (10 μmol/l), 33.5 μl of sterile Milli-Q water, 8 μl of dNTP, 5 μl of LA PCR™ Buffer II and 0.5 μl of TaKaRa LA Taq HS (Takara Bio Inc.). The PCR was performed by the program: 95°C for 5 min, 60°C for 40 s, 72°C for 40 s, 35 cycles. *AZIN2* gene fragments were cloned and sequenced following standard procedures as described previously (KANG *et al*. 2014).

Bioinformatic analysis

The ORF Finder program (http://www.ncbi.nlm.nih.gov/gorf/gorf.html) was employed to analyse the coding sequence of goose *AZIN2*. Online NCBI Blast was used to align nucleotide and amino acid sequences of *AZIN2* homologs. The physiochemical properties and subcellular distribution were analysed using the Protamina (http://web.expasy.org/protparam/) and PSORT II (http://www.genscript.com/psort.html), respectively. The secondary structure of the putative AZIN2 protein was analysed by SOPMA (https://npsa-prabi.ibcp.fr/cgi-bin/npsa_automat.pl?page=/NPSA/npsa_sopma.html). Based on the neighbor-joining method with 1000 bootstrap replicates, a phylogenetic tree was also constructed by the MEGA program.

qRT-PCR

Expression levels of *AZIN2* were measured in an iCycler CFX96 using iTaqTM SYBR® Green Supermix (Bio-Rad, USA). Primers for amplifying *AZIN2* and *GAPDH* were as follows:
AZIN2-S: 5'-CGCTGCTGTGATAAACTCTG-3', 5'-CTTCCTTGGCGGTGATGC-3' and
GAPDH: 5'-GTGGTGCAAGAGGCATTGCTGAC-3', 5'-GCTGATGCTCCCATGTTCGTGAT-3'.
Briefly, the 20 μl reaction consisted of 1 μl of cDNA, 10 μl of Supermix, 0.4 μl of 10 μmol/l of each primer, and 8.2 μl of ddH_2O. PCR conditions for *AZIN2* was 95°C for 10 s, followed by 40 cycles of 95°C for 5 s, 62°C for 30 s and 72°C for 30 s, and then an 80 cycles melting curve was performed. The relative mRNA expression levels of *AZIN2* with three replicates for each sample were calculated relative to *GAPDH* using the $2^{-\Delta\Delta Ct}$ method.

Statistical analysis

Statistical analysis was performed by one-way analysis of variance using the SAS 9.2 statistical software for Windows (SAS Institute Inc., NC, USA) followed by Duncan's multiple range test. All values are presented as the mean ±SEM. A $P<0.05$ was considered to be statistically significant.

Results

Characteristics of goose *AZIN2*

Three partial fragments of the *AZIN2* gene were amplified and sequenced. The *AZIN2* cDNA assembled from the three fragments was 1398 bp in length including a 1374 bp coding sequence that encoded a 457-amino acid protein. The *AZIN2* nucleotide sequence was deposited in the GenBank (GenBank accession no. MF939648). The *AZIN2* cDNA sequence of the goose (*Anser cygnoides*) shared 88%, 69%, and 69% sequence identity with the *AZIN2* genes of *Gallus gallus* (NM_001293656.1), *Mus musculus* (NM_001301841.1), and *Homo sapiens* (NM_001293562.1), respectively. The putative AZIN2 amino acid sequence shared 86%, 59%, and 58% identity to *Gallus gallus* (NP_001280585.1), *Mus musculus* (NP_766463.1), and *Homo sapiens* (NP_001280491.1), respectively.

AZIN2 protein sequence analysis

The theoretical pI of the putative 49.10 kDa AZIN2 protein was 5.28 in the goose. Putative AZIN2 instability index was computed as 48.57. The grand average of hydropathicity was 0.026. AZIN2 secondary structure was predicted to consist of 39.82% alpha helix, 18.60% extended strand, 7.44% beta turn and 34.14% random coil. The predicted subcellular location of goose AZIN2 protein was 47.8% cytoplasmic, 26.1% nuclear, 17.4% mitochondrial, 4.3% cytoskeletal, and 4.3% plasma membrane. The putative goose AZIN2 protein contained a 238-amino acid pyridoxal-dependent decarboxylase (PDX) pyridoxal binding domain, a 123-amino acid PDX C-terminal sheet domain, a 19-amino acid Orn/DAP/Arg decarboxylases family 2 pyridoxal-P attachment site and an 18-amino acid Orn/DAP/Arg decarboxylase family 2 signature 2 (Fig. 1). Based on the putative AZIN2 amino acid sequence, a phylogenetic

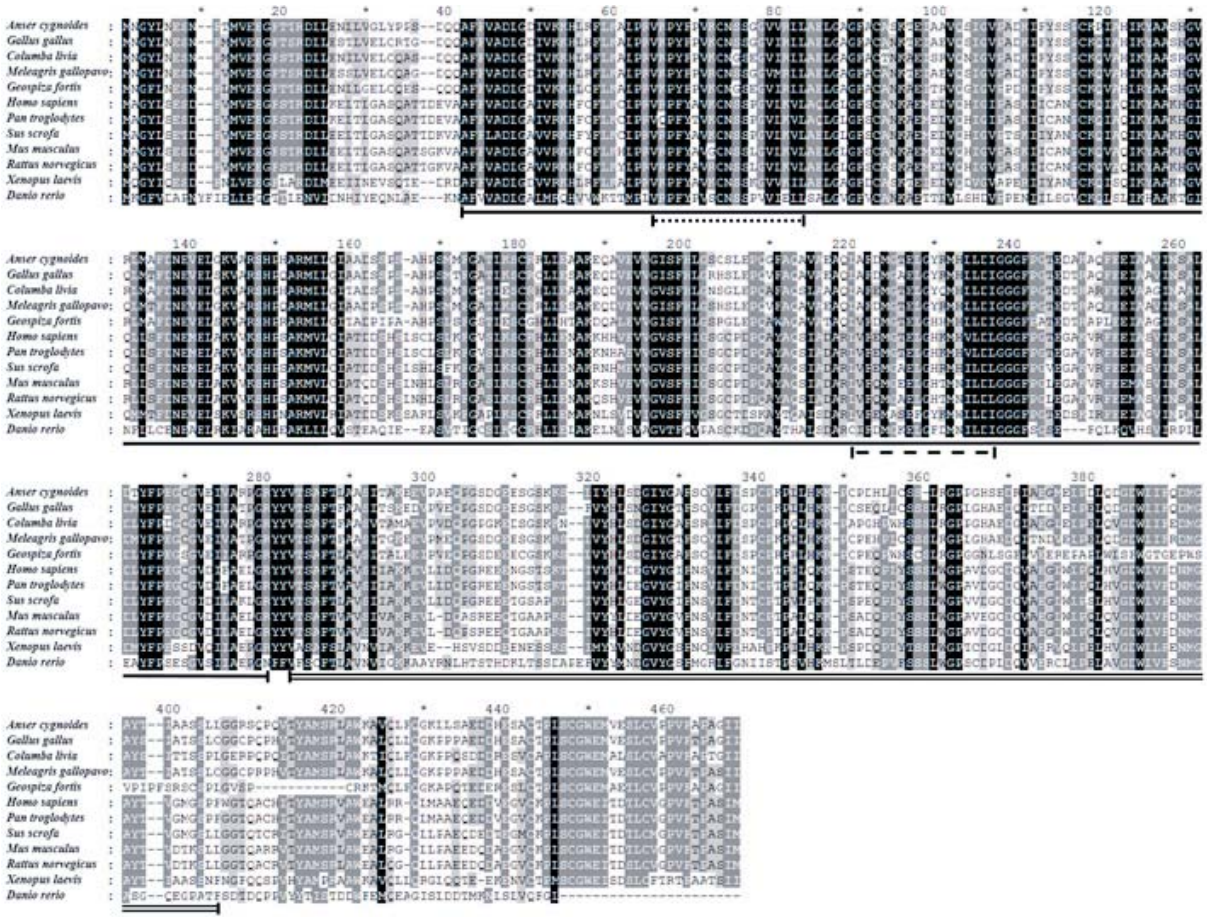

Fig. 1. Multiple alignments of putative AZIN2 amino acid sequences from goose and other species. The single line denotes a pyridoxal-dependent decarboxylase pyridoxal binding domain (position: A43-R280); the double lines denote a pyridoxal-dependent decarboxylase C-terminal sheet domain (position: V283-L405); the dotted line denotes an Orn/DAP/Arg decarboxylases family 2 pyridoxal-P attachment site (position: V65-L83); and the dashed line denotes an Orn/DAP/Arg decarboxylases family 2 signature 2 (position: I220-I237). Accession numbers for sequences used in the alignment: *Anser cygnoides*, *Gallus gallus* (NP_001280585.1), *Columba livia* (NP_001280682.1), *Meleagris gallopavo* (NP_001281204.2), *Geospiza fortis* (NP_001280680.1), *Homo sapiens* (NP_001280491.1), *Pan troglodytes* (XP_016814080.1), *Sus scrofa* (NP_001116665.1), *Mus musculus* (NP_766463.1), *Rattus norvegicus* (NP_001014283.2), *Xenopus laevis* (NP_001079692.1), *Danio rerio* (NP_001007160.2).

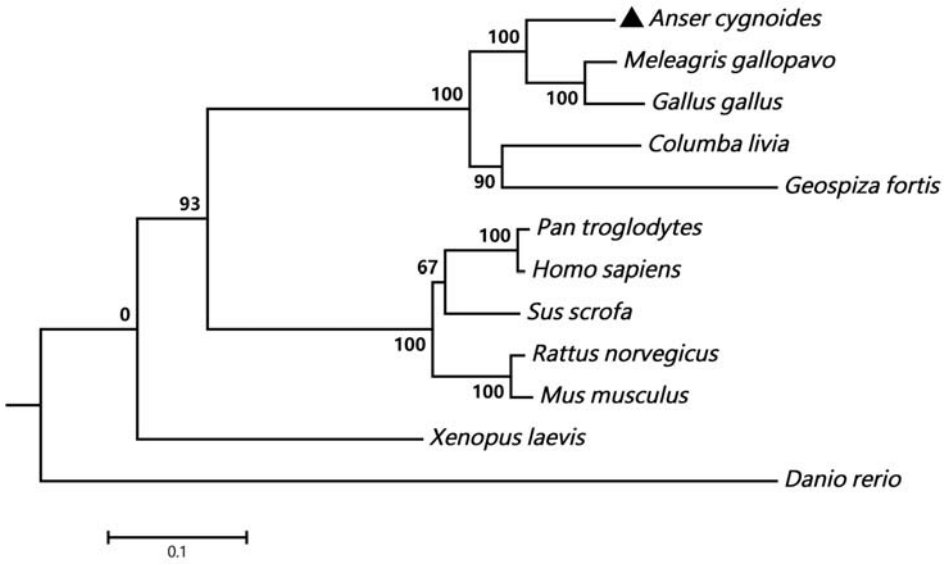

Fig. 2. Phylogenetic tree of AZIN2 amino acid sequences. The AZIN2 sequences shown were as follows: *Anser cygnoides*, *Gallus gallus* (NP_001280585.1), *Columba livia* (NP_001280682.1), *Meleagris gallopavo* (NP_001281204.2), *Geospiza fortis* (NP_001280680.1), *Homo sapiens* (NP_001280491.1), *Pan troglodytes* (XP_016814080.1), *Sus scrofa* (NP_001116665.1), *Mus musculus* (NP_766463.1), *Rattus norvegicus* (NP_001014283.2), *Xenopus laevis* (NP_001079692.1), *Danio rerio* (NP_001007160.2).

tree was constructed, and goose AZIN2 was most similar to that found in *Meleagris gallopavo* and *Gallus gallus* (Fig. 2).

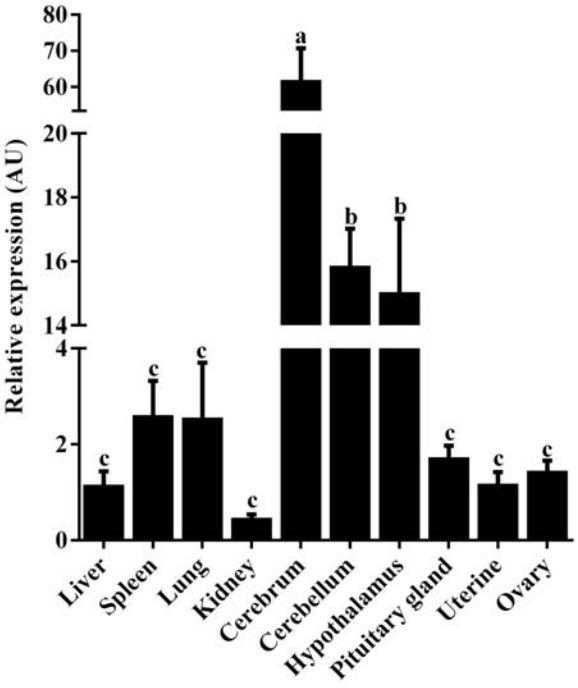

Fig. 3. Expression levels of the *AZIN2* gene in goose tissues. Expression levels of the *AZIN2* gene were normalized to *GAPDH*. Expression levels calculated by the $2^{-\Delta\Delta Ct}$ method were presented in arbitrary units (AU). Values are expressed as the mean ±SEM. Bars without a common letter are significantly different (P<0.05).

AZIN2 expression profiling in goose tissues

The mRNA expression of *AZIN2* was not observed in heart, adrenal gland, breast muscle, thigh muscle and pineal gland tissues in the goose using qRT-PCR. These results were also confirmed by semi-quantitative reverse transcription PCR (data not shown). The highest and lowest expression levels of *AZIN2* in all examined tissues were observed in cerebrum and kidney tissues, respectively (Fig. 3). The mRNA expression levels of *AZIN2* were significantly higher in cerebrum, cerebellum and hypothalamus tissues than in other examined tissues (P<0.05). *AZIN2* expression levels in the cerebrum, cerebellum and hypothalamus were 61.95-, 15.87- and 15.04-fold higher compared to the liver (P<0.05), respectively. We did not find significant differences in expression levels of *AZIN2* in the liver, spleen, lungs, kidneys, pituitary gland, uterus and ovary in the goose (P>0.05).

AZIN2 expression profiles in goose ovarian follicles

The mRNA expression of *AZIN2* was observed in all examined follicles (Fig. 4). During follicular development, significant difference in the mRNA expression levels of *AZIN2* was not observed among the SWF, SYF and F5-F2 follicles (P>0.05). The mRNA expression level of *AZIN2* in the F1 follicle was the highest in all examined follicles and was 6.48-fold higher compared to in the SWF (P<0.05). Significant difference in *AZIN2* expression levels were not detected among any POF follicles (P>0.05).

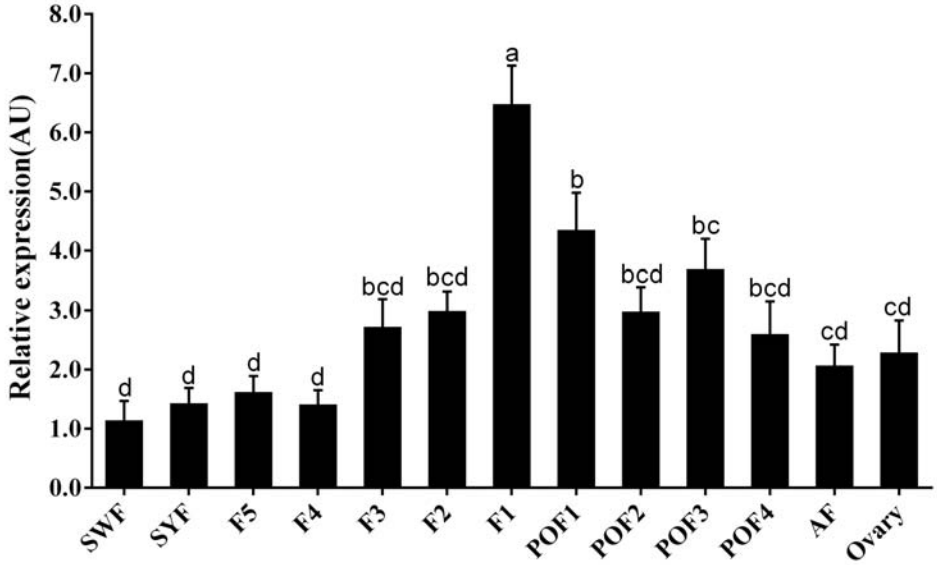

Fig. 4. Expression levels of the *AZIN2* gene in goose follicles and ovary. Expression levels of the *AZIN2* gene were normalized to *GAPDH*. Expression levels calculated by the $2^{-\Delta\Delta Ct}$ method were presented in arbitrary units (AU). Values are expressed as the mean ±SEM. Bars without a common letter are significantly different ($P<0.05$).

Discussion

The goose *AZIN2* coding sequence was cloned and characterized for the first time in this study. The putative AZIN2 protein in the goose had a molecular mass of 49.10 kDa, similar to that of mammal AZIN2 (50 kDa) and goose AZIN1 (50 kDa) (LOPEZ-CONTRERAS *et al.* 2010; MA et al. 2015). As in the case of AZIN1, goose AZIN2 was also a labile protein (PITKANEN *et al.* 2001; RAMOS-MOLINA *et al.* 2014; MA *et al.* 2015). Human AZIN2 retains 45% identity and 66% similarity to AZIN1 at the amino acid level (PITKANEN *et al.* 2001; OLSEN & ZETTER 2011). In this study, our data showed that the identity and the similarity between goose AZIN2 and AZIN1 were 41 and 64%, respectively. The theoretical pI of the putative AZIN1, AZIN2 and ODC protein of the goose was 4.79, 5.28 and 5.00, respectively (MA *et al.* 2015). In the goose, the putative ODC secondary structure consisted of 35.87% alpha helix, 23.7% extended strand, 8.91% beta turn and 31.52% random coil (our unpublished data). MA *et al.* (2015) reported that goose AZIN1 secondary structure was predicted to consist of 36.00% alpha helix, 16.89% extended strand and 47.11% random coil (MA *et al.* 2015). In this study, goose AZIN2 secondary structure consisted of 39.82% alpha helix, 18.60% extended strand, 7.44% beta turn and 34.14% random coil. In geese, the subcellular location of putative AZIN1, AZIN2 and ODC proteins was different. The subcellular distribution of the AZIN1 protein was predicted to be 73.9% in cytoplasmic, 8.7% in nuclear, 13.0% in mitochondrial and 4.3% in secretory vesicles in geese (MA *et al.* 2015). The predicted subcellular location of goose ODC protein was 65.2% cytoplasmic, 21.7% nuclear and 13.0% mitochondrial. Our data showed that the subcellular location of goose AZIN2 protein was 47.8% cytoplasmic, 26.1% nuclear, 17.4% mitochondrial, 4.3% cytoskeletal and 4.3% plasma membrane.

A previous study showed that goose *AZIN1* mRNA was expressed in all examined tissues (MA *et al.* 2015). In this study, the observed mRNA expression levels of *AZIN2* in the heart, adrenal glands, breast muscles, thigh muscles and pineal gland in geese were lower than the detection limits of qRT-PCR used. This suggests that *AZIN1* is ubiquitously expressed and *AZIN2* shows restricted expression in goose tissues. In mammals, studies have revealed that *AZIN2* was mainly expressed in testis and brain (LOPEZ-CONTRERAS *et al.* 2010), but not evenly expressed in all types of cells. *AZIN2* mRNA expression is mainly observed in the testicular germinal haploid cells (LOPEZ-CONTRERAS *et al.* 2009a), whereas in the murine brain *AZIN2* appears to be mainly localized in motor and sensory nucleus, hippocampus and some cerebellar areas (LOPEZ-CONTRERAS *et al.* 2010; RAMOS-MOLINA *et al.* 2012). These results suggest that *AZIN2* has a more restricted pattern of expression than *AZIN1* in both bird and mammalian tissues (LOPEZ-CONTRERAS *et al.* 2010). AZIN2 is exclusively expressed in adrenal medulla of adrenal glands that plays a role in the bio-

synthesis and secretion of catecholamines (LOPEZ-CONTRERAS *et al.* 2009b; LOPEZ-GARCIA *et al.* 2013). However, in present study, the mRNA expression of *AZIN2* was not found in adrenal glands in the goose. The mRNA expression of *AZIN2* in different cells of adrenal glands remains to be measured in birds. Studies have suggested that robust expression of *AZIN2* in the brain is distributed along neural axons and dendrites in a granular or vesicular pattern (MAKITIE *et al.* 2010; RASILA *et al.* 2016). High expression of AZIN2 was also found in human cerebellum (RASILA *et al.* 2016). In this study, high mRNA expression levels of *AZIN2* were observed in cerebrum, cerebellum and hypothalamus tissues in the goose. It is well known that AZIN2 is an inhibitor of OAZ. Thus, it is conceivable that AZIN2 is involved in regulating polyamine homeostasis in the brain. Changes in the expression and activity of different polyamine metabolic enzymes, as well as alternations in polyamine levels, have been associated to different brain insults such as cerebral ischemia and some mental disorders (LI *et al.* 2007; FIORI & TURECKI 2008; LOPEZ-CONTRERAS *et al.* 2010). Taken together, strong AZIN2 expression in the brain suggests that this protein may play important roles in modulating physiological functions of the brain in both mammals and birds, although the actions and mechanisms need to be clarified.

Polyamine synthesis, under endocrine influence, appears necessary for function and differentiation of the somatic cell component of the ovary (THYSSEN *et al.* 2002; FERNANDES *et al.* 2017; QIU *et al.* 2017). Treatment of immature female mice with DFMO (an irreversible inhibitor of ODC) inhibits ovarian growth, antral follicle formation, and the onset of puberty (BASTIDA *et al.* 2005; QIU *et al.* 2017). As commented before, AZIN can restore ODC activity by forming a tight complex with OAZ, thereby releasing ODC from the ODC-OAZ complex (QIU *et al*. 2017). Taking into consideration polyamines and ODC action as a regulator of ovarian function, it is possible that AZINs should play important roles in regulating follicular development. *AZIN1* mRNA expression gradually increased during follicular development and was significantly higher in POF1 follicle than other ovarian follicles. This suggests that AZIN1 plays a key role in follicular development (MA *et al.* 2015). In the present study, significant differences were not detected among the SWF, SYF and F5-F2 follicles, whereas the mRNA expression level of *AZIN2* was significantly higher in the F1 follicle than other follicles. Recent studies suggest that AZINs might be important molecules for modulating cell proliferation and oncogenesis through both the polyamine pathway and additional mediators (LOPEZ-CONTRERAS *et al.* 2010; LOPEZ-GARCIA *et al.* 2013; QIU *et al.* 2017). Taken together, high expression of *AZIN1* in the POF1 follicle and of *AZIN2* in the F1 follicle indicate that AZINs may play an important role in modulating follicular development and ovulation. The actions and molecular mechanisms responsible for these functions remain to be determined.

Funding

This work was financially supported by grant 31201798 from the National Natural Science Foundation of China and grant 20105103120003 from the Specialized Research Fund for the Doctoral Program of Higher Education.

Author Contributions

Research concept and design: B.K., D.M.J.; Collection and/or assembly of data: B.K., T.D., X.X.W.; Data analysis and interpretation: B.K., Z.Y.C., Z.X.Y., D.M.J.; Writing the article: B.K., D.M.J.; Critical revision of the article: B.K, T.D., Z.Y.C., X.X.W., Z.X.Y., D.M.J.; Final approval of article: D.M.J.

Conflict of Interest

The authors declare that they have no conflict of interest.

References

ACOSTA-ANDRADE C., LAMBERTOS A., URDIALES J.L., SANCHEZ-JIMENEZ F., PENAFIEL R., FAJARDO I. 2016. A novel role for antizyme inhibitor 2 as a regulator of serotonin and histamine biosynthesis and content in mouse mast cells. Amino Acids **48**: 2411-2421. http://doi.org/doi:10.1007/s00726-016-2230-3

BASTIDA C.M., CREMADES A., CASTELLS M.T., LOPEZ-CONTRERAS A.J., LOPEZ-GARCIA C., TEJADA F., PENAFIEL R. 2005. Influence of ovarian ornithine decarboxylase in folliculogenesis and luteinization. Endocrinology **146**: 666-674. http://doi.org/doi:10.1210/en.2004-1004

FERNANDES J.R., JAIN S., BANERJEE A. 2017. Expression of ODC1, SPD, SPM and AZIN1 in the hypothalamus, ovary and uterus during rat estrous cycle. Gen. Comp. Endocrinol. **246**: 9-22. http://doi.org/doi:10.1016/j.ygcen.2017.03.005

FIORI L.M., TURECKI G. 2008. Implication of the polyamine system in mental disorders. J. Psychiatry Neurosci. **33**: 102-110.

HOSHINO K., MOMIYAMA E., YOSHIDA K., NISHIMURA K., SAKAI S., TOIDA T., KASHIWAGI K., IGARASHI K. 2005. Polyamine transport by mammalian cells and mitochondria: role of antizyme and glycosaminoglycans. J. Biol. Chem. **280**: 42801-42808. http://doi.org/doi:10.1074/jbc.M505445200

INOUE K., TSUTSUI H., AKATSU H., HASHIZUME Y., MATSUKAWA N., YAMAMOTO T., TOYO'OKA T. 2013.

Metabolic profiling of Alzheimer's disease brains. Sci. Rep. **3**: 2364. http://doi.org/doi:10.1038/srep02364

KAHANA C. 2009. Regulation of cellular polyamine levels and cellular proliferation by antizyme and antizyme inhibitor. Essays Biochem. **46**: 47-61. http://doi.org/doi:10.1042/bse0460004

KANERVA K., MAKITIE L.T., PELANDER A., HEISKALA M., ANDERSSON L.C. 2008. Human ornithine decarboxylase paralogue (ODCp) is an antizyme inhibitor but not an arginine decarboxylase. Biochem. J. **409**: 187-192. http://doi.org/doi:10.1042/BJ20071004

KANERVA K., LAPPALAINEN J., MAKITIE L.T., VIROLAINEN S., KOVANEN P.T., ANDERSSON L.C. 2009. Expression of antizyme inhibitor 2 in mast cells and role of polyamines as selective regulators of serotonin secretion. PLoS One **4**: e6858. http://doi.org/doi:10.1371/journal.pone.0006858

KANG B., JIANG D.M., BAI L., HE H., MA R. 2014. Molecular characterisation and expression profiling of the ENO1 gene in the ovarian follicle of the Sichuan white goose. Mol. Biol. Rep. **41**: 1927-1935. http://doi.org/doi:10.1007/s11033-014-3039-3

KEREN-PAZ A., BERCOVICH Z., PORAT Z., EREZ O., BRENER O., KAHANA C. 2006. Overexpression of antizyme-inhibitor in NIH3T3 fibroblasts provides growth advantage through neutralization of antizyme functions. Oncogene **25**: 5163-5172. http://doi.org/doi:10.1038/sj.onc.1209521

LEFEVRE P.L., PALIN M.F., MURPHY B.D. 2011. Polyamines on the reproductive landscape. Endocr. Rev. **32**: 694-712. http://doi.org/doi:10.1210/er.2011-0012

LI J., DOYLE K.M., TATLISUMAK T. 2007. Polyamines in the brain: distribution, biological interactions, and their potential therapeutic role in brain ischaemia. Curr. Med. Chem. **14**: 1807-1813.

LIU Y.C., LIU Y.L., SU J.Y., LIU G.Y., HUNG H.C. 2011. Critical factors governing the difference in antizyme-binding affinities between human ornithine decarboxylase and antizyme inhibitor. PLoS One **6**: e19253. http://doi.org/doi:10.1371/journal.pone.0019253

LOPEZ-CONTRERAS A.J., LOPEZ-GARCIA C., JIMENEZ-CERVANTES C., CREMADES A., PENAFIEL R. 2006. Mouse ornithine decarboxylase-like gene encodes an antizyme inhibitor devoid of ornithine and arginine decarboxylating activity. J. Biol. Chem. **281**: 30896-30906. http://doi.org/doi:10.1074/jbc.M602840200

LOPEZ-CONTRERAS A.J., RAMOS-MOLINA B., MARTINEZ-DE-LA-TORRE M., PENAFIEL-VERDU C., PUELLES L., CREMADES A., PENAFIEL R. 2009a. Expression of antizyme inhibitor 2 in male haploid germinal cells suggests a role in spermiogenesis. Int. J. Biochem. Cell Biol. **41**: 1070-1078. http://doi.org/doi:10.1016/j.biocel.2008.09.029

LOPEZ-CONTRERAS A.J., SANCHEZ-LAORDEN B.L., RAMOS-MOLINA B., DE LA MORENA M.E., CREMADES A., PENAFIEL R. 2009b. Subcellular localization of antizyme inhibitor 2 in mammalian cells: Influence of intrinsic sequences and interaction with antizymes. J. Cell Biochem. **107**: 732-740. http://doi.org/doi:10.1002/jcb.22168

LOPEZ-CONTRERAS A.J., RAMOS-MOLINA B., CREMADES A., PENAFIEL R. 2010. Antizyme inhibitor 2: molecular, cellular and physiological aspects. Amino Acids **38**: 603-611. http://doi.org/doi:10.1007/s00726-009-0419-4

LOPEZ-GARCIA C., RAMOS-MOLINA B., LAMBERTOS A., LOPEZ-CONTRERAS A.J., CREMADES A., PENAFIEL R. 2013. Antizyme inhibitor 2 hypomorphic mice. New patterns of expression in pancreas and adrenal glands suggest a role in secretory processes. PLoS One **8**: e69188. http://doi.org/doi:10.1371/journal.pone.0069188

MA R., JIANG D., KANG B., BAI L., HE H., CHEN Z., YI Z. 2015. Molecular cloning and mRNA expression analysis of antizyme inhibitor 1 in the ovarian follicles of the Sichuan white goose. Gene **568**: 55-60. http://doi.org/doi:10.1016/j.gene.2015.05.014

MAKITIE L.T., KANERVA K., POLVIKOSKI T., PAETAU A., ANDERSSON L.C. 2010. Brain neurons express ornithine decarboxylase-activating antizyme inhibitor 2 with accumulation in Alzheimer's disease. Brain Pathol. **20**: 571-580. http://doi.org/doi:10.1111/j.1750-3639.2009.00334.x

MURAKAMI Y., ICHIBA T., MATSUFUJI S., HAYASHI S. 1996. Cloning of antizyme inhibitor, a highly homologous protein to ornithine decarboxylase. J. Biol. Chem. **271**: 3340-3342.

OLSEN R.R., ZETTER B.R. 2011. Evidence of a role for antizyme and antizyme inhibitor as regulators of human cancer. Mol. Cancer Res. **9**: 1285-1293. http://doi.org/doi:10.1158/1541-7786.MCR-11-0178

PEGG A.E. 2009. Mammalian polyamine metabolism and function. IUBMB Life **61**: 880-894. http://doi.org/doi:10.1002/iub.230

PITKANEN L.T., HEISKALA M., ANDERSSON L.C. 2001. Expression of a novel human ornithine decarboxylase-like protein in the central nervous system and testes. Biochem. Biophys. Res. Commun. **287**: 1051-1057. http://doi.org/doi:10.1006/bbrc.2001.5703

QIU S., LIU J., XING F. 2017. Antizyme inhibitor 1: a potential carcinogenic molecule. Cancer Sci. **108**: 163-169. http://doi.org/doi:10.1111/cas.13122

RAMOS-MOLINA B., LOPEZ-CONTRERAS A.J., CREMADES A., PENAFIEL R. 2012. Differential expression of ornithine decarboxylase antizyme inhibitors and antizymes in rodent tissues and human cell lines. Amino Acids **42**: 539-547. http://doi.org/doi:10.1007/s00726-011-1031-y

RAMOS-MOLINA B., LAMBERTOS A., LOPEZ-CONTRERAS A.J., KASPRZAK J.M., CZERWONIEC A., BUJNICKI J.M., CREMADES A., PENAFIEL R. 2014. Structural and degradative aspects of ornithine decarboxylase antizyme inhibitor 2. FEBS Open Bio **4**: 510-521. http://doi.org/doi:10.1016/j.fob.2014.05.004

RASILA T., LEHTONEN A., KANERVA K., MAKITIE L.T., HAGLUND C., ANDERSSON L.C. 2016. Expression of ODC Antizyme Inhibitor 2 (AZIN2) in Human Secretory Cells and Tissues. PLoS One **11**: e0151175. http://doi.org/doi:10.1371/journal.pone.0151175

SILVA T.M., CIRENAJWIS H., WALLACE H.M., OREDSSON S., PERSSON L. 2015. A role for antizyme inhibitor in cell proliferation. Amino Acids **47**: 1341-1352. http://doi.org/doi:10.1007/s00726-015-1957-6

THOMAS T., THOMAS T.J. 2001. Polyamines in cell growth and cell death: molecular mechanisms and therapeutic applications. Cell. Mol. Life Sci. **58**: 244-258. http://doi.org/doi:10.1007/PL00000852

THYSSEN S.M., HOCKL P.F., CHAMSON A., LUX-LANTOS V.A., LIBERTUN C. 2002. Effects of polyamines on the release of gonadotropin-releasing hormone and gonadotropins in developing female rats. Exp. Biol. Med. (Maywood) **227**: 276-281.

e-ISSN 1734-9168
http://www.isez.pan.krakow.pl/en/folia-biologica.html

Folia Biologica (Kraków), vol. 66 (2018), No 1
https://doi.org/10.3409/fb_66-1.04

Biochemical Profile, Liver and Kidney Selenium (Se) Status during Acanthamoebiasis in a Mouse Model

Natalia ŁANOCHA-ARENDARCZYK, Irena BARANOWSKA-BOSIACKA, Karolina KOT, Bogumiła PILARCZYK, Agnieszka TOMZA-MARCINIAK, Joanna KABAT-KOPERSKA, and Danuta KOSIK-BOGACKA✉

Accepted: April 24, 2018 *Published online May 18, 2018* *Issue online June 22, 2018*

Original article

ŁANOCHA-ARENDARCZYK N., BARANOWSKA-BOSIACKA I., KOT K., PILARCZYK B., TOMZA-MARCINIAK A., KABAT-KOPERSKA J., KOSIK-BOGACKA D. 2018. Biochemical profile, liver and kidney selenium (Se) status during acanthamoebiasis in a mouse model. Folia Biologica (Kraków) **66**: 33-40.

The aim of the present study was to determine biochemical parameters and Se concentrations in the main detoxication organs in immunocompetent and immunosuppressed mice infected by *Acanthamoeba* sp. at the early stage of infection. The mice were divided into 4 groups: immunocompetent non-infected control (C), immunocompetent infected (A), immunosuppressed infected (AS), and immunosuppressed non-infected (CS) mice. Biochemical parameters in serum were determined using an automated clinical chemistry analyzer, ARCHITECT C8000, while selenium concentration in the liver and kidney were determined by spectrofluorimetry. We observed a significant downregulation in chlorine plasma level in the blood of A vs CS groups. We found a significantly higher serum AST level in the A group than in group C. The *Acanthamoeba* sp. infection did not influence liver Se in immunocompetent mice but significantly increased liver Se levels in mice with compromised immunity. Kidney Se concentration was significantly higher in group AS compared to A. We observed a novel strong relation between Se hepatic concentration and liver enzymes in the AS group (aspartate aminotransferase, AST and alanine aminotransferase, ALT). Moreover, Se liver concentration correlated with plasma AST in group A. Immunological status affected Se levels in the liver and kidney of mice infected by *Acanthamoeba* sp. This parasite influenced the activity of serum AST regardless of the host's immunological status. Furthermore, elevated concentrations of hepatic Se were associated with increased levels of plasma ALT and AST.

Key words: Biochemical parameters, selenium, liver, kidney, *Acanthamoeba* sp., immunological status.

Natalia ŁANOCHA-ARENDARCZYK, Karolina KOT, Danuta KOSIK-BOGACKA✉, Department of Biology and Medical Parasitology, Pomeranian Medical University, Powstancow Wielkopolskich 72-111 Szczecin, Poland.
kodan@pum.edu.pl
Irena BARANOWSKA-BOSIACKA, Department of Biochemistry and Medical Chemistry, Pomeranian Medical University, Powstancow Wielkopolskich 72-111 Szczecin, Poland.
Bogumiła PILARCZYK, Agnieszka TOMZA-MARCINIAK, Department of Animal Reproduction Biotechnology and Environmental Hygiene, West Pomeranian University of Technology, Doktora Judyma 6, 71-466, Szczecin, Poland.
Joanna KABAT-KOPERSKA, Department of Nephrology, Transplantology and Internal Medicine, Pomeranian Medical University, Powstancow Wielkopolskich 72-111 Szczecin, Poland.

Acanthamoeba sp. are opportunistic protozoan organisms which most often cause lethal brain invasion resulting in granulomatous amebic encephalitis (GAE) (VISVESVARA *et al* 2007; TRABELSI *et al.* 2012). Their biotope may also be the cornea, with contact lens-wearing being a major risk factor of *Acanthamoeba* keratitis (CARNT & STAPLETON 2016). Moreover, there are also reports of cutaneous acanthamoebiasis, *Acanthamoeba* rhinosinusitis, osteo-cutaneous and lung invasions

(SHARMA *et al.* 2017; TEKNOS *et al.* 2000; WINSETT *et al.* 2017). Acanthamoebiasis is most often found in patients with immune deficiency, and invasions are facilitated by the intake of immunosuppressive drugs (SALAMEH *et al.* 2015; BRONDFIELD *et al.* 2017). Most publications focusing on brain acanthamoebiasis are associated with organ transplantation, including the liver and kidney. *Acanthamoeba* sp. may affect the normal functioning of the liver and kidney, but little is known about the pathomechanism of infection and relations in the parasite-host system in acanthamoebiasis. Trace elements including selenium (Se) modulate immune functions, influencing the susceptibility of the host to infection (RIVERA *et al.* 2002). Selenium is an essential trace element and an antioxidant at the cellular level, reducing free radical damage and oxidative stress (JELICKS *et al.* 2011). Moreover, Se is a cofactor for glutathione peroxidase (GPx), selenoprotein P, and thioredoxin reductase, playing a significant role in maintaining redox homeostasis and sufficient activity of immunocompetent cells, and in the release of inflammatory mediators (TINGGI 2008). This element has a diverse effect on the immune system, being immunosuppressive at high doses, and immunostimulatory at low doses. Selenium and selenoproteins are not only responsible for initiating and/or enhancing immunity, but also take part in immunoregulation which is crucial for preventing excessive responses leading to autoimmunity or chronic inflammation (STEINBRENNER *et al.* 2015).

Selenium's role in parasitic protozoan invasions has been observed in experimentally induced infections with *Trypanosoma* sp., *Cryptosporidium* sp., *Toxoplasma gondii* and *Plasmodium* sp. (HUANG & YANG 2002; IRIBHOGBE *et al.* 2013; DA SILVA *et al.* 2014). Selenium supplementation decreases the parasitemia of *Trypanosoma* sp. infections and reduces important parameters associated with diseases such as anemia and parasite-induced organ damage (DA SILVA *et al.* 2014). Moreover, Se has potential antimalarial activity and may be of benefit in malaria therapeutics (IRIBHOGBE *et al.* 2013). Se supplementation or depletion may be beneficial depending on the particular infectious agent and state of the host (JELICKS *et al.* 2011). Selenium status may vary in an acute phase response to stress or infection (MAEHIRA *et al.* 2002). Parasitic diseases are sometimes accompanied by elevated and/or reduced Se concentrations in the liver and kidney, and may alter the regulation of trace mineral metabolism and homeostasis (PILARCZYK *et al.* 2008). The liver is the central organ for Se regulation, producing Se forms to regulate whole-body Se (DUNTAS & HUBALEWSKA-DYDEJCZYK 2015). VÄLIMÄKI *et al.* (1987) observed that Se concentrations were lower in blood and liver tissue in patients with liver disorders (cirrhosis and hepatitis). PILARCZYK *et al.* (2008) did not report any effect of *Toxocara canis* on the levels of Se in the liver and kidney of infected mice. Importantly, parasite pathological changes in the host may also lead to alterations in the biochemical parameters of serum including liver enzymes, protein, albumin, lipid levels and renal function biomarkers such as urea, creatinine and several trace elements (DAGNACHEW *et al.* 2015; MOREIRA *et al.* 2016). The effect of *Acanthamoeba* sp. infection on the biochemical profile may be of paramount importance on the pathophysiological outcome, similar to other protozoan infections (DAGNACHEW *et al.* 2015). There is no information of how *Acanthamoeba* sp. alters Se concentrations in the liver and kidney, nor serum biochemical parameters in experimentally infected hosts, taking into account host immunological status. Therefore, in the present preliminary study, the main goal was to determine biochemical parameters and Se concentrations in the main detoxication organs in immunocompetent and immunosuppressed mice infected by *Acanthamoeba* sp. at the early stage of infection.

Material and Methods

This study was approved by the Local Ethical Committee for Experiments on Animals in Szczecin (No. 29/2015, dated 22 June 2015) and in Poznań (No. 64/2016 dated 9 September 2016).

Acanthamoeba sp. strain

We used *Acanthamoeba* AM 22 strain from a previous study (LANOCHA *et al*. 2009). Protozoan amoebae were isolated from the bronchoaspirate of a 53-year-old man with low immunity levels. The amoebae were grown on agar plates (NN Agar) covered with a suspension of deactivated (at 70°C for 1 h) *Escherichia coli* and incubated at 37°C for 72 h according to standard parasitological methods.

Experimental animals

Experimental acanthamoebiasis in a mouse model were performed as previously described by ŁANOCHA-ARENDARCZYK *et al*. (2018). Briefly, the study was conducted on 32 male Balb/c mice (6-weeks old) obtained from a licensed breeder – the Centre of Experimental Medicine, Medical University in Białystok, Poland. The infected (A and AS) and control (C and CS) animals were housed in groups of 5 and 6 mice per cage, respectively. The mice were kept in controlled conventional conditions (temperature 22±1°C, relative humidity approximately 50% and 12/12 h light-dark cycle) in the Animal Facility of the Pomeranian Medical University in Szczecin. The animals were fed Labofeed H (Morawski, Kcynia, PL0410004p,

Poland) and water *ad libitum* from a stoppered-bottle with a nose-activated nozzle.

The experimental procedures were carried out in strict accordance with good animal practice with the recommendations in the Guide for the Care and Use of Laboratory Animals (https://grants.nih.gov/grants/olaw/ guide-for-the-care-and-use-of-laboratory-animals.pdf). Balb/c mice were immunosuppressed by administering 0.22 mg (10 mg/kg) of methylprednisolone as methylprednisolone sodium succinate (MPS, Solu-Medrol, Pfizer, Europe MA EEIG) in 0.1 ml of 0.9% saline intraperitoneally (i.p.) for 5 days (-4, -3, -2, -1, 0 days) before amoeba inoculation. The dose of MPS was based on data from MARKOWITZ *et al*. (1978). This procedure allowed for the development of an experimental model similar to that of immunosuppressed patients. MPS is administered, among others, to patients treated for acute rejection episodes (ŁANOCHA-ARENDARCZYK *et al.* 2018).

The mice (n=32) were divided into 4 groups:

– immunocompetent non-infected mice (C, n=6)

– immunocompetent mice infected with *Acanthamoeba* sp. (A, n=10)

– immunosuppressed mice infected with *Acanthamoeb*a sp. (AS, n=10)

– immunosuppressed uninfected mice (CS, n=6)

In studies on the influence of parasites on the host, groups of 6-10 individuals form an experimental standard allowing for reliable statistical analysis. The animals (groups A and AS) were inoculated intra-nasally with 3 µl of suspension containing 10-20 thousand amoebae. Control mice (groups C and CS) were given the same volume of sterile physiological solution (3 µl of 0.9% NaCl solution). The mice in all groups were anesthetized by an overdose of pentobarbital sodium (200 mg/kg b.wt. i.p.). The mice were sacrificed at 8 days post *Acanthamoeba* sp. infection (at the early stage of infection). During necropsy the livers and kidneys were collected for Se concentration analysis.

Blood sample collection for biochemical analysis

Whole blood from the hearts of the mice was sampled by the 1.2 ml blood collection system S *Monovette* SERUM. We determined the concentrations of sodium (Na), potassium (K), chlorine (Cl), total protein (TP), C-reactive protein (CRP), albumin, creatinine (CR), urea, aspartate aminotransferase (AST), alanine aminotransferase (ALT), total cholesterol (TC), triglyceride (TG), high-density lipoprotein (HDL) and low-density lipoprotein cholesterol (LDL). A suite of biochemical analyses for the parameters was carried out using an automated clinical chemistry analyzer, ARCHITECT C8000 (Abbott, USA).

Selenium concentrations in liver and kidney

Selenium concentration was determined by spectrofluorimetry with a SHIMADZU RF-5001 PC analyzer. Livers and kidneys were wet digested in concentrated HNO_3 (230°C/180 min) and $HClO_4$ (310°C/ 20 min). 9% HCl was added to the digested samples to reduce selenate VI to selenate IV. Subsequently, selenate IV was complexed with 2,3-diaminonaftalene (Sigma) and the resulting complex was extracted with cyclohexane (Chempur). Fluorescence was measured from the organic layer (cyclohexane) at 518 nm emission wavelength and 378 nm excitation wavelength. The accuracy of the analytical method was based on NCS-ZC 71001 (beef liver) reference material from China NatiAnalysis Center for Iron and Steel (Beijing, China). The determined Se concentration was 90.9% of the standard value. Two replicates were performed for each sample, and statistical analysis used the average of the data, expressed in milligrams per kilogram wet weight (ww).

Statistical analysis

Analyses used Statistica 10.0 software (StatSoft). In order to determine compliance with the expected normal distribution of results, a Kolmogorov-Smirnov test with Lilliefors correction ($P<0.05$) was used. The arithmetic means (AM), standard deviations of the AM (SD), and medians (Med) were calculated for each studied group. Nonparametric tests (Kruskal- Wallis and Mann-Whitney U tests) were used as data deviated from a normal distribution. Differences between groups were analyzed with the Mann-Whitney U test for comparison of 2 groups and the Kruskal-Wallis test for comparison of 4 groups. The significance level was $P<0.05$. To determine a possible relationship between Se concentration in the liver and kidney in the analyzed infected groups and serum biochemical parameters (ALT and AST levels as important indicators of hepatocyte structural damage), we calculated the Spearman rank correlation coefficient (r_S) and determined the signfiicance.

Results

The biochemical findings in the infected and control groups with respect to the host's immunological status are presented in Table 1. The levels of sodium and potassium were not significantly different among the groups. A significant decrease in chlorine serum level was observed in the blood of the infected immunocompetent mice relative to the uninfected immunosuppressed animals ($U=23.0$, $P=0.05$). Analysis of serum liver enzyme activities showed that the highest levels of AST and ALT

Table 1

Biochemical parameters of serum results of *Acanthamoeba* sp. infected mice with respect to the host's immunological status.

Parameter/group			C n=6	A n=10	AS n=10	CS n=6	P (K-W test)
Na	mmol/l	AM±SD Median Range	153.0±2.16 152.0 151.0-156.0	152.5±1.0 153.0 151.0-153.0	151.2±1.4 151.0 149.0-154.0	152.6±1.26 153.0 151.0-154.0	0.40 NS
K	mmol/l	AM±SD Median Range	7.01±0.59 7.10 6.4-7.8	5.93±0.21 6.01 5.7-6.1	7.51±1.50 7.21 5.2-11.1	6.52±0.79 6.30 5.8-7.6	0.10 NS
Cl	mmol/l	AM±SD Median Range	110.0±3.7 109.5 107.0-114.0	108.5±0.58** 108.5 108.0-109.0	111.4±1.90 112.0 107.0-114.0	113.0±1.15** 113.0 112.0-114.0	0.004
TP	g/l	AM±SD Median Range	48.75±3.1 48.0 46.0-53.0	41.14±4.0 49.0 42.8-51.0	48.10±3.90 47.5 44.0-58.0	46.50±3.11 45.5 44.0-51.0	0.90 NS
CRP	mg/l	AM±SD Median Range	<0.02	<0.02	<0.02	<0.02	–
Albumin	g/l	AM±SD Median Range	25.25±1.26 25.0 23.0-27.0	27.0±0.82 27.0 26.0-28.0	23.8±1.50 24.0 20.0-26.0	24.0±0.80 24.0 23.0-25.0	0.58 NS
CR	mg/dl	AM±SD Median Range	0.35±0.03 0.35 0.31-0.36	0.36±0.03 0.37 0.32-0.40	0.40±0.03 0.40 0.30-0.40	0.36±0.02 0.35 0.35-0.38	0.25 NS
Urea	g/l	AM±SD Median Range	48.4±9.18 53.0 37.0-56.0	53.4±3.78 53.0 48.0-57.0	52.8±7.0 52.0 41.0-69.0	53.3±5.09 53.5 47.0-59.0	0.46 NS
AST	U/l	AM±SD Median Range	272.2±132.1* 273.0 141.0-471.0	546.3±357.9* 511.0 203.0-1174.0	673.8±292.5 559.0 137.0-1128.0	411.5±147.2 411.5 282.0-541.0	0.001
ALT	U/l	AM±SD Median Range	113.20±36.6 117.0 58.0-153.0	116.43±68.6 105.0 48.0-230.0	191.4±136.2 169.5 35.0-538.0	96.8±32.5 91.5 63.0-141.0	0.56 NS
TC	mg/dl	AM±SD Median Range	72.20±2.95 74.0 68.0-75.0	73.14±4.81 74.0 66.0-81.0	73.80±7.60 72.0 63.0-91.0	73.25±7.76 74.5 63.0-81.0	0.49 NS
TG	mg/l	AM±SD Median Range	122.0±2.65 121.0 120.0-125.0	129.0±26.0 129.0 103.0-155.0	99.5±31.1 92.0 60.0-167.0	70.0±10.9 68.5 60.0-83.0	0.32 NS
HDL	mg/l	AM±SD Median Range	41.20±3.63 40.0 37.0-45.0	41.20±2.11 41.0 38.0-45.0	41.9±8.90 40.0 29.0-60.0	42.25±5.92 42.0 40.0-53.0	0.35 NS
LDL	mg/l	AM±SD Median Range	1.20±0.45 1.0 1.0-2.0	1.57±0.53 2.0 1.0-2.0	1.90±1.10 2.0 1.0-5.0	2.0±0.82 2.0 1.0-3.0	0.51 NS

A – immunocompetent *Acanthamoeba*-infected mice; C – immunocompetent uninfected control group; AS – immunosuppressed *Acanthamoeba*-infected mice; CS – immunosuppressed uninfected mice; Na – sodium, K – potassium, Cl – chlorine, TP – total protein, CRP – C-reactive protein, CR – creatinine, AST – aspartate aminotransferase, ALT – alanine aminotransferase, TC – total cholesterol, TG – triglyceride, HDL – high-density lipoprotein, LDL – low-density lipoprotein cholesterol; AM – arithmetic mean; SD – standard deviation; P – level of significance; P (K-W test) – P-value Kruskal-Wallis test; NS – non-significant difference; Mann-Whitney U-test, P<0.05: *A vs C, ** A vs CS (P-value is not adjusted for multiple comparisons).

Table 2

Selenium (Se) concentrations in the liver and kidney in control and infected mice

Parameter	C (n=6)	A (n=10)	AS (n=10)	CS (n=6)	P (K-W test)
Liver					
AM±SD Median Range	0.44±0.26** 0.48 0.08-0.75	0.46±0.23* 0.53 0.15-0.69	0.89±0.21* 0.91 0.14-1.18	0.99±0.21** 0.96 0.89-1.22	0.001
Kidney					
AM±SD Median Range	0.49±0.20 # 0.50 0.24-0.71	0.61±0.07*,# 0.59 0.53-0.71	1.69±1.24* 1.02 0.72-6.86	0.91±0.05 0.90 0.83-0.99	0.001

A – immunocompetent *Acanthamoeba*-infected mice; C – immunocompetent control group uninfected mice; AS – immunosuppressed *Acanthamoeba*-infected mice; CS – immunosuppressed uninfected mice; AM – arithmetic mean; SD – standard deviation; P – level of significance; P (K-W test) – P-value Kruskal-Wallis test; Mann-Whitney U-test, P<0.05: *A vs AS, **C vs CS and # C vs A (P value is not adjusted for multiple comparisons).

were observed in the AS group and mean values did not exceed 680 and 192 U/l, respectively. We found a significantly higher serum AST level in *Acanthamoeba*-infected immunocompetent mice than in control immunocompetent animals (U=21.0, P=0.02). There was no significant difference in TP, CRP, albumin, CR or urea. Evaluation of lipid levels did not reveal significant differences in TC, HDL and LDL. Significant differences in TG analysis were not found among the groups, but relatively higher mean values were recorded in the immunocompetent animals from the A and C groups, >122 mg/l.

Average Se levels in the livers of the examined groups can be arranged in the following descending order: CS>AS>A>C. The highest Se concentration in livers of *Acanthamoeba*-infected animals was observed in immunosuppressive mice and ranged from 0.14 mg/kg ww to 1.18 mg/kg ww. We observed a significantly lower Se liver concentration in *Acanthamoeba*-infected immunocompetent mice than in the *Acanthamoeba*-infected immunosuppressed group (U=15, P=0.001) (Table 2). There was a significant difference in hepatic Se levels between the C and CS groups: 0.48 and 0.96 mg/kg ww, respectively. *Acanthamoeba* infection did not influence the accumulation of Se in the liver of immunocompetent animals but significantly increased in mice with low immunity.

The highest mean Se level in the kidney was observed in the *Acanthamoeba*-infected immunosuppressed animals, at ~1.70 mg/kg ww. Nephric Se concentration in the immunocompetent mice was higher in the infected group compared to the control. We found a significantly higher Se kidney concentration in immunosuppressed infected mice than in immunocompetent infected animals (U=34.5, P=0.01).

To determine the possible association between Se concentration in the liver and kidney in the analyzed groups and serum biochemical parameters (AST and ALT), we calculated the Spearman rank correlation coefficient (r_S) and determined its significance. We observed statistically significant correlations between the Se liver concentration and ALT serum level (r_S=0.87; P=0.01) as well as AST serum level (r_S=0.77, P=0.01) in infected immunosuppressed mice (AS group). Moreover, we noted positive significant correlation for Se concentration in the liver and AST serum level (r_S=0.70; P=0.02) in immunocompetent *Acanthamoeba* sp. infected mice (group A). There were no significant relationships between Se nephric level in the analyzed groups and serum biochemical parameters.

Discussion

Limited data from studies on *Acanthamoeba* sp. infection show that the livers of mice infected by these amoebae are subject to extensive necrosis and a considerable reduction in glycogen levels in hepatocytes. In the kidneys, necrotic changes are reported in tubules and glomeruli (GÓRNIK & KUŹNA-GRYGIEL 2005). We could not find data on biochemical parameters in experimental acanthamoebiasis, with the clinical image of this infection in patients being very diverse and depending on the efficiency of the host's immune

system. In a study by TILAK *et al*. (2008), a patient with *Acanthamoeba* peritonitis on continuous ambulatory peritoneal dialysis had normal levels of electrolytes Na^+ and K^+, and kidney function tests revealed normal ranges of urea, creatinine, serum protein and albumin. Moreover, no changes were observed in liver function. WEBSTER *et al.* (2012) in an immunocompetent patient with GAE observed that liver enzymes and renal function also remained stable. Similar to our model, KHANNA *et al.* (2015), in a rare case of meningoencephalitis caused by *Aspergillus* sp. and *Acanthamoeba* sp. coinfection, did not show changes in serum sodium and potassium levels, and urea and creatinine were in normal ranges.

The liver is exposed to many systemic infectious pathogens including, among others, hepatotropic organisms which may directly or indirectly cause liver pathology. Changes in serum ALT and AST are considered important indicators of hepatocyte structural damage. Hepatic enzymes are present in some tissues, including cardiac muscle, liver and brain, in which they take part in energy metabolism involving the transamination of amino acids (LIMDI & HYDE 2003; ADEYEMI & AKANJI 2011). In cases of cellular damage, AST and ALT can leak out into the general circulation leading to elevated activity (EL-SAYED *et al*. 2016; AL-SALAHY *et al.* 2016). This study demonstrated that the highest concentrations of AST and ALT were observed in the infected immunosuppressed mice. Moreover, AST level increased in infected immunocompetent compared to non-infected animals. EL-SAYED *et al*. (2016) showed a significant increase of liver enzymes in the serum of patients infected with the opportunistic parasite *Toxoplasma gondii.* Similarly, AL-SALAHY *et al.* (2016) reported significantly higher serum ALT and AST in patients with malaria caused by *Plasmodium falciparum.* YUSUF *et al.* (2012) in experimental trypanosomiasis showed that an increase in the activity of ALT may be due to tissue damage alone, and also as a result of the destruction of trypanosomes by the host defense system. MOREIRA *et al.* (2016) revealed a renal alteration characterized by an increase in urea and creatinine in *Leishmania infantum* infected hamsters. Our experimental acanthamoebiasis showed no significant difference in total protein, CRP, albumin, creatinine or urea.

Cholesterol may have an important role in cellular immunity, and a low cholesterol level may have destructive effects on lymphocytes and macrophages facilitating development and progression of pneumonia infection (SAHIN & YILDIZ 2013). However, the mechanisms involved in lipid changes related to parasite infections remain unclear. Lipid profiling in this study included TC, HDL and LDL, which were all constant, except TG in the immunocompetent animals, with lowest levels noted in non-infected mice with low immunity after corticoid administration. MARTÍNEZ-SUBIELA *et al.* (2004) suggest that glucocorticoids do not produce an increase in lipid mediators and parameters of lipid profile. There is some evidence of a relationship between acanthamoebiasis and changes in serum triglyceride metabolism in the host. The highest, but nonetheless insignificant, level of triglyceride was observed in *Acanthamoeba*-infected immunocompetent mice and was 1.3 times greater than in infected mice with low immunity. Some researchers suggest that the increase in triglyceride, e.g. in dog babesiosis, may be associated with increased hepatic production or with the inflammatory host response (CARPENTIER & SCRUEL 2002; MRLJAK *et al.* 2014).

Trace elements including Se are essential for the functioning of immunocompetent cells, and the liver is the main organ in the metabolism and homeostasis of Se (AMINI *et al.* 2009). This study demonstrated several biochemical disturbances in *Acanthamoeba*-infected mice and a connection between Se concentration in the liver in the analyzed groups and serum biochemical parameters. Selenium levels in the liver and kidney of immunosuppressed *Acanthamoeba*-infected mice were higher than in immunocompetent animals, which may be connected with Se retention. Nephric Se levels in immunocompetent mice were higher in infected group compared to the control. Se levels in serum and tissues of infected hosts are usually lower than in the control. LOGUERCIO *et al.* (2001) observed that liver cirrhosis induced a decrease in Se level and oxidative stress, as documented by a significant correlation between Se and glutathione. Oxidative stress may be a result of suboptimal Se and Zn concentrations (SCHOMBURG 2014). In contrast, YANG *et al*. (2016) showed that elevated plasma Se levels were associated not only with nonalcoholic fatty liver disease, but with increased levels of triglycerides, ALT and AST.

This study demonstrated non-significant, but decreasing hepatic Se level only in infected, immunosuppressed mice compared to control animals with low immunity. PILARCZYK *et al.* (2008) showed a nephric Se concentration in *T. canis* infected mice at the control level, not exceeding 0.69 mg/kg ww. Moreover, parasite infection did not change Se level in the kidney, which is in line with results in this study in immunocompetent infected hosts.

In patients treated with corticosteroids with anti-inflammatory and immunosuppressive properties, changes in trace elements may be a consequence of the defense response of the organism, mediated by inflammatory-like substances (AL-ZUBAIDI 2001; ÖNAL *et al.* 2011). In patients with multiple sclerosis, intravenous administration of methylprednisolone results in decreased serum Se

compared to control, as Se can act as an antioxidant in the extracellular space and in the cell cytosol, in association with the cell membranes, all of which have the potential to influence the immune processes (AL-ZUBAIDI 2001; MILLER *et al.* 2001). In our animal model of *Acanthamoeba*-infected and non-infected mice, which were administered methylprednisolone intraperitoneally, Se concentrations in the liver and kidney were greater than without the steroids.

Imbalances in the metabolism of trace metals may lead to metal interactions with potential pathophysiological significance (LANOCHA-ARENDARCZYK *et al.* 2015). In the experimentally induced acanthamoebiasis in our study, we observed a novel strong relationship between hepatic Se concentration and liver enzymes (AST and ALT) in infected mice with low immunity. Moreover, Se liver concentration correlated with serum AST in immunocompetent infected mice.

Our results may lead to a better understanding of the pathogenesis of acanthamoebiasis and an improvement in diagnostic efficiency, particularly in patients with low immunity. Immunological status influenced Se level in the liver and kidney of *Acanthamoeba*-infected mice. The infection did not influence the accumulation of Se in the liver of immunocompetent animals but significantly increased accumulation in mice with low immunity. Infection with this pathogenic amoeba affected the activity of serum AST regardless of the host's immunological status. Furthermore, the elevated hepatic Se concentrations were associated with increased levels of serum ALT and AST. Hepatic and nephric Se levels and biochemical markers in animals infected by *Acanthamoeba* sp. might depend on host immunological reactions, but the role of the immune system in the pathogenesis of an *Acanthamoeba* infection is still unclear.

Funding

The study was financed as research project no. WLBiMl-431-04/S/12/2017 by Pomeranian Medical University in Szczecin.

Author Contributions

Research concept and design: N.Ł-A ., I.B.-B., B.P., J.K.-K., D.K.-B.; Collection and/or assembly of data: N.Ł-A., I.B.-B., K.K., B.P., A.T.-M., D.K.-B.; Data analysis and interpretation: N.Ł-A., K.K., D.K.-B.; Writing the article: N.Ł-A., K.K., D.K.-B.; Critical revision of the article: N.Ł-A., D.K.-B.; Final approval of article: N.Ł-A., K.K., B.P., A.T.-M., J.K.-K., D.K.-B.

Conflict of Interest

The authors declare no conflict of interest.

References

ADEYEMI O.S., AKANJI M.A. 2011. Biochemical changes in the kidney and liver of rats following administration of ethanolic extract of *Psidium guajava* leaves. Hum. Exp. Toxicol. **30**: 1266-1274. https://doi.org/10.1177/0960327110388534

AL-SALAHY M., SHNAWA B., ABED G., MANDOUR A., AL-EZZI A. 2016. Parasitaemia and Its Relation to Hematological Parameters and Liver Function among Patients Malaria in Abs, Hajjah, Northwest Yemen. Interdiscip. Perspect. Infect. Dis. 2016: 5954394. https://doi.org/10.1155/2016/5954394

AL-ZUBAIDI M.A. 2001. The Effect of Interferon Beta-1b and Methylprednisolone Treatment on the Serum Trace Elements in Iraqi Patients with Multiple Sclerosis. J. Clin. Diagn. Res. **6**: 994-998.

AMINI M., NAHREVANIAN H., KHATAMI S., FARAHMAND M., MIRKHANI F., JAVADIAN S. 2009. Biochemical association between essential trace elements and susceptibility to *Leishma niamajor* in BALB/c and C57BL/6 mice. Braz. J. Infect. Dis. **13**: 83-85.

BRONDFIELD M.N., REID M.J., RUTISHAUSER R.L., COPE J.R., TANG J., RITTER J.M., MATANOCK A., ALI I., DOERNBERG S.B., HILTS-HORECZKO A., DEMARCO T., KLEIN L., BABIK J.M. 2017. Disseminated *Acanthamoeba* infection in a heart transplant recipient treated successfully with a miltefosine-containing regimen: Case report and review of the literature. Transpl. Infect. Dis. **19**. https://doi.org/10.1111/tid.12661

CARNT N., STAPLETON F. 2016. Strategies for the prevention of contact lens-related *Acanthamoeba* keratitis: a review. Ophthalmic. Physiol. Opt. **36**: 77-92. https://doi.org/10.1111/opo.12271

CARPENTIER Y.A., SCRUEL O. 2002. Changes in the concentration and composition of plasma lipoproteins during the acute phase response. Curr. Opin. Clin. Nutr. Metab. Care, **5**: 153-158.

DA SILVA M.T., SILVA-JARDIM I., THIEMANN O.H. 2014. Biological implications of selenium and its role in trypanosomiasis treatment. Curr. Med. Chem. **21**: 1772-1780.

DAGNACHEW S., BEZIE M., TEREFE G., ABEBE G., BARRY J.D., GODDEERIS B.M. 2015. Comparative clinico-haematological analysis in young Zebu cattle experimentally infected with *Trypanosoma vivax* isolates from tsetse infested and non-tsetse infested areas of Northwest Ethiopia. Acta. Vet. Scand. **57**: 24. https://doi.org/10.1186/s13028-015-0114-2

DUNTAS L.H., HUBALEWSKA-DYDEJCZYK A. 2015. Selenium and inflammation – potential use and future perspectives. US Endocrinol. **11**: 97102.

EL-SAYED N.M., RAMADAN M.E., RAMADAN M.E. 2016. *Toxoplasma gondii* infection and chronic liver diseases: evidence of an association. Trop. Med. Infect. Dis. **1**: 7. https://doi.org/10.3390/tropicalmed1010007

GÓRNIK K., KUŹNA-GRYGIEL W. 2005. Histological studies of selected organs of mice experimentally infected with *Acanthamoeba* spp. Folia Morphol. (Warszawa) **64**: 161-167.

HUANG K., YANG S. 2002. Inhibitory effect of selenium on *Cryptosporidium parvum* infection *in vitro* and *in vivo*. Biol. Trace. Elem. Res. **90**: 261-272.

IRIBHOGBE O.I., AGBAJE E.O., OREAGBA I.A., AINA O.O., OTA A.D. 2013. Oxidative stress and micronutrient therapy in malaria: an in vivo study in *Plasmodium berghei* infected mice. Pak. J. Biol. Sci. **16**: 160-167.

JELICKS L.A., DE SOUZA A.P., ARAUJO-JORGE T.C., TANOWITZ H.B. 2011. Would selenium supplementation

aid in therapy for Chagas disease? Trends. Parasitol. **27**: 102-105. https://doi.org/10.1016/j.pt.2010.12.002

KHANNA V., TILAK K., PRABHU M., PRIYA P., KHANNA R. 2015. Rare case of meningoencephalitis due to *Aspergillus* and *Acanthamoeba* coinfection. Hum. Parasit. Dis. **7**: 19-23.

LANOCHA N., KOSIK-BOGACKA D., MACIEJEWSKA A., SAWCZUK M., WILK A., KUŹNA-GRYGIEL W. 2009. The Occurrence *Acanthamoeba* (Free Living Amoeba) in Environmental and Respiratory. Acta. Protozool. **48**: 271-279.

LANOCHA-ARENDARCZYK N., KOSIK-BOGACKA D.I., PROKOPOWICZ A., KALISINSKA E., SOKOLOWSKI S., KARACZUN M., ZIETEK P., PODLASIŃSKA J., PILARCZYK B., TOMZA-MARCINIAK A., BARANOWSKA-BOSIACKA I., GUTOWSKA I., SAFRANOW K., CHLUBEK D. 2015. The effect of risk factors on the levels of chemical elements in the tibial plateau of patients with osteoarthritis following knee surgery. Biomed. Res. Int. 2015: 650282. https://doi.org/10.1155/2015/650282

ŁANOCHA-ARENDARCZYK N., BARANOWSKA-BOSIACKA I., KOT K., GUTOWSKA I., KOLASA-WOŁOSIUK A., CHLUBEK D., KOSIK-BOGACKA D. 2018. Expression and activity of COX-1 and COX-2 in *Acanthamoeba* sp.-infected lungs according to the host immunological status. Int. J. Mol. Sci. **19**:121. https://doi.org/10.3390/ijms19010121

LIMDI J.K., HYDE G.M. 2003. Evaluation of abnormal liver function tests. Postgrad. J. **79**: 307-312.\

LOGUERCIO C., DE GIROLAMO V., FEDERICO A., FENG S.L., CRAFA E., CATALDI V., GIALANELLA G., MORO R., DEL VECCHIO BLANCO C. 2001. Relationship of blood trace elements to liver damage, nutritional status, and oxidative stress in chronic nonalcoholic liver disease. Biol. Trace. Elem. Res. **81**: 245-254.

MAEHIRA F., LUYO G.A., MIYAGI I., OSHIRO M., YAMANE N., KUBA M., NAKAZATO Y. 2002. Alterations of serum selenium concentrations in the acute phase of pathological conditions. Clin. Chim. Acta. **316**: 137-146.

MARKOWITZ S.M., SOBIESKI T., MARTINEZ A.J., DUMA R.J. 1978. Experimental *Acanthamoeba* infections in mice pretreated with methylprednisolone or tetracycline. Am. J. Pathol. **92**: 733-744.

MARTÍNEZ-SUBIELA S., GINEL P.J., CERÓN J.J. 2004. Effects of different glucocorticoid treatments on serum acute phase proteins in dogs. Vet Rec **154**: 814-817.

MILLER S., WALKER S.W., ARTHUR J.R., NICOL F., PICKARD K., LEWIN M.H. 2001. Selenite protects the human endothelial cells from oxidative damage and it induces thioredoxin reductase. Clin. Sci. (London) **100**: 543-550.

MOREIRA N.D., VITORIANO-SOUZA J., ROATT B.M., VIEIRA P.M., COURA-VITAL W., CARDOSO J.M., REZENDE M.T., KER H.G., GIUNCHETTI R.C., CARNEIRO C.M., REIS A.B. 2016. Clinical, hematological and biochemical alterations in hamster (*Mesocricetus auratus*) experimentally infected with *Leishmania infantum* through different routes of inoculation. Parasit. Vectors **9:** 181. https://doi.org/10.1186/s13071-016-1464-y

MRLJAK V., KUČER N., KULEŠ J., TVARIJONAVICIUTE A., BRKLJAČIĆ M., CRNOGAJ M., ZIVIČNJAK T., SMIT I., CERON J.J., RAFAJ R.B. 2014. Serum concentrations of eicosanoids and lipids in dogs naturally infected with *Babesia canis*. Vet. Parasitol. **201**: 24-30. https://doi.org/10.1016/j.vetpar.2014.01.002

ÖNAL S., NAZIROĞLU M., ÇOLAK M., BULUT V., FLORES-ARCE M.F. 2011. Effects of different medical treatments on serum copper, selenium and zinc levels in patients with rheumatoid arthritis. Biol. Trace. Elem. Res. **142**: 447-455. https://doi.org/10.1007/s12011-010-8826-7

PILARCZYK B., DOLIGALSKA M.J., DONSKOW-SCHMELTER K., BALICKA-RAMISZ A., RAMISZ A. 2008. Selenium supplementation enhances the protective response to *Toxocara canis* larvae in mice. Parasite. Immunol. **30**: 394-402. https://doi.org/10.1111/j.1365-3024.2008.01039.x

RIVERA M.T., DE SOUZA A.P., MORENO A.H., XAVIER S.S., GOMES J.A., ROCHA M.O., CORREA-OLIVEIRA R., NEVE J., VANDERPAS J., ARAUJO-JORGE T.C. 2002. Progressive Chagas' cardiomyopathy is associated with low selenium levels. Am. J. Trop. Med. Hyg. **66**: 706-712.

SAHIN F., YILDIZ P. 2013. Distinctive biochemical changes in pulmonary tuberculosis and pneumonia. Arch. Med. Sci. **30**: 656-661. https://doi.org/10.5114/aoms.2013.34403

SALAMEH A., BELLO N., BECKER J., ZANGENEH T. 2015. Fatal granulomatous amoebic encephalitis caused by *Acanthamoeba* in a patient with kidney transplant: A Case Report. Open. Forum. Infect. Dis. **2**: ofv104. https://doi.org/10.1093/ofid/ofv104

SCHOMBURG L. 2014. Selenium in sepsis-substitution, supplementation or pro-oxidative bolus? Crit. Care. **18**: 444. https://doi.org/10.1186/cc13963

SHARMA M., SUDHAN S.S., SHARMA S., MEGHA K., NADA R., KHURANA S. 2017. Osteo-cutaneous acanthamoebiasis in a non-immunocompromised patient with a favorable outcome. Parasitol. Int. **66**: 727-720. https://doi.org/10.1016/j.parint.2017.08.003

STEINBRENNER H., AL-QURAISHY S., DKHIL M.A., WUNDERLICH F., SIES H. 2015. Dietary selenium in adjuvant therapy of viral and bacterial infections. Adv. Nutr. **6**: 73-82. https://doi.org/10.3945/an.114.007575

TEKNOS T.N., POULIN M.D., LARUENTANO A.M., LI K.K. 2000. *Acanthamoeba rhinosinusitis*: characterization, diagnosis, and treatment. Am. J. Rhinol. **14**: 387-391.

TILAK R., SINGH R.G., WANI I.A., PAREKH A., PRAKASH J., USHA U. 2008. An unusual case of *Acanthamoeba* peritonitis in a malnourished patient on continuous ambulatory peritoneal dialysis (CAPD). J. Infect. Dev. Ctries. **2**: 146-148.

TINGGI U. 2008. Selenium: its role as antioxidant in human health. Environ. Health. Prev. Med. **13**: 102-108. https://doi.org/10.1007/s12199-007-0019-4

TRABELSI H., DENDANA F., SELLAMI A., SELLAMI H., CHEIKHROUHOU F., NEJI S., MAKNI F., AYADI A. 2012. Pathogenic free-living amoebae: epidemiology and clinical review. Pathol. Biol. **60**: 399-405. https://doi.org/10.1016/j.patbio.2012.03.002

VÄLIMÄKI M., ALFTHAN G., PIKKARAINEN J., YLIKAHRI R., SALASPURO M. 1987. Blood and liver selenium concentrations in patients with liver diseases. Clin. Chim. Acta. **166**: 171-176.

VISVESVARA G.S., MOURA H., SCHUSTER F.L. 2007. Pathogenic and opportunistic free-living amoebae: *Acanthamoeba* spp., *Balamuthia mandrillaris*, *Naegleria fowleri* and *Sappinia diploidea*. FEMS Immunol. Med. Mic. **50**: 1-26.

WEBSTER D., UMAR I., KOLYVAS G., BILBAO J., GUIOT M.C., DUPLISEA K., QVARNSTROM Y., VISVESVARA G.S. 2012. Treatment of granulomatous amoebic encephalitis with voriconazole and miltefosine in an immunocompetent soldier. Am. J. Trop. Med. Hyg. **87**: 715-718. https://doi.org/10.4269/ajtmh.2012.12-0100

WINSETT F., DIETERT J., TSCHEN J., SWABY M., BANGERT C.A. 2017. A rare case of cutaneous acanthamoebiasis in a renal transplant patient. Dermatol. Online. J. **15**: 23.

YANG Z., YAN C., LIU G., NIU Y., ZHANG W., LU S., LI X., ZHANG H., NING G., FAN J., QIN L., SU Q. 2016. Plasma selenium levels and nonalcoholic fatty liver disease in Chinese adults: a cross-sectional analysis. Sci. Rep. **17**: 372-388. https://doi.org/10.1038/srep37288

YUSUF A.B., UMAR I.A., NOK A.J. 2012. Effects of methanol extract of *Vernonia amygdalina* leaf on survival and some biochemical parameters in acute *Trypanosoma brucei brucei* infection. Afr. J. Biochem. Res. **6**: 150-158.

e-ISSN 1734-9168
http://www.isez.pan.krakow.pl/en/folia-biologica.html

Folia Biologica (Kraków), vol. 66 (2018), No 1
https://doi.org/10.3409/fb_66-1.05

Effects of Ultra-violet Radiation on Cellular Proteins and Lipids of Radioresistant Bacteria Isolated from Desert Soil

Wasim SAJJAD, Salman KHAN, Manzoor AHMAD, Muhammad RAFIQ, Malik BADSHAH, Wasim SAJJAD, Sahib ZADA, Samiullah KHAN, Fariha HASAN, and Aamer Ali SHAH

Accepted April 28, 2018 *Published online June 20, 2018* *Issue online June 22, 2018*

Original article

SAJJAD W., KHAN S., AHMAD M., RAFIQ M., BADSHAH M., SAJJAD W., ZADA S., KHAN S., HASAN F., SHAH A.A. 2018. Effects of ultra-violet radiation on cellular proteins and lipids of radioresistant bacteria isolated from desert soil. Folia Biologica (Kraków) **66**: 41-52.

Organisms in hot, arid environment have to cope with adverse life conditions such as desiccation, temperature and lack of nutrients. The phylogenetic diversity of ultra-violet (UV) radiation resistant bacteria from desert soil was investigated by culture and molecular-based analysis. The bacterial strains were characterized for their tolerance to UV doses, salt concentration and heavy metals. The effect of UV radiation (UVR) on cellular lipids and proteins was studied by lipid peroxidation and protein carbonylation assay. 9 UV resistant bacteria were isolated and identified through biochemical tests and 16S rRNA sequencing. These bacterial strains were grouped into four phyla: *Firmicutes, Proteobacteria, Deinococcus-Thermus* and *Actinobacteria*. The genus *Deinococcus* was found to be resistant to high UV dosage in comparison to other genera, as indicated by maximum survival rate. The bacteria were found to grow at a wide range of temperature and pH, resistant to high salt concentration and various metal ions. The UV resistant selected strains exhibited minor damages to proteins and lipids as a result of exposure to UV radiation as compared to *Escherichia coli* (ATCC 10536), a UV sensitive bacteria. The results indicated that these microbes might harbor a sophisticated phenotypic character and molecular repair mechanism that can prolong their survival under extreme radiation.

Key words: Radio-resistant, phylogenetic analysis, *Deinococcus-Thermus*, protein carbonylation, lipid peroxidation.

Wasim SAJJAD, Salman KHAN, Manzoor AHMAD, Muhammad RAFIQ, Malik BADSHAH, Wasim SAJJAD, Sahib ZADA, Samiullah KHAN, Fariha HASAN, Aamer Ali SHAH✉, Department of Microbiology, Faculty of Biological Sciences, Quaid-i-Azam University, Islamabad 45320, Pakistan.
alishah@qau.edu.pk
Wasim SAJJAD, Department of Biogenetics, National University of Medical Sciences, Rawalpindi 46000, Pakistan.
Muhammad RAFIQ, Department of Microbiology Abdul Wali Khan University Mardan, Khyber Pakhtoonkhwa Pakistan.
Wasim SAJJAD, Key Laboratory of Petroleum Resources, Gansu Province/Key Laboratory of Petroleum Resources Research, Institute of Geology and Geophysics, Chinese Academy of Sciences, Lanzhou, PR China; University of Chinese Academy of Sciences, Beijing, PR China.
Sahib ZADA, Department of Allied Health Sciences, Iqra National University Peshawar, Khyber Pakhtoonkhwa Pakistan.

Radio-resistant is the term referred to the group of organisms that live under and can efficiently recover when exposed to radiation. These organisms can surprisingly endure both ionizing and non-ionizing radiation, which can be lethal to other species (SINGH & GABANI 2011). Ionizing radiation-resistant microbes have been isolated from a wide range of environments including dried food, irradiated meat and fish, high level nuclear wastes at Savannah River in South Carolina, hot and dry desert, and warm freshwater geothermal spring at Hanford in Washington (RAINEY *et al*. 2005). Extreme ionizing radiation resistance has been observed in several members of the domains *Bacteria* and *Archaea* (FREDRICKSON *et al*. 2004). Of the genera containing ionizing radiation-

resistant organisms, *Deinococcus* and *Rubrobacter* followed by *Kineococcus* and *Kocuria* show the highest levels of resistance (PHILLIPS *et al*. 2002).

Ultraviolet radiation (UVR) is an important stress factor for bacterial communities. It is known to induce oxidative stress in aquatic bacteria by production of reactive oxygen species (ROS) formed via photodynamic reactions involving intracellular or extracellular photosensitizers (PATTISON & DAVIES 2006; SANTOS *et al*. 2013a,b). These ROS can react with cellular constituents, most notably proteins and lipids, leading to altered membrane permeability and/or disruption of transmembrane ion gradients that eventually cause cell death (BARRERA 2012). The cellular and biological consequences of ROS are strongly influenced by metal ion homeostasis (HALLIWELL & GUTTERIDGE 2015). In bacterial cells which are exposed to UVB radiation, the potential synergistic effect of some transition metals like Cu^{+2}, Mn^{+2} and Zn^{+2} have also been reported (SANTOS *et al*. 2013a). Intercellular Cu^{+2} uptake, presence of high intracellular Mn^{2+} and Zn^{2+} uptake by UV resistant microbes are the adaptive response to peroxide stress by blocking the Fenton and Haber-Weiss reactions (BAGWELL *et al*. 2008; DALY *et al*. 2010). Production of different compatible solutes such as trehalose and ectoine in extreme environments plays a significant role in ionizing radiation protection (BEBLO-VRANESEVIC *et al*. 2017). Ionizing radiation resistance in *Halobacterium salinarum* is most likely achieved by a "metabolic route" with a combination of tightly coordinated physiological processes (ROBINSON *et al*. 2011). Therefore, it is necessary to investigate the diversity of ultraviolet resistant microorganisms in order to understand the biological mechanisms involved in survival under UVR stress.

The current study focused on determination of phylogenetic diversity of UV resistant bacteria in desert soil of Lakki Marwat and Bahawalpur deserts, Pakistan. The effect of UV radiation on intracellular lipids and proteins was also investigated by using standard oxidation assays.

Material and Methods

Sampling

Soil samples (2 different samples from 15 cm depth) were collected aseptically from Lakki Marwat and Bahawalpur deserts, Pakistan, in sterilized polyethylene zipper bags following a standard microbiological procedure, carefully transported to the laboratory and stored at 4°C for further processing.

Metal analysis of desert soil

Sample preparation

The soil samples (2 samples) were dried at room temperature for 5 days and sieved (2 mm sieve). 1 g of the soil was acidified with 0.5 ml of concentrated nitric acid and 10 ml of per-chloric acid (70% $HClO_4$). The mixture was heated till white, dense fumes of $HClO_4$ appeared (RAURET 1998). The digested samples were cooled to room temperature, filtered through Whatman # 41 and boiled to remove oxides of nitrogen and chlorine. Finally, the soil samples were subjected to Cu^{+2}, Ni^{+2}, Zn^{+2}, Mn^{+2}, Cr^{+2}, Fe^{+2}, Pb^{+2}, Cd^{+2}, Ca^{+2}, Mg^{+2} and Na^{+2} analysis using an atomic absorption spectrophotometer (AAS) on a Perkin-Elmer 460 Spectrophotometer.

Isolation of radio-resistant microorganisms

The soil samples were serially diluted and plated on TGY (tryptone glucose yeast extract) agar by the spread plate method. The plates were exposed to UV radiation in 119x69×52 cm UV chamber supplied with a 20W and 280nm UV light source (germicidal lamp) for a specified time (30-300 seconds). The UV fluence rate (energy/area/time) to the test sample was measured with He=Ee×t in units of J/m^2 (SAJJAD *et al*. 2017). The total UV dose was determined by time of exposure to UV fluence rate. All UV irradiation procedures were performed under red light to prevent photo-reactivation.

Radiant exposure (He) = the energy that reaches a surface area due to irradiance (Ee) maintained for a time duration (t).

UV radiation tolerance

The UVR resistance among bacterial isolates was determined by a method previously described by MATTIMORE and BATTISTA (1996) with some modifications in order to calculate % survivability. The UV-resistant bacteria isolated were grown in TGY broth up to OD_{600} 0.5, and then spread on TGY agar. The plates were exposed to UV-B (280nm) for the variable doses (30-180 sec) and subsequently incubated at 30ºC. The surviving fraction was calculated after 24 hrs by determining the titer of culture after irradiation divided by unirradiated control.

Identification of UV resistant microbes

Biochemical and physiological characteristics

Cellular morphology was examined by phase-contrast microscopy (Labomed Lx400). The bac-

teria were grown on TGY agar plates at wide temperature 15-45°C, pH 4.0-9.0 and NaCl (0-16%) ranges for 3 days to determine optimum growth conditions. The strains were also tested for catalase, cytochrome oxidase as well as hydrolysis of starch, casein, and gelatin by methods described in MURRAY *et al*. (1981).

Sequence alignment and phylogenetic analysis

The genomic DNA of all bacterial strains was extracted using a DNA extraction kit (QIAGEN). The 16S rRNA gene sequences were amplified using universal primers (F-27:AGAGTTTGATCMTGGCTCAG, R-1492:TACGGYTACCTTGTTACGACTT). A reaction mixture containing GoTaq Green Master Mix Promega (25 µl), primer 27F (2 µl), primer 1492R (2 µl), DNA extract (3 µl), and *Nuclease-Free* Water (50 µl) was prepared. The reaction was carried out in a MJ Mini Personal Thermal Cycler (BIO RAD). In the PCR cycle initial denaturation was completed at 95°C for 3 minutes, followed by denaturation (30 cycles) for 1 min at 95°C, annealing at 55°C for 1 min and finally extension for 1 min at 72°C and final extension at 72°C for 7 min. The PCR product was analyzed by agarose gel (1%) electrophoresis. The amplified PCR products were sequenced at Macrogen Service Center (Geunchun-gu, Seoul, South Korea). The obtained sequences were identified using the BLAST tool at the NCBI database and homologs were phylogenetically analyzed using Molecular Evolutionary Genetic Analysis (MEGA) version 6 (TAMURA *et al*. 2013). All the UV resistant isolates were compared with previously reported microorganisms submitted to NCBI.

Metal resistance

Stock solutions (1000 ppm) of various transition metals (Co^{+2}, Cu^{+2}, Cr^{+2}, Fe^{+2}, Mn^{+2} and Zn^{+2}) were prepared in deionized and filter-sterilized water from the corresponding metallic salts. The effect of metal ions on bacterial strains was determined by inoculating them on TGY agar supplemented with different metals at variable concentrations (20-400 ppm) and incubated at 30°C for 48 h.

Effect of UVB on lipids and proteins of UV resistant bacteria

Cultures grown overnight in TGY broth were harvested by centrifugation at 10,000 rmp for 10 mins. The pellets of the respective bacterial strain (10^6 cells/ml) were irradiated with UVB. The UV dose (2000 J/m^2) was calculated by a method described previously (SAJJAD *et al*. 2017). An aliquot of cell suspension was collected before and after irradiation, washed with ultrapure water, and immediately used for lipid and protein extraction.

Lipid peroxidation assay

Lipid peroxidation results in formation of malondialdehyde (MDA), a lipid peroxidation marker. The TBA (Thiobarbituric acid) assay was performed by the method described by PÉREZ *et al.* (2007) with some modification, in order to assess the MDA concentration. Total lipid extract was recovered, according to a standard protocol as previously described (BLIGH & DYER 1959). 250 µl of lipid samples from irradiated and un-irradiated culture were mixed with 125 µl of 20% trichloroacetic acid (TCA). The supernatant was collected, mixed with 0.5 ml $FeSO_4$ (0.07 M) and incubated at 37°C for 1 h. 300 µl of this solution was mixed with 0.8% TBA reagent (200 µl), 8% SDS (200 µl) and incubated at 100°C for 1 h. The absorbance of chromophore was measured at 535 nm. The MDA concentration is presented as µM of MDA produced per mg of lipids using a molar extinction coefficient of 1.56×10^5 M/cm (KONUKOĞLU *et al*. 1999). The experiment was run in triplicate and a UV sensitive *E. coli* (ATCC 10536) was used as a control.

Intracellular protein carbonylation

Protein carbonylation, an indicator of protein oxidation, was measured using the DNPH (2,4-dinitrophenyl hydrazine) method (MISRA *et al*. 2004). Both irradiated and un-irradiated cell suspensions were centrifuged and pellets were resuspended in 10 mM Tris-HCl (pH 8.0), sarkosyl (1.5% v/v) and incubated at room temperature for 20 min (OJANEN *et al*. 1993). The total protein concentration was estimated by a method previously described by LOWRY *et al*. (1951). The protein extract (2 mg/ml) in 50 mM PBS (pH 7.4) was incubated with 400 µl of 10 mM DNPH in 2 M HCl for 2hrs in the dark. Protein was precipitated, resuspended in 6 M guanidine hydrochloride. The supernatant was analyzed spectrophotometrically at 370nm. A protein control was run in parallel where DNPH was replaced with 2 M HCl. The protein carbonyl content was expressed in mM/mg of protein.

Statistical analysis

To assess the significance of the results the following tests were applied: Student's t-test for pairwise comparisons, single factor and two-way ANOVA for analysis between and within groups, and Tukey's HSD test for multiple comparisons. A P value less than 0.05 was considered significant. The effects of UV on cellular lipids and pro-

teins were estimated and all the strains were compared with a UV sensitive strain *E. coli* ATCC 10536. Bacterial cell sensitivities were studied by plotting the data between the % survivability and their respective UV doses (Jm^{-2}).

Results

Metal analysis of soil samples

The sampling areas, both selected from Lakki Marwat and Bahawalpur deserts, were characterized by high solar radiation and temperature fluctuations between day and night. Figure 1 shows the physiochemical analysis of soil samples collected from two different deserts. Both samples contained high concentrations of Mn^{+2} followed by Mg^{+2}, Fe^{+2} and Pb^{+2} but very low concentrations of Cd^{+2}, Cu^{+2} and Cr^{+2} ions. A two-way ANOVA used to check the differences between the two deserts, showed a significant difference using metal-type as blocking factor ($P<0.05$). Moreover, a pairwise t-test showed that the average characteristic of Lakki Marwat dessert is significantly higher than the Bahawalpur desert ($P=0.02$).

Isolation of ultraviolet radiation (UVR) resistant microbes

Soil samples were exposed to UV radiation from 30 to 300 sec with an energy dose of about 300-3300 J/m^2. A total of 9 representative colonies were selected after incubation at 37°C for a week, morphological characteristics (shown in Table 1) were noted and then purified.

Resistance to UV in correlation with % survivability

The bacterial strains were exposed to UVR dosage ranges from 300-3300 J/m^2 and their survival rate was determined. Following exposure to different doses of UVR, the colony-forming units (CFUs) of irradiated samples were significantly lower than un-irradiated samples ($P=0.001$) (Fig. 2). The initial dose of UVR ($2.0x10^3$ J/m^2) was found to be lethal for most of the bacterial population, hence considered as LD_{50}. A gradual decrease in CFU was observed upon an increase in UV dose up to a certain extent, a rapid decline in individual populations was observed beyond that limit. Among these 9 bacterial strains, the survival rates of strains WMA-LM9, WMA-LM30 and WMA-BD1 were noted as 79%, 68%, and 45%, respectively, even after exposure to high energy dosage (3.3×10^3) and considered as UV resistant bacteria. Strain WMA-LM19 was found to be the most sensitive that could withstand up to 1.30×10^3 J/m^2 energy. Pairwise t-test shows there is a significant affect of UV dose on the survival of isolates where $P<0.05$.

Identification of UV resistant bacterial strains

Morphology

A diverse bacterial population was observed on un-irradiated TGY plates in comparison to the irradiated TGY plates where only yellow, orange, pink, or red colonies were observed. A decrease in colony forming units (CFU) per gram of soil samples was observed upon increase in UVR dose. After UV irradiation, the UVR resistant strains were

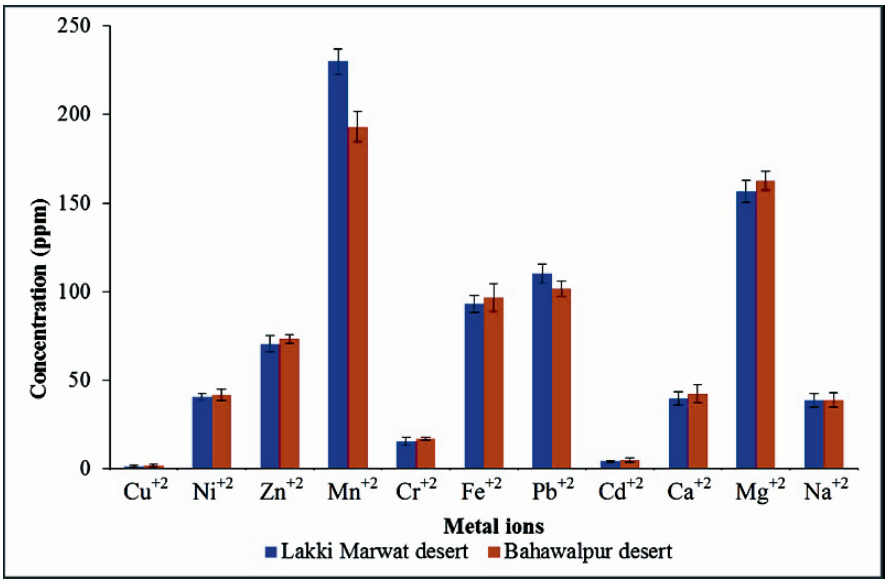

Fig. 1. Metal analysis (in ppm) of soil samples collected from Lakki Marwat and Bahawalpur deserts.

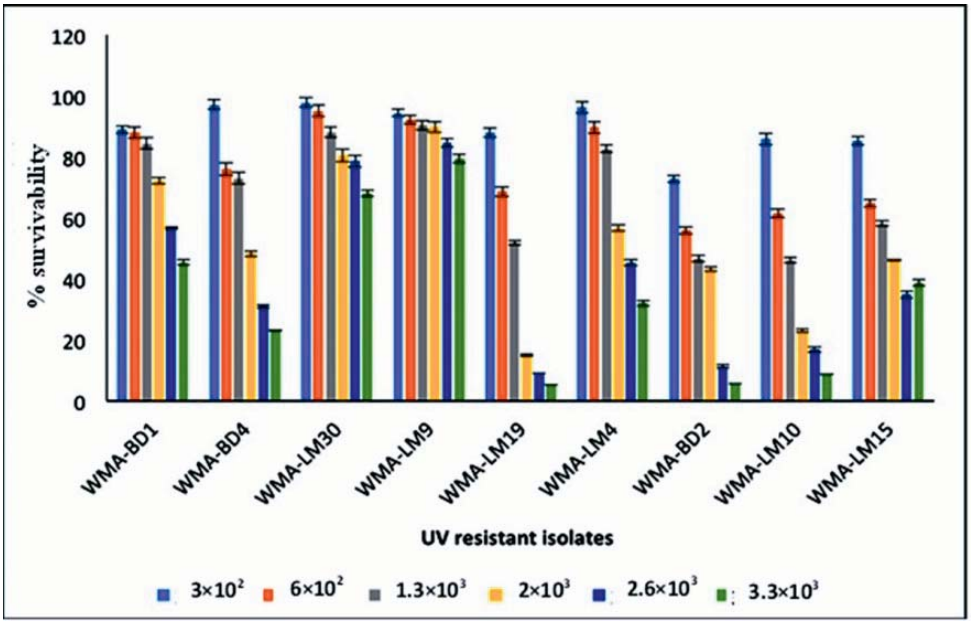

Fig. 2. Survivability of total UVR resistant isolates from desert soil at varying UV-B exposure. % survivability was measured using the formula $N_1/N_0 \times 100$. N_1 is the number of colonies after UV irradiation while N_0 number of colonies prior to exposure. The bars show mean±SD (whiskers).

Table 1

Microscopic characteristics with cultural morphology of UV resistant bacteria isolated from desert soil samples

Culture code	Sampling site	Morphology	Microscopy
WMA-BD1	Bahawalpur desert	Small to medium sized light orange colored mucoid and circular, raised colonies with entire margins	G+ve cocci
WMA-BD2	Bahawalpur desert	Large light off-white oval shaped colonies dry surface forming crystal like structure when aggregates	G+ve rods
WMA-BD4	Bahawalpur desert	Medium to large yellow colored circular raised colonies with entire margins	G+ve rods
WMA-LM4	Lakki Marwat desert	Small to medium sized off-white smooth and circular, flat colonies with entire margins	G+ve rods
WMA-LM9	Lakki Marwat desert	Medium brick red colored colonies mucoid circular with entire margins	G+ve cocci
WMA-LM10	Lakki Marwat desert	Large raised white in color with sticky surface colonies with irregular margins	G-ve rods
WMA-LM15	Lakki Marwat desert	Large flat off-white in color oval shape dry colonies with entire margins	G-ve rods
WMA-LM19	Lakki Marwat desert	Large off-white in color flat colonies with shiny surface circular with entire margins	G-ve rods
WMA-LM30	Lakki Marwat desert	Medium brick red colored colonies with dry surface circular with entire margins occur singly or tetrads	G+ve cocci

examined both morphologically and microscopically; Table 1 shows the cellular morphology and Gram's reaction of all UV resistant bacteria.

Biochemical and physiological characteristics of UV resistant microbes

Biochemical, physiological and other characteristics such as temperature, pH range and salt tolerance among all UVR resistant bacteria were also determined. Table 2 shows biochemical and other physiological characteristics of these UVR resistant strains. The results indicated that all these strains have potential to grow at a wide temperature (20-45°C) and pH (6-10) range, high salt concentration (2-16%), and also produce different hydrolytic enzymes like amylase, protease, gelatinase, and DNase as shown in the Table 2.

Table 2

Biochemical and physiological characteristics of UV resistant isolates from Lakki Marwat and Bahawalpur desert soils

Characteristics	Bacterial Strains								
	WMA-BD1	WMA-BD2	WMA-BD4	WMA-LM4	WMA-LM9	WMA-LM10	WMA-LM15	WMA-LM19	WMA-LM30
Temperature (°C)	20-35	25-40	20-37	25-37	10-30	20-45	25-45	20-45	10-30
pH	7-9	7-10	7-9	7-9	7-8	6-10	6-9	6-10	7-8
Salt tolerance	12%	10%	10%	14%	2%	10%	16%	12%	6%
Catalase	+	+	+	+	+	+	+	+	+
Oxidase	–	–	–	–	–	+	+	+	–
Amylase	+	+	+	–	+	+	+	+	–
Protease	–	+	+	+	+	+	+	+	+
Gelatinase	+	+	–	–	+	+	+	+	+
DNase	+	–	–	–	+	+	+	+	–

Molecular characterization and phylogenetic analysis of UVR bacteria

The phylogenetic diversity was evaluated by partial sequencing of the 16S rRNA gene of 9 bacterial strains representative of each dominant morphotype cultured on plates. The sequencing results clearly divided all these strains into 4 phyla: *Actinobacteria* (1 isolate), *Proteobacteria* (3 isolates), *Firmicutes* (3 isolates) and the *Deinococccus-Thermus* group (2 isolates). *Proteobacteria* showed a distant relationship to the genera *Stenotrophomonas* with 93-99% of similarity. 2 strains were clustered near phylum *Deinococcus-Thermus* and showed 99% similarity to *Deinococcus* sp., considered to be among the most UV resistant organisms up till now. 3 *Firmicutes* clustered near the genera *Bacillus* (2) and *Staphylococcus* (1) with 99% similarity. Finally, 1 Actinobacteria was distantly related to the genus *Kocuria* with 99% similarity, as shown in Table 3. It is noteworthy that the 16S rRNA gene sequences of 9 bacterial strains were closely related to database sequences derived from arid, semi-arid environments and polluted soils (Table 3).

Nucleotide sequence and accession numbers

The 16S rRNA sequences of all pure cultures were deposited in the GenBank database under accession numbers: KT008382 (*Stenotrophomonas maltophilia* WMA-LM10); KT008383 (*Stenotrophomonas* sp. WMA-LM19); KT008384 (*Deinococcus* sp. WMA-LM30); KT008385 (*Bacillus licheniformis* WMA-BD2); KT008386

Table 3

GenBank accession number, closest related species, query coverage, 16S rRNA sequence homologues, and % survivability of Ultraviolet radiation (UV-B) resistant isolates from desert samples

Isolates	GenBank Accession Number	Closest related species	Query coverage %	Similarity score %	UVR resistance J/m^2	Survival rate (%)
WMA-BD1	KT008387	*Kocuria turfanensis*	100	99	3.3×10^3	45.45
WMA-BD2	KT008385	*Bacillus licheniformis*	100	99	2.0×10^3	43.18
WMA-BD4	KT008386	*Staphylococcus lugdunensis*	100	99	2.0×10^3	48.27
WMA-LM4	KT008388	*Bacillus pumilus*	99	99	2.60×10^3	45.28
WMA-LM9	KT008389	*Deinococcus radiopugnans*	100	99	3.30×10^3	79.47
WMA-LM10	KT008382	*Stenotrophomonas maltophilia*	100	99	1.30×10^3	46.15
WMA-LM15	KT008390	*Bacillus subtilis*	100	99	3.30×10^3	38.72
WMA-LM19	KT008383	*Stenotrophomonas* sp.	99	93	1.30×10^3	51.69
WMA-LM30	KT008384	*Deinococcus* sp.	100	100	3.30×10^3	68.03

Table 4

Effect of the metal ions (in ppm) on growth of UVR resistant selected bacteria from desert samples on TGY agar plates. The minimum metal ion concentration (ppm) that inhibits the growth of UVR resistant isolates is shown in the table

Strain code	Cd	Zn	Cr	Fe	Cu	Mn
WMA-BD1	380	160	360	360	280	300
WMA-BD2	200	200	320	360	200	260
WMA-BD4	240	240	300	360	200	240
WMA-LM4	360	280	360	300	240	200
WMA-LM9	200	80	380	280	200	220
WMA-LM10	240	200	300	360	200	300
WMA-LM15	220	280	360	360	240	340
WMA-LM19	280	120	280	360	200	280
WMA-LM30	280	200	360	200	280	340

(*Staphylococcus lugdunensis* WMA-BD4); KT008387 (*Kocuria turfanensis* WMA-BD1); KT008388 (*Bacillus pumilus* WMA-LM4); KT008389 (*Deinococcus radiopugnans* WMA-LM9); KT008390 (*Bacillus subtilis* WMA-LM15) (Table 3).

Metal resistance

The isolated radioresistant bacteria were more resistant to Mn^{+2}, Co^{+2}, Cr^{+2}, and Ni^{+2}, which could be directly correlated to UVR resistance as shown in Table 4. Some interesting changes in cultural characteristics of strains WMA-LM9, WMA-LM30 and WMA-LM19 were observed on medium supplemented with Mn^{+2}, such as an increase in colony size and bright coloration. A high capacity for intracellular Cu^{+2} ion sequestration was detected in strains WMA-BD1, WMA-LM15, WMA-LM9, WMA-LM30 (240-280ppm) that provided protection against the damaging effects of ionizing radiation as shown in Fig. 3.

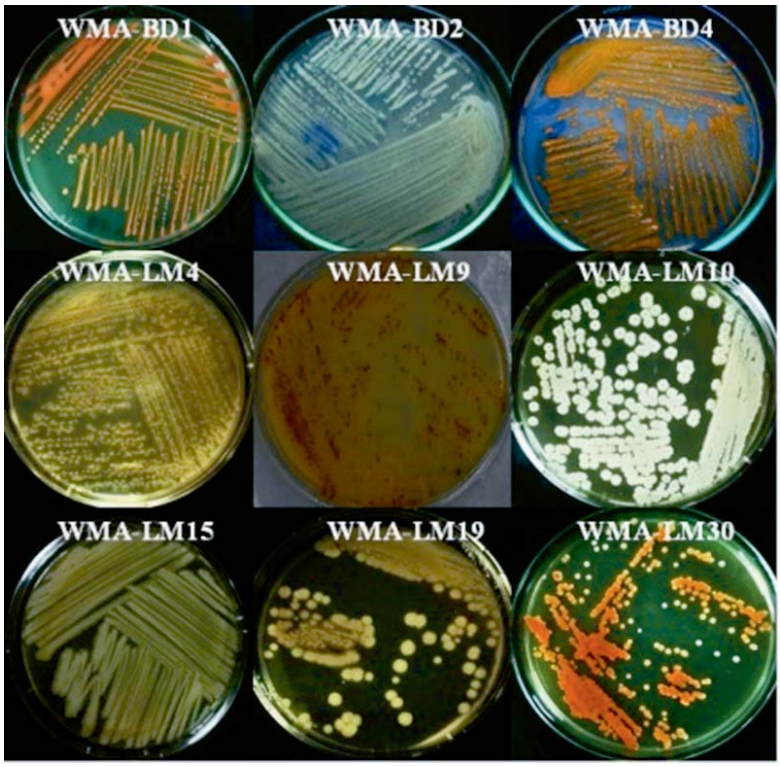

Fig. 3. Morphology of different UV resistant isolates from two desert soils on tryptone glucose yeast (TGY) agar plates supplemented with metal ions.

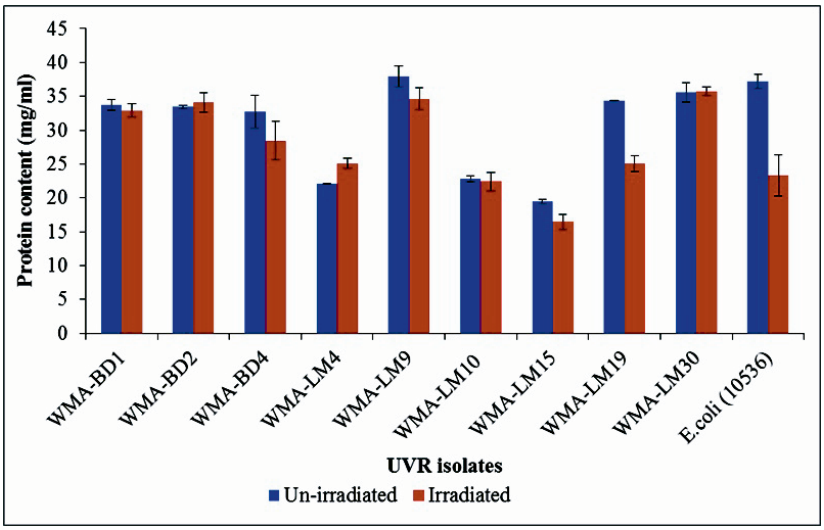

Fig. 4. Effect of UVB on total cell protein content in mg/ml. The bars show mean±SD (whiskers).

Effect of UVB on whole cell proteins

The effect of UVR on whole cell protein from radioresistant bacteria was determined. The bacteria presented strong protection to cellular protein upon exposure to UVR, in comparison to a UVR sensitive *E. coli* (ATCC 10536), used as a control. Figure 4 shows the amount of protein (mg/ml) measured from both irradiated and non-irradiated bacteria, strains WMA-LM9, WMA-LM30, WMA-BD1 and WMA-BD2 were observed for maximum amount of protein after exposure to a high UVR dose. UVB strongly damaged the whole cell protein of *E. coli* 10536, a sensitive strain. The radioresistant UV treated strains in this study showed little damage in intracellular proteins as compared to the untreated strains. The pairwise t-tests shows $P<0.05$ ($P=0.002$). Statistical analysis showed a significant difference in protein contents of sensitive strain *E. coli* and UV resistant isolates using Tukey's multiple comparisons test ($P<0.014$). The results show a better preventive system for UV in UV resistant strains than *E. coli* ATCC 10536.

Lipid and protein oxidation of UVR isolates

UV radiation-induced oxidative stress causes damage to cellular lipids and proteins that ultimately results in cell death. The effect of UV on cellular lipids and proteins was measured. A UV sensitive *E. coli* (10536) strain was used as a control. *E. coli* (10536) displayed significant damage to its cellular lipids (Fig. 5) and proteins (Fig. 6) upon UV exposure with lipid peroxidation up to 12 µM/mg and protein oxidation of 189 mM/mg. A difference between *E. coli* was observed in protein and lipids damages in comparison to the ra-

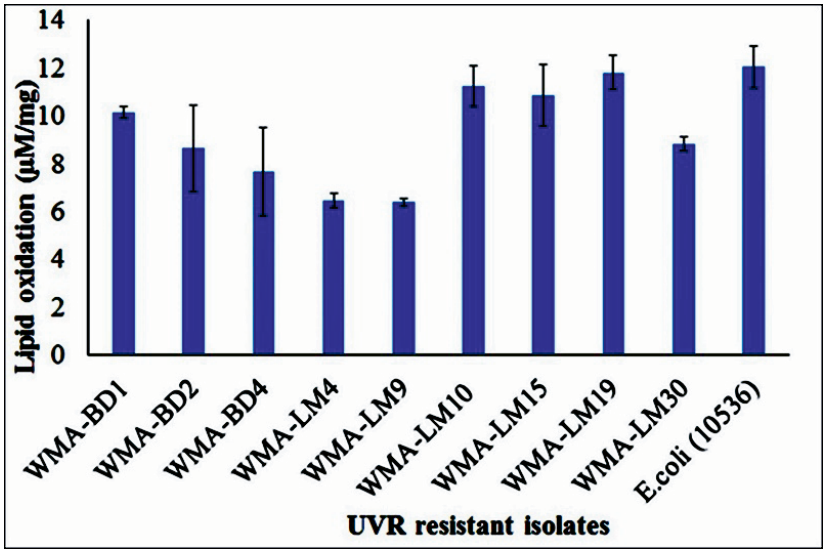

Fig. 5. Lipid peroxidation assay in UV-treated isolates from desert soil. The bars show mean±SD (whiskers).

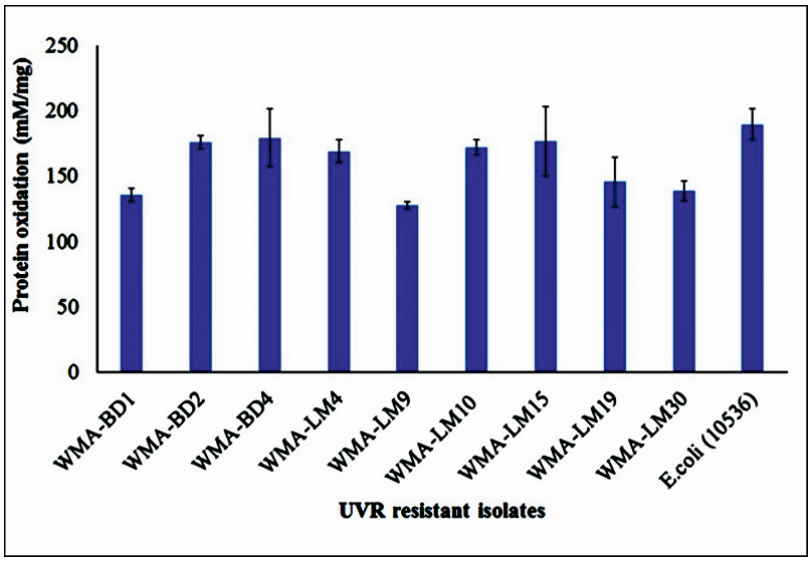

Fig. 6. Protein oxidation assay in UV-treated isolates from desert soil. The bars show mean±SD (whiskers).

dioresistant microbes, revealing their resistance to UV radiation. Figures 5 and 6 show that strains WMA-LM9, WMA-LM30 and WMA-BD1 exhibited lower protein oxidation (P=0.0099), while lipid oxidation was lower in strains WMA-LM4, WMA-LM9 and WMA-BD4 (P=0.0199) in comparison to the control strain. The data was analysed by using a two-way ANOVA and Tukey's HSD test. Moreover, a pairwise t-test shows P<0.02, and the results were considered highly significant.

Discussion

The current study was conducted to investigate the bacterial community inhabiting extreme environments including high hypersaline and high UV radiation habitats. Their survival in spite of higher UV dosage as well as resistance to salt and metal ions are some of the interesting characteristics of these microbes. The molecular mechanisms behind these phenomena need to be investigated. The soil samples were analyzed for the presence of various metal ions: Mn^{+2}, Mg^{+2}, Fe^{+2}, and Pb^{+2} were found to be the most abundant divalent cations followed by Ca^{+2}, Ni^{+2}, and Zn^{+2}. Research conducted on several biological systems has highlighted the role of transition metal ions in protection against the detrimental effects of radiation, desiccation and H_2O_2 (DALY *et al*. 2004; GHOSH *et al*. 2011). During sand formation in deserts, the manganese oxides in rock varnish very effectively blocking the transmission of ultraviolet radiation (DORN & OBERLANDER 1981). Our results demonstrated a significant role of the metal ions in two deserts and UV-resistant microbe survival in such dry and extreme environs. The microbes inhabiting the desert can synthesize different oxides of manganese on their outer surfaces which can act as a sunscreen to block the UV radiation. These manganese oxides also give a characteristic dark color to desert soil (FLEISHER *et al*. 1999).

Based on comparison of 16S rRNA gene sequences, most of the UVR resistant bacteria were Gram positive and assigned to four different clusters: *Fermicutes*, *Deinococcus-Thermus, Proteobacteria* and *Actinobacteria*. β-*Proteobacteria* and *Firmicute*s have been reported earlier with maximum survival rate at high UV dosage (BAATI *et al*. 2010; MORENO *et al*. 2012). FREDRICKSON and colleagues (2004) described *Proteobacteria*-related species from nuclear waste-contaminated sediments that exhibited resistance to 2.5 kGy of gamma radiation, with 0.0017% survival.

Most of the bacteria produced colored pigments on TGY agar, as indicated by colored colonies, that may absorb radiation in order to protect the cells from damage. The production of UVR-absorbing compounds might be induced as a result of exposure to radiation stress (DIB *et al*. 2009). We have reported a bacterium with 93% similarity to *Stenotrophomonas* sp. that showed enlargement in its colony size and pink to red coloration upon radiation exposure in the presence of Mn^{+2}. The rapid increase in cell number and size after exposure to UV needs deeper studies in order to explain the mechanism triggered by radiation that enhances cellular survival and replication (MCGLYNN & LLOYD 2002). Previously a number of researchers have reported radio-resistant bacteria from desert soil, this strategy might be the result of evolution in order to protect cells from desiccation (RAINEY *et al*. 2005). In *Deinococcus* the S-layer protein DR-2577 binds deinoxan-

thin under desiccation stress that in turn shields the bacterium from UV light and could behave as a first line of defense against radiation (FARCI *et al*. 2016). The ability of these UV resistant microbes to survive in several extreme conditions is suggested to be a result of three combined mechanisms: prevention, tolerance and repair (WHITE *et al*. 1999).

Metals like Mn^{+2}, Cu^{+2}, Zn^{+2} and Co^{+2} enhance the survivability of UVR resistant microbes because these metals block the Fenton reactions that indirectly prevent formation of several toxic oxides and by-products which can alter the cell membrane (BAATI *et al*. 2010; SANTOS 2011). In this study, all the bacteria isolated from desert soils showed high resistance to various metal ions. A high capacity for intracellular copper ion sequestration was detected in *Kineococcus* radiotolerans (*Actinobacteria*) that might be a reason for its survival against ionizing radiation (ASGARANI *et al*. 2012; PAULINO-LIMA *et al*. 2016). Research has highlighted the role of manganese (Mn^{2+}) ions in the prevention of oxidative damage to cells upon exposure to UV radiation, gamma-irradiation, heat and H_2O_2 (BARNES *et al*. 2008; MCEWAN 2009; DALY *et al.* 2010; SLADE & RADMAN 2011). Zinc (Zn^{2+}) uptake is also a key component of the adaptive response to peroxide stress (GABALLA & HELMANN 2002), protecting copper-treated *Escherichia coli* against superoxide killing (KORBASHI *et al*. 1989) and countering the effects of oxidative stress in *Lactococcus lactis* (SCOTT *et al*. 2000). The ability of these microbes in such extreme environment makes them an attractive choice for in-situ bioremediation of radioactive wastes. Bacteria are susceptible to harmful effects of UV radiation due to their small size, short generation time and absence of effective UV-protective pigmentation (GARCIA-PICHEL 1994). The effect of UV radiation on all the bacterial strains isolated from desert soil showed different survival rates as well as lipid peroxidation and protein carbonylation. *Deinococcus* was found to be the most resistant with a high survival rate and low level of lipid and protein damage in comparison to *E. coli* (10536) ATCC (Fig. 4). SANTOS *et al*. (2013b) reported that exposure to UVR causes alteration in lipids and protein structures as a result of peroxidation and carbonylation, respectively, which were confirmed by gas chromatography.

In addition to DNA damages by high UV exposure, changes in lipid membranes and protein tertiary structure also play an important role in bacterial inactivation. The targets (e.g., nucleic acids, proteins, lipids) for UV radiation inactivation may differ among the genus, species and strains and thus all these factors contribute the duration of cell survival under high UV radiation. It has also been suggested that UV-induced DNA damage in Gram-positive bacteria is lower than that of Gram-negative bacteria because of a shielding effect by the cell wall (JAGGER 1985). The presence of Mn/Fe ratio is another factor that can contribute to cell resistance under high radiation. The presence of a high concentration of Fe^{+2} in *Shewanella oneidensis* MR-1 makes it sensitive to UV radiation. The intracellular Fe^{+2} promotes the formation of ROS via Fenton type reactions (QIU *et al*. 2005). The efficiency of defence in extreme environments and highly sophisticated molecular repair mechanisms may differ among bacteria and play an important role in cellular resistance.

Conclusion

We have demonstrated that UV radiation has a clear effect on the microbes and other living cells. The resistant microbes produce compounds of great interest which can be used as sunscreen and UV protectants. Our study argues for increased exploration of the desert environment for UV resistant microbes in Pakistan. These results open exciting possibilities for investigating bacterial lenience to desiccation, radiation and survey in the deserts. The implication of the results is conferred from an environmental and industrial perspective and with admiration to potential expansion in UV-based disinfection technologies.

Acknowledgements

We highly acknowledge the Department of Microbiology, Quaid-I-Azam University, Islamabad, Pakistan for providing facilities to accomplish this study. The contribution of Biochemistry department Quaid-I-Azam University, Islamabad, Pakistan is highly appreciated.

Author Contributions

Research concept and design: A.A.S.; Collection and/or assembly of data: W.S., S.K., M.A., S.Z.; Data analysis and interpretation: W.S., M.R., W.S.; Writing the article: W.S; Critical revision of the article: M.B.

Conflict of Interest

The authors declare no conflict of interest.

References

ASGARANI E., SOUDI M.R., BORZOOEE F., DABBAGH R. 2012. Radio-resistance in psychrotrophic *Kocuria* sp. ASB 107 isolated from Ab-e-Siah radioactive spring. J. Environ. Radioact. **113**: 171-176.

BAATI H., AMDOUNI R., GHARSALLAH N., SGHIR A., AMMAR E. 2010. Isolation and characterization of moderately halophilic bacteria from tunisian solar saltern. Curr. Microbiol**. 60**: 157-161.

BAGWELL C.E., MILLIKEN C.E., GHOSHROY S., BLOM D.A. 2008. Intracellular copper accumulation enhances the growth of *Kineococcus radiotolerans* during chronic irradiation. Appl. Environ. Microbiol. **74**: 1376-1384.

BARNES P.W., FLINT S.D., SLUSSER J.R., GAO W., RYEL R.J. 2008. Diurnal changes in epidermal UV transmittance of plants in naturally high UV environments. Physiologia Plantarum **133**: 363-372.

BARRERA G. 2012. Oxidative stress and lipid peroxidation products in cancer progression and therapy. ISRN Oncology. 2012.

BEBLO-VRANESEVIC K., GALINSKI E.A., RACHEL R., HUBER H., RETTBERG P. 2017. Influence of osmotic stress on desiccation and irradiation tolerance of (hyper)-thermophilic microorganisms. Arch. Microbiol. **199**: 17-28.

BLIGH E.G., DYER W.J. 1959. A rapid method of total lipid extraction and purification. Canadian J. Biochem. Physiol. **37**: 911-917.

DALY M.J., GAIDAMAKOVA E.K., MATROSOVA V.Y., KIANG J.G., FUKUMOTO R., LEE D.Y., WEHR N.B., VITERI G.A., BERLETT B.S., LEVINE R.L. 2010. Small-Molecule Antioxidant Proteome-Shields in *Deinococcus radiodurans*. PLoS One **5**: e12570.

DALY M.J., GAIDAMAKOVA E.K., MATROSOVA V.Y., VASILENKO A., ZHAI M., VENKATESWARAN A., HESS M., OMELCHENKO M.V., KOSTANDARITHES H.M., MAKAROVA K.S., WACKETT L.P., FREDRICKSON J.K., GHOSAL D. 2004. Accumulation of Mn(II) in *Deinococcus radiodurans* facilitates gamma-radiation resistance. Science **306**: 1025-1028.

DIB J.R., WEISS A., NEUMANN A., ORDOÑEZ O., ESTÉVEZ M.C., FARÍAS M.E. 2009. Isolation of bacteria from remote high altitude Andean lakes able to grow in the presence of antibiotics. Recent Pat. Antiinfect Drug Discov. **4**: 66-76.

DORN R.I., OBERLANDER T.M. 1981. Microbial origin of desert varnish. Science **213**: 1245-1247.

FARCI D., SLAVOV C., TRAMONTANO E., PIANO D. 2016. The S-layer Protein DR_2577 Binds *Deinoxanthin* and under Desiccation conditions protects against UV-radiation in *Deinococcus radiodurans*. Front. Microbiol. **7**: 155.

FLEISHER M., LIU T., BROECKER W.S., MOORE W. 1999. A clue regarding the origin of rock varnish. Geophys Res. Lett. **26**: 103-106.

FREDRICKSON J.K., ZACHARA J.M., BALKWILL D.L., KENNEDY D., LI S.M., KOSTANDARITHES H.M., DALY M.J., ROMINE M.F., BROCKMAN F.L. 2004. Geomicrobiology of high-level nuclear waste-contaminated vadose sediments at the Hanford site, Washington state. Appl. Environ. Microbiol. **70**: 4230-4241.

GABALLA A., HELMANN J.D. 2002. A peroxide-induced zinc uptake system plays an important role in protection against oxidative stress in *Bacillus subtilis*. Mol. Microbiol**. 45**: 997-1005.

GARCIA-PICHEL F. 1994. A model for internal self-shading in planktonic organisms and its implications for the usefulness of ultraviolet sunscreens. Limnol. Oceanogr. **39**: 1704-1717.

GHOSH S., RAMIREZ-PERALTA A., GAIDAMAKOVA E., ZHANG P., LI Y.Q., DALY M.J., SETLOW P. 2011. Effects of Mn levels on resistance of *Bacillus megaterium* spores to heat, radiation and hydrogen peroxide. J. Appl. Microbiol. **111**: 663-670.

HALLIWELL B., GUTTERIDGE J.M. 2015. Free Radicals in Biology and Medicine. Oxford University Press, USA.

JAGGER J. 1985. Solar UV Actions on Living Cells. Praeger Publishing, New York.

KONUKOĞLU D., AKÇAY T., DINÇER Y., HATEMI H. 1999. The susceptibility of red blood cells to autoxidation in type 2 diabetic patients with angiopathy. Metabolism **48**: 1481-1484.

KORBASHI P., KATZHENDLER J., SALTMAN P., CHEVION M. 1989. Zinc protects *Escherichia coli* against copper-mediated paraquatinduced damage. J. Biol. Chem. **264**: 8479-8482.

LOWRY O.H., ROSEBROUGH N.J., FARR A.L., RANDALL R.J. 1951. Protein measurement with the folin phenol reagent. J. Biol. Chem. **193**: 265-275.

MATTIMORE V., BATTISTA J.R. 1996. Radioresistance of *Deinococcus radiodurans*: functions necessary to survive ionizing radiation are also necessary to survive prolonged desiccation. J. Bacteriol. **178**: 633-637.

MCEWAN A.G. 2009. New insights into the protective effect of manganese against oxidative stress. Mol. Microbiol. **72**: 812-814.

MCGLYNN P., LLOYD R.G. 2002. Genome stability and the processing of damaged replication forks by RecG. Trends Genet. **18**: 413-419.

MISRA H.S., KHAIRNAR N.P., BARIK A., PRIYADARSINI K.I., MOHAN H., APTE S.K. 2004. Pyrroloquinoline-quinone: a reactive oxygen species scavenger in bacteria. FEBS Letters **578**: 26-30.

MORENO M.L., PIUBELI F., BONFA M.R.L., GARCÍA M.T., DURRANT L.R., MELLADO E. 2012. Analysis and characterization of cultivable extremophilic hydrolytic bacterial community in heavy-metal contaminated soils from the Atacama Desert and their biotechnological potentials. J. Appl. Microbiol. **113**: 550-559.

MURRAY R.G.E., COSTILOW R.N., NESTER E.W., WOOD W.A., KRIEG N.R., PHILLIPS G.B.. 1981. Manual of Methods for General Bacteriology. American Society for Microbiology, Washington, DC.

OJANEN T., HELANDER I.M., HAAHTELA K., KORHONEN T.K., LAAKSO T. 1993. Outer membrane proteins and lipopolysaccharides in pathovars of *Xanthomonas campestris*. Appl. Environ. Microbiol. **59** : 4143-4151.

PATTISON D.I., DAVIES M.J. 2006. Actions of ultraviolet light on cellular structures. (In: Cancer: Cell Structures, Carcinogens and Genomic Instability. Birkhäuser Basel): 131-157.

PAULINO-LIMA I.G., FUJISHIMA K., NAVARRETE J.U., GALANTE D., RODRIGUES F., AZUA-BUSTOS A., ROTHSCHILD L.J. 2016. Extremely high UV-C radiation resistant microorganisms from desert environments with different manganese concentrations. J. Photochem. Photobiol. B: Biol. **163**: 327-336.

PÉREZ J.M., CALDERÓN I.L., ARENAS F.A., FUENTES D.E., PRADENAS G.A., FUENTES E.L., SANDOVAL J.M., CASTRO M.E., ELÍAS A.O., VÁSQUEZ C.C. 2007. Bacterial toxicity of potassium tellurite: unveiling an ancient enigma. PLoS One, **2**: p.e211.

PHILLIPS R.W., WIEGEL J., BERRY C.J., FLIERMANS C., PEACOCK A.D., WHITE D.C., SHIMKETS L.J. 2002. *Kineococcus radiotolerans* sp. nov., a radiation- resistant, Gram positive bacterium. Int. J. Syst. Evol. Microbiol. **52**: 933-938.

QIU X., SUNDIN G.W., WU L., ZHOU J., TIEDJE J.M. 2005. Comparative analysis of differentially expressed genes in *Shewanella oneidensis* MR-1 following exposure to UVC, UVB, and UVA radiation. J. Bacteriol. **187**: 3556-3564.

RAINEY F.A., RAY K., FERREIRA M., GATZ B.Z., NOBRE M.F., BAGALEY D., SMALL A.M. 2005. Extensive diversity of ionizing-radiation-resistant bacteria recovered from Sonoran Desert soil and description of nine new species of the genus *Deinococcus* obtained from a single soil sample. Appl. Environ. Microbiol. **71**: 5225-5235.

RAURET G. 1998. Extraction procedures for the determination of heavy metals in contaminated soil and sediment. Talanta **46**: 449-455.

ROBINSON C.K., WEBB K., KAUR A., JARUGA P., DIZDAROGLU M., BALIGA N.S., PLACE A., DIRUGGIERO J. 2011. A major role for nonenzymatic antioxidant processes in the radioresistance of *Halobacterium salinarum*. J. Bacteriol. **193**: 1653-1662.

SAJJAD W., AHMAD M., KHAN S., ILYAS S., HASAN F., CELIK C., MCPHAIL K., SHAH A.A. 2017. Radio-protective and antioxidative activities of astaxanthin from newly isolated radio-resistant bacterium *Deinococcus* sp. strain WMA-LM9 Ann. Microbiol. **67**: 1-13.

SANTOS A.L., GOMES N., HENRIQUES I., ALMEIDA A., CORREIA A., CUNHA A. 2013a. Role of transition metals in UV-B-induced damage to bacteria. Photochem. Photobiol. **89**: 640-648.

SANTOS A.L., LOPES S., BAPTISTA I., HENRIQUES I., GOMES N.C.M., ALMEIDA A., CORREIA A., CUNH A. 2011. Diversity in UV sensitivity and recovery potential among bacterioneuston and bacterioplankton isolates. Lett. Appl. Microbiol**. 52**: 360-366.

SANTOS A.L., MOREIRINHA C., LOPES D., ESTEVES A.C., HENRIQUES I., ALMEIDA A., CORREIA A., CUNHA A. 2013b. Effects of UV radiation on the lipids and proteins of bacteria studied by mid-infrared spectroscopy. Environ. Sci. Technol. **4**: 6306-6315.

SCOTT C., RAWSTHORNE H., UPADHYAY M., SHEARMAN C.A., GASSON M.J., GUEST J.R., GREEN J. 2000. Zinc uptake, oxidative stress and the FNR-like proteins of *Lactococcus lactis*. Fems Microbiol. Lett. **192**: 85-89.

SINGH O.V., GABANI P. 2011. Extremophiles: radiation resistance microbial reserves and therapeutic implications. J. Appl. Microbiol. **110**: 851-861.

SLADE D., RADMAN M. 2011. Oxidative stress resistance in *Deinococcus radiodurans.* Microbiol. Mol. Biol. R. **75**: 133-191.

TAMURA K., STECHER G., PETERSON D., FILIPSKI A., KUMAR S. 2013. MEGA6: Molecular evolutionary genetics analysis version 6.0. Mol. Biol. Evol. **30**: 2725-2729.

WHITE O., EISEN J.A., HEIDELBERG J.F., HICKEY E.K., PETERSON J.D., DODSON R.J., MOFFAT K.S. 1999. Genome sequence of the radioresistant bacterium *Deinococcus radiodurans* R1. Science **286**: 1571-1577.